Převodníky pro pulzní kvantovou optomechaniku

Odevzdáno pro splnění požadavků získání titulu

Ph.D.

NIKITA VOSTROSABLIN

Školitel: Prof. Mgr. Radim Filip, Ph.D
Konzultant: Andrey Rakhubovsky, Ph.D

Palacký University
Olomouc

UNIVERZITA PALACKÉHO V OLOMOUCI, PŘÍRODOVĚDECKÁ FAKULTA, KATEDRA OPTIKY

září 2020

Pulsed quantum optomechanical interfaces

Submitted in partial fulfillment of the requirements for the degree of

Doctor of Philosophy

by

NIKITA VOSTROSABLIN

Supervisor: Prof. Mgr. Radim Filip, Ph.D
Ph.D. Consultant: Andrey Rakhubovsky, Ph.D

Palacký University
Olomouc

PALACKY UNIVERSITY OLOMOUC. FACULTY OF SCIENCE
DEPARTEMENT OF OPTICS

September, 2020

DECLARATION

I here by declare that the thesis entitled “Thesis Title” submitted by me, for the award of the degree of *Doctor of Philosophy* to Palacký University is a record of bonafide work carried out by me under the supervision of Prof. Mgr. Radim Filip, Ph.D. and with consultations provided by Andrey Rakhubovsky, Ph.D.

I further declare that the work reported in this thesis has not been submitted and will not be submitted, either in part or in full, for the award of any other degree or diploma in this institute or any other institute or university.

I certify that:

- I was collaborating on all analytical and numerical analysis in chapters 3, 4, 5 and 6.
- This doctoral Thesis is based on four original impact publications listed in the section **LIST OF PUBLICATIONS**, which summarize the main results reached during my Ph.D. studies.
- I agree with the further usage of the thesis according to the requirements of Palacký University and the Department of Optics.

Place: Olomouc

Date: **Signature of the Candidate**

ABSTRACT

This Thesis is based on four original publications and concludes my theoretical research during the years of my Ph.D. studies.

Firstly we proposed a new way to deterministically transfer an arbitrary quantum state of light to the mechanical oscillator. It is shown that it is possible to enhance the coupling of light to matter with the help of only local Gaussian operation on the light. This approach is proved to help to transfer negativity of Winger function from light to mechanics.

Next, we introduced a scheme efficiently entangling two distant mechanical oscillators mediated by the optical or microwave field. At the time the work was performed, there have been no mechanical oscillators coupled at the quantum level demonstrated. The proposed scheme assumes a certain coupling between the mechanical systems – the quantum nondemolition (QND) one, which is very useful for basic continuous-variable quantum gates.

We also studied quantum transducers which are very important for the development of quantum technology. The proposed transducer is based on a sequence of long-pulsed interactions between the systems of interest (optical or microwave fields) and the mediating system (mechanical oscillator). We showed that with the help of the geometric phase effect it is possible to eliminate the noisy influence of the mechanical mediator.

To follow the development of quantum optomechanics, we explored the very similar transducer, but in the regime of high-intensive ultra-short pulses (stroboscopic regime). It was unclear before whether the geometric phase effect will be sufficient to obtain a robust transducer in this regime. Our proposal is suitable for arbitrary wavelengths of radiation which might stimulate a much broader class of feasible quantum transducers mediated by mechanical systems.

We believe that this thesis supported research and advanced the field making important theoretical explorations that open the way for future experimental implementations and studies of other setups based on similar principles.

Keywords: *Quantum Optomechanics*, *Quantum Optics*, *Quantum technology*, *Gaussian states*, *Gaussian operations*, *Quantum state transfer*, *Quantum transducer*, *Quan-*

tum correlations, *Gaussian entanglement*.

ACKNOWLEDGEMENT

First of all, I would like to express my deepest gratitude to my supervisor Radim Filip and my Ph.D. consultant Andrey Rakhubovsky. Radim was the example of the best possible *chief*, being able to inspire, guide, and help in any possible way he could. I think there are not enough words to express my appreciation, but I would like to thank him for all the support and understanding he provided to me during these years, and more importantly for the chance to study and work in his team. Andrey spent enormous time and effort helping me during my Ph.D. studies, and he is the person responsible the most for the fact that I finalized this Thesis. It is really hard to estimate his impact, but at least I would love to emphasize that my perspective on scientific work and work in general is mostly formed under his influence. I would like to thank him for all of his patience and engagement, even though I wasn't the best student possible.

I would like to address my great thanks to Ulrik L. Andersen and Ulrich B. Hoff for the fruitful and enriching discussions during my stay abroad. In this regard, I also would like to thank the Technical University of Denmark for hosting me during this stay.

I acknowledge the financial support of the Palacký University in Olomouc and the Czech Ministry of Education, Youth and Sports. Besides, I would like to express my deepest thanks to the Czech Republic in general as this beautiful country was very hospitable to me.

I thank two of my colleagues - Lukáš Lachman and Gleb Mazin for continued help with paper work related to Ph.D. and for scientific discussions we had.

I would love to mention my family for their support even though they didn't have any idea what I was doing all these years.

My special and deepest appreciation goes to my wife, who was very loving and understanding all these years, regardless of all my ups and downs. She always was very ironic and patient to any of my crazy undertakings and she is the person for whom I don't have to explain anything – I will be always supported.

Thank you!

Place: Olomouc

Date: 14/09/2020 **Nikita Vostrosablin**

TABLE OF CONTENTS

LIST OF FIGURES

To my grandfather and grandmother who are not with us anymore

Introduction

In 2016 a team of representatives of European academic and administrative institutions formulated [48] a common strategy for Europe to stay at the front of the second quantum revolution. This strategy has been named the "Quantum Manifesto" and it distinguishes four main directions in which quantum technologies could bring the next breakthrough. Those are quantum communication, simulations, sensors, and computers. As will be shown in the overview below, quantum optomechanics is an useful platform for all listed core fields. No less important, quantum optomechanics is very promising in expanding our understanding of quantum mechanics in general, including the study of classical-to-quantum transition [40] or quantum gravity [75, 193]. Because of these reasons, the field is getting more and more attention in recent years.

Origins of the field

Optomechanics relies traditionally on the radiation pressure phenomenon. Generally speaking, optomechanics refers to the radiation-pressure induced interaction between light and the mechanical harmonic oscillator. It is based on the idea that light-induced pressure can affect the mechanical properties of the oscillator being the subject of this pressure. To some degree, one could state, that we can trace back its origins to the famous experiments on measurements of the radiation pressure force conducted by Lebedev [115], and Nichols and Hull [153]. In the 20th century, the invention of laser made it possible to explore the radiation force at the new level, leading to the creation of optical tweezers after Ashkin's demonstration of a small dielectric ball being trapped by focused laser beams [10], to experiments with laser-trapped atoms [185, 165] and atomic Bose-Einstein condensates [4, 47].

A very important milestone in the formation of contemporary cavity optomechanics was the works of Vladimir Braginsky and colleagues in the 1960s-1970s, where they showed the action of light on a harmonically suspended mirror. In their works [28, 26] it was theoretically shown that in the case when the mirror is incorporated into a Fabry-Pérot cavity, its motion could be damped or amplified based on how the driving light frequency is tuned with respect to the optical resonance frequency of the cavity. The experimental demonstration in the microwave domain followed in the 1970 [27]. The idea of cavity optomechanics started being implemented in the 70s and 80s to the

detection of gravitational waves with Michelson-type laser interferometers [224]. This lead to the first detection of gravitational waves in 2015 [2].

The recent growth of interest to the quantum optomechanics is related to the possibility of a good level of control of the quantum states of various mechanical oscillators. However, these states are very fragile and present a big challenge in their experimental implementation. This fragility is related to the fact that quantum systems are never completely isolated from the environment [192]. When interacting with the environment a quantum system becomes entangled with a large number of environmental degrees of freedom, which influences what we can observe after measuring the system. Quantum interference effects become effectively suppressed and this process is known as *quantum decoherence* or *environment-induced decoherence* [238, 234, 191]. In other words, the external influences from the environment mask the quantum properties of large objects, and the most pervasive environmental factor is the *thermal noise*. To reach the regime in which it is possible to observe quantum effects, one first has to suppress this noise. The partial compensation of the thermal noise can be achieved by cooling a mechanical oscillator to its lowest energy state - *ground state*.

Optomechanical cooling

The principle of optomechanical cooling is based on the dynamical backaction effects and the resulting optomechanical damping rate [227, 138]. The very first experimental observation of possibility of the damping of mechanical motion of a harmonic oscillator with radiation pressure was performed by Vladimir Braginsky and coworkers in 1970 [27]. The experiment was based on a microwave cavity, where the modification of the damping rate of the end-mirror pendulum could be observed. The same year Ashkin demonstrated [10] laser-trapped dielectric ball. Cooling in the resolved sideband regime was achieved in 1995 by Blair and others [21] with high-Q niobium resonant mass gravitational antenna getting noise temperatures of 2 mK.

Another method of optomechanical cooling - optical feedback cooling, based on a feedback mechanism controlling the motion of a mechanical mirror via the radiation pressure of a laser beam, was implemented in 1999 [44]. In 2004 the dynamical backaction cooling with the help of photothermal forces was achieved [145] in the optical domain and then in 2006 using radiation pressure forces [7, 77, 189].

Aformentioned experiments operated in the regime where the optical decay rate of the cavity (κ) was exceeding the mechanical frequency Ω_m. However, an important requirement for many applications is the so-called resolved-sideband regime $\kappa \ll \Omega_m$ (or sometimes - good cavity regime). The first experiment to demonstrate that was performed in a microwave domain with a high-Q cryogenic sapphire transducer, where it served to reduce the effective noise temperature [46]. Then in 2008, it was first

demonstrated in the optical domain [190]. Since then a number of experiments with novel systems have been carried out in this regime [207, 205, 123].

It is a challenge to reach the quantum ground state of micromechanical oscillators at low frequencies. The strategy is to combine cryogenic precooling with dynamical backaction laser cooling. Initial attempts in this direction resulted in a few dozen quanta level of cooling in the optical domain [82, 162, 188]. But later experiments demonstrated first-ever cooling of mechanical mode below one quantum of energy for microwave [204] and optical [179] domains. In [156] authors performed the ground state cooling by the means of a conventional cryogenic refrigerator.

It's also worth mentioning achievements in cooling with other geometries like microtoroidal resonators [215].

Important progress has been made in recent years. In the experiment with highly sideband-resolved silicon optomechanical crystal, the cooling near the ground state with mean thermal phonon occupancy being around 0.09 quanta was demonstrated [172]. Another experiment showed the sideband cooling of the multimode optomechanical system consisting of two nearly degenerate mechanical oscillators coupled to a microwave cavity [155]. There was a progress in a feedback cooling of a room temperature mechanical oscillator to nearly its ground state by combining integrated nanophotonics with phononic band gap engineering [84].

Another milestone to mention is a progress in the cooling of levitated nanoparticles with feedback technique relying on Coulomb force and optimized using a machine learning algorithm [45], in a resolved-sideband cooling in the presence of laser phase noise [146] and using cavities populated solely by coherent scattering [52, 211].

Recently demonstration of cooling via sideband asymmetry [201] emerged.

Quantum state preparation and control

Optomechanical systems are a promising platform for the realization of non-classical states of a mechanical oscillator due to recent experimental advances in optomechanical devices providing low dissipation and high Q factors. Back in 1997, it was shown [23] that the Fabry-Perot-type optomechanical system can be potentially used for the preparation of a plethora of non-classical states for both the cavity field and the mirror itself.

There were a number of studies proposing the preparation of single phonon excitations. For example, in [178] authors proposed a system where the mechanical resonator is coupled to multiple laser-driven resonances of the optical cavity. By lowering the resonance frequency of the oscillator with the help of an inhomogeneous electrostatic field, the level of non-linearity was significantly enhanced leading to the possibility to prepare individual phonon Fock states. In [171] it was shown that in case the optome-

chanical coupling is strong enough (comparable to or larger than the optical decay rate and the mechanical frequency), it is possible to develop a negative Wigner function for the steady state of a mechanical oscillator. Finally, in [22] a multimode optomechanical system stabilizing the mechanical oscillator at the level of first energy excitation was proposed.

Another direction of research is the preparation of squeezed states. In [110] steady-state quantum squeezing of a mechanical resonator beyond 3 dB was proposed. The scheme implied two driving lasers with different amplitudes and used a dissipative mechanism with the driven cavity acting as an engineered reservoir. Experimental demonstration of quantum squeezing of a mechanical resonator followed in 2015 [229] with the microwave driving that resulted in 1 dB level of squeezing. The same year, another experimental demonstration emerged [168] with the level of squeezing about 1.1 dB for a micromechanical resonator. Recently a mechanical squeezing based on a sequence of four pulsed optomechanical interactions with pulse length much shorter than the mechanical period was proposed [17].

In the last few years, there has been a lot of progress in the preparation of entangled states of mechanical oscillators. Entanglement between pulsed radiation and mechanical mode has been demonstrated [161]. In [177] the entanglement between two chip-based micromechanical resonators placed on a solid-state platform and separated by 20 centimeters was achieved. The superposition state of mechanical excitations was created in [220] where authors demonstrated a Duan-Lukin-Cirac-Zoller-type [57] mechanical quantum memory controlled through an optical interface operating at telecom frequencies. The optomechanical Bell test was performed [137] using two silicon optomechanical oscillators violating Bell inequality by more than 4 standard deviations. Another demonstration of the entanglement in the steady state between two massive micromechanical oscillators in the microwave domain was conducted in [154]. We should also mention recent experiments in preparation of optical/microwave entanglement via mechanical element [15, 38, 184]. A number of new theoretical proposals to generate entangled states of radiation field and mechanics [42, 85], of mechanical systems [42, 122, 183] and even whole optomechanical systems [103] emerged in recent years.

Importantly, similar to quantum electrodynamics and quantum optics, the control of the quantum state of a mechanical oscillator requires operation in the strong coupling regime where the energy exchange between the mechanical system and the electromagnetic field is not distorted by dissipation and decoherence. Significant effort is concentrated on achieving this regime in optomechanical systems. In [81] the first demonstration of normal mode splitting was realized. It is important as the normal mode splitting is the characteristic of strongly coupled systems. Teufel and colleagues carried out a series of experiments with the demonstration of strong optomechanical coupling [206]. Another important experiment [215] demonstrated quantum coherent coupling with a

micro-mechanical oscillator. In recent years new platforms emerged which demonstrated a strong and ultra-strong coupling [62, 182] together with a new approach of engineering conventional bulk optomechanical devices [74, 64, 199] resulting in higher Q-factors and enhanced optomechanical coupling.

Among other works it is worth mentioning new proposals to generate nonclassical states in stroboscopic regime [31] which includes squeezing and entangling of mechanical modes, an extensive research in the direction of creation of non-Gaussian states [118, 235, 194, 202, 108] and recent demonstration of subpoissonian phonon distribution [129].

Quantum communication with optomechanics

Optomechanics is considered today as one of the important candidates to create operational quantum networks for quantum information distribution and processing, due to slower speed and lower losses of acoustic waves which allow for the design of efficient elements for delaying, filtering and storing of electric signals [141]. One of the important ways to transfer an arbitrary quantum state between two objects that are possibly distinct in nature and distant from each other is to use quantum teleportation [16]. There were a number of theoretical proposals to realize teleportation protocol in optomechanical systems for the case of continuous variables, including the schemes entangling mechanical mode with radiation field [133, 166, 94] and remote mechanical resonators [65]. However, to date, there is no experimental realization of quantum optomechanical teleportation. Some of the recent theoretical works explore discrete-variable teleportation in the pulsed regime [119] and simulate state-of-the-art gigahertz optomechanical devices [163].

Transferring quantum states from one site to another is a very important task of quantum processing and networking. Quantum teleportation is not the only way to achieve that goal, especially this is not necessary when the systems are not spatially separated. One of the limitations of quantum teleportation is the fragility of the entanglement which is needed to be established between the parties. Instead, the basic coupling between light and the mechanical system could be used. The systems interconnecting optical, mechanical and microwave modes has been proposed in a number of works for continuous-wave [186, 222, 209, 210, 236], pulsed [101, 142, 95, 174] and stroboscopic regimes [95]. Experimental demonstration followed for continuous-wave one [93, 5, 6, 116]. New approaches have been taken to the quantum transducers' experimental realization. A system combining silicon photonics, cavity optomechanics, and superconducting circuits demonstrated efficient transduction between the microwave and the telecom bands at millikelvin temperatures [9]. In another experiment [71] authors used an integrated, on-chip electromechanical setup with the mechanical mode

being in its quantum ground state. Finally, in [92] a mechanically-mediated microwave-to-optical converter has been implemented with 47% of conversion efficiency. This converter operated at millikelvin temperatures and used the feed-forward protocol to reduce added noise. Some more details on the topic of optomechanical transducers can be found in Chapter 5.

Metrological and sensing applications

Finally, we would like to mention other possible practical applications where quantum optomechanics can bring a lot of value.

The researches in the field of detection of gravitational waves launched the exploration of the quantum limits of measurement's precision. The Heisenberg uncertainty principle imposes a limit on precision of simultaneous knowledge about conjugated quadratures, which leads to the base measurement limit known as the *standard quantum limit (SQL)* [25, 76]. The first idea of surpassing this limit belongs to Braginsky [25], where he proposed so-called *quantum non-demolition (QND) measurements* - the method of projectively measuring a quadrature with measurement operator commuting with freely moving mirror's Hamiltonian. This measurement shouldn't affect the mirror's evolution, and the quadrature could be known with arbitrary precision by repeating the measurement an infinite number of times. This approach was also studied by Kip Thorne [208], Vladimir Braginsky [29], William Unruh [212], and Carlton Caves [37]. In recent years the SQL was beat via back-action evading techniques in electromechanics [49] and optomechanics [195, 194], and using a negative-effective-mass oscillator in optical domain [151].

Other applications include quantum-enhanced magnetometry like [117], where authors used a silicon-chip-based cavity optomechanical magnetometer with squeezed light to increase its sensitivity.

It is possible to build optomechanical accelerometers as demonstrated [109] with a setup based on photonic-crystal nanocavity monolithically integrated with nanotethered test mass or with a single chip-based device based on subwavelength grating pair and rotated serpentine springs [126].

Mass sensing is another application of optomechanics as described for instance in [124] with sub-pg mass sensitivity in a large microtoroid optomechanical oscillator.

New and improved optomechanical platforms

Quantum optomechanics is a fast-growing field. In the last years, we witnessed a lot of improvements and advances.

Recent achievements in engineering can be noticed in the experiment with nanopho-

tonic interface with levitated dielectric nanoparticle [132] demonstrating single-photon optomechanical coupling of three orders of magnitude larger than previously reported, or in the demonstration of linear, quadratic and tertiary optomechanical interactions in the resolved-sideband regime together with the demonstration of high quantum cooperativity for levitated nanoparticle [51]. New techniques of coherent scattering for levitated nanoparticles [53, 228, 80, 198] which allowed motional ground-state cooling [52] should be noticed. New advances in electromagnetic fabrication have been demonstrated in [180] where authors created flux-mediated optomechanical coupling with a single-photon coupling strength, reaching state-of-the-art rates, and in [164], where ultrastrong parametric coupling between the superconducting cavity and mechanical mode has been achieved.

It is important to mention new platforms that emerged in the last years. Among them are levitated optomechanics and electromechanics [149, 79, 139] or quantum magnetomechanics [182], which we already mentioned few times in this chapter, or new hybrid devices like the one directly and parametrically manipulating the mechanical nanobeam resonator of a cavity electromechanical system [24], systems with circuit quantum electrodynamics [43], flux-mediated optomechanics [107] or Brillouin-coupling-enabled optomechanics with superfluid helium droplets [62].

CHAPTER 1

Basic concepts of quantum optics

1.1 Quantization of electromagnetic field

As the light is the central essence of the field of quantum optics required to prepare, operate and measure optomechanical systems, we first need to briefly introduce some of the concepts of the mathematical description of the electromagnetic field in both classical and quantum cases. In the next two sections, we will discuss how the quantum representation of light is related to classical concepts, and why it was necessary to introduce quantization and we will present references for further details.

1.2 Classical representation of light

In the classical theory of *electromagnetism* [112, 98], the electromagnetic field is considered as a solution of the famous *Maxwell's* equations [140]. Under the assumption of electromagnetic field propagating in vacuum, these equations take the following form:

$$\nabla \mathbf{E} = 0, \tag{1.1a}$$

$$\nabla \mathbf{B} = 0, \tag{1.1b}$$

$$\nabla \times \mathbf{E} = -\frac{\partial \mathbf{B}}{\partial t}, \tag{1.1c}$$

$$\nabla \times \mathbf{B} = \varepsilon_0 \mu_0 \frac{\partial \mathbf{E}}{\partial t} \tag{1.1d}$$

where $\mathbf{E}$ and $\mathbf{B}$ are three-dimensional vectors being called *electric vector* and *magnetic induction* correspondingly and ε_0 and μ_0 are universal constants – permittivity and permeability of free space respectively.

Another way to describe the electromagnetic field useful after the quantization is with the help of so-called *potential formulation* [98], where the electric vector and magnetic induction are expressed through the *vector-potential* $\mathbf{A}(\mathbf{r}, t)$ as follows:

$$\mathbf{E} = -\frac{\partial \mathbf{A}}{\partial t}, \tag{1.2a}$$

$$\mathbf{B} = \nabla \times \mathbf{A}. \tag{1.2b}$$

Vector-potential $\mathbf{A}$ is defined up to curl-free component, and *Coulomb gauge* is used as a part of the definition:

$$\nabla \mathbf{A} = 0. \tag{1.3}$$

This gauge is used when no sources of electromagnetic field are present and it is particularly useful in quantum electrodynamics. In quantum-mechanical description the quantization of only vector-potential is necessary [98].

Substituting (1.2a) and (1.2b) to (1.1c) and (1.1d), we get the following wave equation:

$$\nabla^2 \mathbf{A}(\mathbf{r}, t) = \frac{1}{c^2} \frac{\partial^2 \mathbf{A}(\mathbf{r}, t)}{\partial t^2}, \tag{1.4}$$

where we introduced the speed of light in vacuum $c = 1/\sqrt{\varepsilon_0 \mu_0}$. Expression (1.4) is called the *wave equation* for vector potential. We now can express the vector potential as a sum of two complex components [219]:

$$\mathbf{A}(\mathbf{r}, t) = \mathbf{A}^{(+)}(\mathbf{r}, t) + \mathbf{A}^{(-)}(\mathbf{r}, t), \tag{1.5}$$

where $\mathbf{A}^{(-)} = [\mathbf{A}^{(+)}]^*$ and $\mathbf{A}^{(+)}$ contains all the amplitudes which vary as $e^{-i\omega t}$ whereas $\mathbf{A}^{(+)}$ contains all the amplitudes which vary as $e^{i\omega t}$. Let us consider field restricted in a volume of space then we can expand the vector potential as a linear combination of orthogonal modes $\mathbf{u}_k(\mathbf{r})$:

$$\mathbf{A}^{(+)} = \sum_k c_k \mathbf{u}_k(\mathbf{r}) e^{-i\omega_k t}, \tag{1.6}$$

which form a complete orthonormal set:

$$\int_V \mathbf{u}_k^*(\mathbf{r}) \mathbf{u}_{k'}(\mathbf{r}) d\mathbf{r} = \delta_{kk'}, \tag{1.7}$$

where k describes elements of wave-vector $\mathbf{k}$ and polarization. This allows considering a discrete set of modes instead of an infinite continuum and simplify the description of their amplitudes c_k. Substituting (1.6) to wave equation (1.4) we get an equation for the mode function $\mathbf{u}_k(\mathbf{r})$:

$$\left(\nabla^2 + \frac{\omega_k^2}{c^2} \right) \mathbf{u}_k(\mathbf{r}) = 0, \tag{1.8}$$

which is called the *Helmholtz* equation. The solution of this equation leads to different possible types of spatial modes $\mathbf{u}_k(\mathbf{r})$, depending on the boundary conditions. The vector potential can be written now based on (1.5):

$$\mathbf{A}(\mathbf{r}, t) = \sum_{k=0}^{\infty} \sqrt{\frac{\hbar}{2\omega_k \varepsilon_0}} \left(a_k \mathbf{u}_k(\mathbf{r}) e^{-i\omega_k t} + a_k^\dagger \mathbf{u}_k^*(\mathbf{r}) e^{i\omega_k t} \right), \tag{1.9}$$

with $k \in \mathbb{N}$, $\hbar$ being the reduced Planck constant and $a_k = \sqrt{\frac{2\omega_k \varepsilon_0}{\hbar}} c_k$.

Substituting (1.9) to (1.2a) we can get an expression for the electric field which reads as follows:

$$\mathbf{E}(\mathbf{r}, t) = i \sum_k \sqrt{\frac{\hbar \omega_k}{2\varepsilon_0}} \left(a_k \mathbf{u}_k(\mathbf{r}) e^{-i\omega_k t} - a_k^\dagger \mathbf{u}_k^*(\mathbf{r}) e^{i\omega_k t} \right), \tag{1.10}$$

with normalization factors guarantying amplitudes $a_k, a_k^\dagger$ being dimensionless. As the electric field is the only measurable on optical frequencies, (1.10) is a key point for the next section.

1.3 Quantum representation of light

In the 19th century the study of black-body radiation [134] and photoelectric effect [91] both demonstrated that classical representation of light is not able to describe all observed phenomena. In 1905 Albert Einstein, in purpose to explain experimental data, proposed [59] that the energy is transferred by discrete portions. This was a key step to the development of quantum mechanics.

To switch from classical theory to quantum one *the canonical quantization* procedure is needed. It was introduced by Paul Dirac in his doctoral thesis [54]. The method is to replace canonical conjugate variables, $\{q_i, p_j\} = \delta_{ij}$, by Hermitian operators satisfying canonical commutation relation $[\hat{q}_i, \hat{p}_j] = i\delta_{ij}$. The Poisson bracket of two functions f and g of a set of variables $(q_1, ..., q_N, p_1, ..., p_N)$ is defined as $\{f, g\} = \sum_{i=1}^N \left(\frac{\delta f}{\delta q_i} \frac{\delta g}{\delta p_i} - \frac{\delta f}{\delta p_i} \frac{\delta g}{\delta q_i} \right)$, whereas the commutator is defined as $[\hat{A}, \hat{B}] = \hat{A}\hat{B} - \hat{B}\hat{A}$ and reflects the importance of the operation's order.

In our case, we choose amplitudes a_k and $a_k^\dagger$ to be replaced by the operators satisfying boson commutation relations [219]:

$$[\hat{a}_i, \hat{a}_j^\dagger] = \delta_{ij}, \quad [\hat{a}_i, \hat{a}_j] = [\hat{a}_i^\dagger, \hat{a}_j^\dagger] = 0 \tag{1.11}$$

These operators are called *creation* ($\hat{a}^\dagger$) and *annihilation* ($\hat{a}$) operators. Based on that, we can now derive the expression for the Hamiltonian of the electromagnetic field in quantum representation. Classical Hamiltonian compatible with Maxwell equations (1.1) in a quantization box is represented in the following way [125]:

$$\hat{H}_{cl} = \frac{1}{2} \int \left(\varepsilon_0 \mathbf{E}^2 + \mu_0 \mathbf{H}^2 \right) d\mathbf{r} \tag{1.12}$$

After substituting expression for $\mathbf{E}$ (1.10) and corresponding expression for $\mathbf{H}$ to (1.12),

we obtain the following:

$$\hat{H}_q = \sum_k \hbar\omega_k \left(\hat{a}_k^\dagger \hat{a}_k + \frac{1}{2} \right). \tag{1.13}$$

The term $\frac{1}{2}\hbar\omega_k$ represents the energy of vacuum fluctuations in mode k. Such quantum fluctuations will play a key role later.

It is important to notice that creation and annihilation operators do not represent any directly measurable observables. But as it may be seen from the way they have been introduced above, they can be linked to the actual optical field observables:

$$\hat{X}_k = \frac{1}{\sqrt{2}} \left(\hat{a}_k + \hat{a}_k^\dagger \right), \tag{1.14a}$$

$$\hat{P}_k = -\frac{i}{\sqrt{2}} \left(\hat{a}_k - \hat{a}_k^\dagger \right), \tag{1.14b}$$

which are called *amplitude* and *phase quadrature operators* (referred later as just *quadratures*). Advantageously, in quantum optics they can be directly measured by homodyne detection [13], in addition to measurement of the photon number $N_k = a_k^\dagger a_k$. These quadratures are the subject of the more general *Heisenberg's uncertainty principle* [89] which states that two canonically conjugated variables are limited in the certainty of the determination of their exact values from initial conditions. This uncertainty is defined by the relation between the variances of (1.14):

$$\langle (\delta\hat{X}_k)^2 \rangle \langle (\delta\hat{P}_k)^2 \rangle \geq \frac{1}{4}, \tag{1.15}$$

where $\delta\hat{O} = \hat{O} - \langle \hat{O} \rangle$ for an arbitrary operator $\hat{O}$.

In the following sections, we stop the usage of "hat-notion" for operators as we already defined all operators we will use.

1.4 Fock states

The eigenvalues of Hamiltonian (1.13) are $\hbar\omega_k(n_k + \frac{1}{2})$ with n_k taking non-negative integer values. The eigenstates $|n_k\rangle$ are called *number* or *Fock states* [219], and they are also the eigenstates of the number operator N_k. The Fock states represent discrete basis states with certain occupancy of the system by quanta of energy (*photon* in case of optical field).

These states obey following orthogonality and completeness conditions:

$$\langle n_k | m_k \rangle = \delta_{mn}, \quad \sum_{n_k=0}^{\infty} |n_k\rangle\langle n_k| = 1. \tag{1.16}$$

The norm of these states is finite and, hence they form a complete set of basis vectors in Hilbert space. Below we consider only a single mode case omitting the lower indices.

Application of annihilation and creation operators to Fock states leads to the following:

$$a|n\rangle = \sqrt{n}|n-1\rangle, \quad a^\dagger|n\rangle = \sqrt{n+1}|n+1\rangle, \tag{1.17}$$

clearly showing where the terms "annihilation" and "creation" came from. The expectation values of annihilation and creation operators and field quadratures are zero in Fock state:

$$\langle a\rangle = \langle n|a|n\rangle = \langle a^\dagger\rangle = 0, \quad \langle X\rangle = \langle P\rangle = 0, \tag{1.18}$$

which is a manifestation of the fact that the phase of the Fock state is not certain. It is worth noticing that the variance of the quadratures is linearly proportional to the occupation number n:

$$\langle(\delta X)^2\rangle = \langle(\delta P)^2\rangle = n + \frac{1}{2}, \tag{1.19}$$

therefore, such states never have a quadrature variance below $1/2$ of vacuum state (see below). On the other hand, photon-number uncertainty is vanishing for all the Fock states.

Another important example of the Fock states is the so-called *vacuum state* $|0\rangle$. This state has the zero-point energy of the system. As it is clearly seen from the eigenvalues of the Hamiltonian (1.13), this energy is equal to $\hbar\omega/2$ and is non-zero as well as the field quadrature variances for this state. This means that there is always some level of minimal noise in any quadrature operator present in the system. Because the variance of this noise is the same as for coherent states introduced in the next section, we refer to it as *the shot noise*.

1.5 Coherent states

Because of the undefined phase and zero quadrature mean Fock states are not convenient to describe optical fields approaching classical light waves, for example, maser radiation or phase-stabilized laser light. It is more convenient to use *coherent states* for this purpose [78]. As one could see from this section these states have a more precisely defined phase and less precisely defined number of photons – see Fig. 1.1, where the coherent state is represented as uncertainty circle (whose area is defined by Heisenberg uncertainty principle) with defined phase ϕ_1. Coherent states can be introduced through Fock states using unitary displacement operator $D(\alpha) = \exp(\alpha a^\dagger - \alpha^* a)$ with α being a complex number. The coherent state $|\alpha\rangle$ is defined from the vacuum state as follows:

$$|\alpha\rangle = D(\alpha)|0\rangle. \tag{1.20}$$

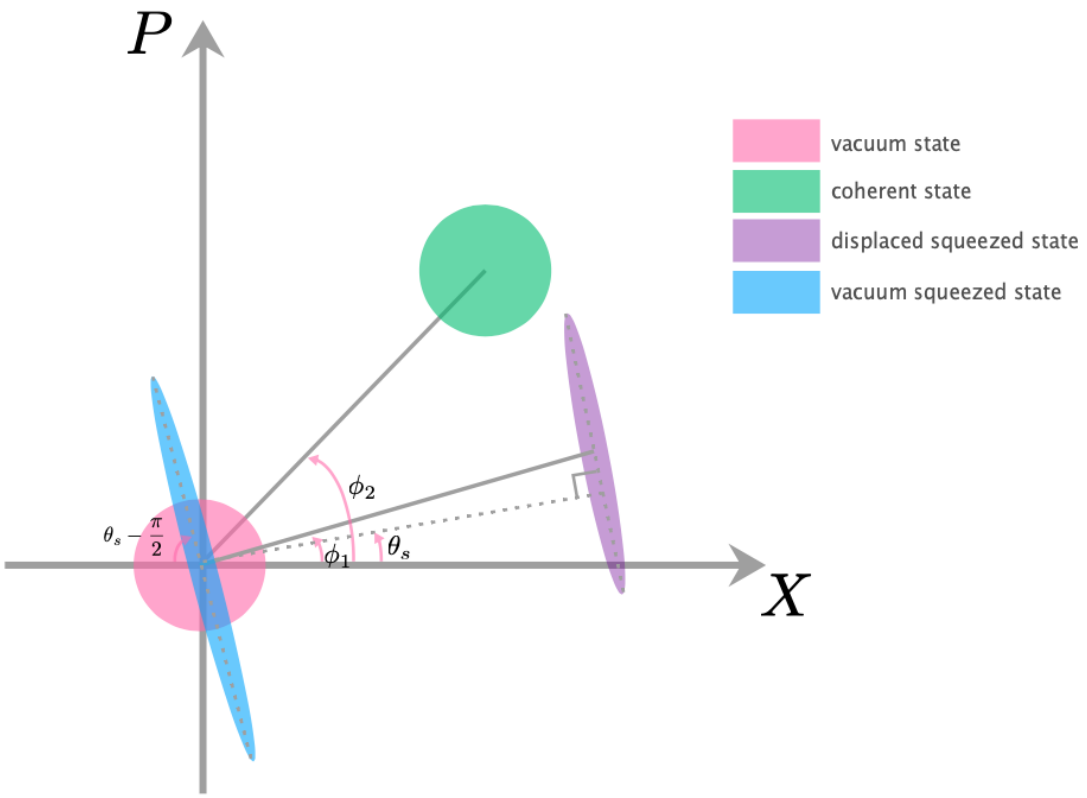

Fig. 1.1 Schematic diagram of the uncertainty areas in the phase space of vacuum, coherent, displaced squeezed and vacuum squeezed states. Vacuum state is a red circle at the origin, which area is defined by the Heisenberg uncertainty principle. A coherent state is represented as a green circle with a minimum uncertainty area displaced from the origin. Displaced squeezed state is represented as purple ellipse being a result of squeezing of vacuum state and displacing it from the origin. Vacuum squeezed state is shown as a blue ellipse at the origin.

From this definition it can be easily derived that coherent state is an eigenstate of annihilation operator:

$$a|\alpha\rangle = \alpha|\alpha\rangle, \tag{1.21}$$

and two additional properties follow as well:

$$\langle\alpha|a^\dagger = \alpha^*\langle\alpha|, \quad \langle\alpha|\alpha\rangle = 1. \tag{1.22}$$

In the classical coherence theory, the complex value α of coherent state is related to the electromagnetic field amplitude.

Another important property of coherent state is that the photon number of a given state is not defined precisely, but rather by probability distribution which is a Poisson distribution:

$$P(n) = |\langle n|\alpha\rangle|^2 = \frac{|\alpha|^{2n}}{n!}e^{-|\alpha|^2}. \tag{1.23}$$

It follows from the Poisson distribution that the mean value and the variance of the

number operator are equal. As the Poissonian distribution corresponds to a stream of statistically independent photons, such light is shot-noise limited.

Coherent states are the states with minimum uncertainty and the variances of the quadratures are equal to those of vacuum state:

$$\langle(\delta X)^2\rangle = \langle(\delta P)^2\rangle = \frac{1}{2}. \tag{1.24}$$

From the properties of coherent states described above it is straightforward to calculate mean values of field quadratures:

$$\langle X\rangle = \sqrt{2}\Re\alpha, \quad \langle P\rangle = \sqrt{2}\Im\alpha. \tag{1.25}$$

It can be seen from these expressions that the phase of coherent state is better defined and, as for classical wave, is proportional to $\arg\alpha$ in contrast to Fock states.

1.6 Squeezed states

Coherent states belong to the more general class of minimum-uncertainty states called *squeezed states* [219]. Quadrature squeezed states are the states with less noise in one quadrature than the shot noise level. To not violate the uncertainty principle, the second quadrature should contain quadrature noise at the level greater than the shot noise. This can be represented in phase-space as a squeezed circle (see Fig.1.1) and expressed as follows:

$$\langle(\delta Q_\phi)^2\rangle \leq \frac{1}{2}, \quad \langle(\delta Q_{\phi+\frac{\pi}{2}})^2\rangle \geq \frac{1}{2}, \tag{1.26}$$

for a more general set of quadratures defined as:

$$Q_\phi = X\cos\phi + P\sin\phi, \quad Q_{\phi+\frac{\pi}{2}} = -X\sin\phi + P\cos\phi. \tag{1.27}$$

As can be seen from these equations, coherent states are the special case of squeezed states with variances being equal to shot noise level.

In general, squeezing of a state $|\psi\rangle$ can be performed by applying the unitary squeeze operator $S(\xi)$ on this state [36]:

$$S(\xi) = e^{\frac{1}{2}(\xi^* a^2 - \xi a^{\dagger 2})}, \tag{1.28}$$

where $\xi = r_s e^{2i\theta_s}$, with r_s being squeeze parameter and θ_s - squeeze angle. Differently to displacement operation (1.20) achievable by linear driving, here we need second-order nonlinearity to squeeze the state.

In case the squeezing operator is applied to the vacuum state the resulting state is

called a vacuum squeezed state. See Fig.1.1 where it is represented as a blue ellipse at the origin.

Another case of the squeezed state is the displaced squeezed coherent state which is obtained after the displacement operator is applied to the squeezed vacuum (see Fig.1.1 where it is represented as a purple ellipse displaced from origin):

$$|\alpha, \xi\rangle = D(\alpha)S(\xi)|0\rangle. \tag{1.29}$$

When $\theta_s = 0$ the state is called amplitude squeezed, whereas for $\theta_s = \pi/2$ – phase squeezed. The conjugate quadrature variances of this state for $\theta_s = 0$ are given by:

$$\langle(\delta X)^2\rangle = \frac{1}{2}e^{-2r_s}, \quad \langle(\delta P)^2\rangle = \frac{1}{2}e^{2r_s}, \tag{1.30}$$

thus satisfying the uncertainty principle $\langle(\delta X)^2\rangle\langle(\delta P)^2\rangle = \frac{1}{4}$.

From reduced variance (1.30) below $1/2$ follows that squeezed states cannot be reached by any mixture of coherent states representing classical waves in quantum optics. Therefore, they belong to the nonclassical states. The same is true for the Fock states, however, their nonclassical aspect is different. Coherent states cannot reach the variance of the photon number below its mean, but amplitude squeezed states can. This variance is however limited if the mean photon number is restricted. This limit can be overcome when we use the Fock states. These two most common representatives of nonclassical states however differ much more in the following representations of the electromagnetic fields.

1.7 Representations of the electromagnetic field

An appropriate description of the electromagnetic field requires a systematic quantum statistical approach, but simultaneously, it has to be computable and ideally, visualize the state in terms of classical waves to compare with classical optics. The electromagnetic field consists of an infinite number of modes, but they can be considered independent, although could be statistically correlated, and we can proceed with single-mode description simplification.

In this section, we introduce several possible statistical representations of the electromagnetic field.

To describe states with only a partial knowledge, we introduce the trace-one positive semidefinite *density operator*:

$$\rho = \sum_i p_i |\psi_i\rangle\langle\psi_i|, \tag{1.31}$$

where p_i is the probability that the system is in the pure state $|\psi_i\rangle$. This operator allows

describing a more general mixed quantum state in that diagonal basis, which is an incoherent statistical mixture of pure states as we know from classical statistics. In the extreme case of a pure state, when our knowledge is maximal, the density operator has the idempotence property $\rho^2 = \rho$ – so-called purity condition.

1.7.1 Glauber–Sudarshan P_{GS} function

The overlapping coherent states form an overcomplete set of states, however still decomposing unity operator, so they can be used as a basis set. The representation of the density operator in the form:

$$\rho = \int P_{GS}(\alpha)|\alpha\rangle\langle\alpha| d^2\alpha \tag{1.32}$$

was firstly introduced by Glauber and Sudarshan [78, 200]. Naively, $P_{GS}(\alpha)$ may be considered as the analog of the probability distribution for the α. However, it should be noticed that $P_{GS}(\alpha)$ can take negative values for some quantum states or singular more than Dirac delta function. For these states no description using classical coherence theory is possible. It complicates both the calculations and also visualization of nonclassical states using $P_{GS}(\alpha)$ function. This can be shown by the example of squeezed states. The variances of quadratures can be expressed in the following form [219]:

$$\langle(\delta X)^2\rangle = \frac{1}{2} + \int \frac{P_{GS}(\alpha)}{2} \left[(\alpha + \alpha^*) - (\langle\alpha\rangle) + \langle\alpha^*\rangle)\right]^2 d^2\alpha, \tag{1.33a}$$

$$\langle(\delta P)^2\rangle = \frac{1}{2} + \int \frac{P_{GS}(\alpha)}{2} \left[\left(\frac{\alpha - \alpha^*}{i}\right) - \left(\frac{\langle\alpha\rangle - \langle\alpha^*\rangle}{i}\right)\right]^2 d^2\alpha \tag{1.33b}$$

It is clearly seen that condition for squeezing ($\langle(\delta X)^2\rangle < \frac{1}{2}$) requires $P_{GS}(\alpha)$ to take negative values. The same holds for second quadrature P if it is squeezed.

States with positive $P_{GS}(\alpha)$ can be considered in classical description with $P_{GS}(\alpha)$ being probability distribution of the stochastic random variable α. They exhibit same effects as described in the classical coherence theory if the standard optical detectors are used.

1.7.2 Wigner function

In 1932 Eugene Wigner introduced [226] a quasiprobability distribution function, while he was studying quantum corrections to quantum mechanics. This function can be expressed as the Fourier transform of the quantum characteristic function $\chi(\eta)$. This quantum characteristic function is directly measurable [88] and can be expressed through the

density operator in the following form:

$$\chi(\eta) = \mathrm{Tr}(\rho D(\eta)) \tag{1.34}$$

and the Wigner function turns to the integral formula as follows:

$$W(\alpha) = \frac{1}{\pi} \int \exp\left(\eta^* \alpha - \eta \alpha^*\right) \chi(\eta) d^2\eta. \tag{1.35}$$

The relation between Wigner function and $P(\alpha)$ distribution can be easly obtained using (1.32) and (1.34):

$$W(\alpha) = \frac{2}{\pi} \int P(\beta) \exp(-2|\beta - \alpha|^2) d^2\beta. \tag{1.36}$$

As we can see the Wigner function is a convolution of P function with a Gaussian kernel. Therefore, Wigner function is less singular and negative than the P_{GS} function and can be more broadly used to compute and visualize nonclassical states.

Often it is useful to express Wigner function in terms of quadratures X and P. We can do this remembering that $a = \frac{1}{\sqrt{2}}(X + iP)$. Assuming that $|x\rangle$ is the eigenstate of X, we can rewrite Wigner function in the following form:

$$W(x,p) = \frac{1}{\pi} \int_{-\infty}^{\infty} \langle x + y|\rho|x - y\rangle e^{-2ipy/\hbar} dy \tag{1.37}$$

Similarly to the P function, this function can be negative in the region of parameters where the system clearly demonstrates non-classical behaviour. However, it is always regular which simplifies the visualization. If the Wigner function is positive, it can be used as hidden variable model to simulate predictions from finite sample of the measured data. On the other hand, if it becomes negative, such the states exhibit quantum non-Gaussianity. These features are not obtainable from any mixture of the all displaced squeezed states and represent new higher level of nonclassical aspects. However, there are criteria how to detect quantum non-Gaussian states for a positive Wigner function as well [111].

It might be of use to mention how Wigner function looks like for some of the quantum states of electromagnetic field.

1. *Coherent state with* $\alpha = \frac{X+iP}{\sqrt{2}}$

$$W_{|\alpha\rangle}(x,p) = \frac{1}{\pi} \exp\left(-[(p-P)^2 + (x-X)^2]\right) \tag{1.38}$$

2. *Squeezed state with $\theta_s = 0$*

$$W_{|\alpha,\xi\rangle}(x,p) = \frac{1}{\pi}\exp\left(-[(x-X)^2 e^{-2r_s} + (p-P)^2 e^{2r_s}]\right) \tag{1.39}$$

3. *Fock n-th state*

$$W_{|n\rangle}(x,p) = \frac{2}{\pi}(-1)^n L_n(4r^2)e^{-2r^2}, \tag{1.40}$$

with $r^2 = x^2 + p^2$, and $L_n(x)$ being the Laguerre polynomial.

Apparently, this Wigner function of nonclassical Fock state becomes negative for $n > 0$, in the contrast to positive Wigner function of any displaced squeezed state. It proves that the Fock states with $n > 0$ are quantum non-Gaussian. Moreover, the criteria [111] proves that such quantum non-Gaussianity of Fock states survives arbitrary optical loss.

1.7.3 Husimi Q representation

Another possible representation is *Q representation* or so-called *Husimi representation*. It was first introduced by Kôdi Husimi in 1940 [97] and can be interpreted as the diagonal matrix elements of the density operator in a pure coherent state:

$$Q(\alpha) = \frac{1}{\pi}\langle\alpha|\rho|\alpha\rangle \tag{1.41}$$

As this convolution smears out P_{GS} function even more, Q function is non-negative and is bounded by value $1/\pi$ from above. Similarly to the Wigner function, it is a Gaussian convolution of the P_{GS} function:

$$Q(\alpha) = \frac{1}{\pi}\int P_{GS}(\beta)e^{-|\alpha-\beta|^2}d^2\beta. \tag{1.42}$$

This function has the advantage of existing for the states, for which the P_{GS} function is not regular and unlike Wigner function it is always positive.

As the Wigner function, it is measurable, even by ordinary double homodyne detection, and can be always used to do finite sample simulations. However, the nonclassical effects are very small here, hardly visible, and deconvolution to obtain the Wigner function or even P_{GS} function is generally not a sufficiently stable procedure. Therefore, the Wigner function is the most suitable phase-space representation for the majority of experiments with nonclassical states in quantum optics.

As mentioned at the beginning of this section, we considered only one-mode states. However, this representation is not always sufficient, and more general multi-mode representation is needed. The rule of thumb is to replace field operator with the individual operators for all the modes, and field state by the product of field states. This rule can give more complicated results for the case the superpositions of product states are considered or for the measurements that involve products of different mode operators. It is

therefore desirable to use another representation if our states can be well approximated by the Gaussian states in the phase space or if we are interested only to covariances of X and P variables.

1.8 Quantum correlations of Gaussian states

Single-mode quantum states can demonstrate properties, which can't be described in terms of classical physics. Another fundamental aspect of quantum behaviour is the possibility of more than one quantum systems to be correlated with each other in the way that no local operations and classical communication could achieve. These correlated states can have much diverse quantum features that we demonstrated on the difference of single mode squeezed and Fock state. We will consider this on the example of bipartite Gaussian states used dominantly in the quantum optomechanics described in this Thesis.

Gaussian states are continous-variable states whose Wigner functions are Gaussian. Some of the states of electromagnetic field described in previous sections are examples of Gaussian states, like coherent or displaced squeezed states. The bipartite Gaussian state of two subsystems A and B, with quadratures forming a vector $f = [X_A, P_A, X_B, P_B]^{\mathrm{T}}$ where upper index T stands for the matrix transposition operation, can be fully characterized by a vector of means $\mu = [\langle X_A\rangle, \langle P_A\rangle, \langle X_B\rangle, \langle P_B\rangle]^{\mathrm{T}}$ and a covariance matrix [...] with elements $V_{ij} = \frac{1}{2}\langle f_i f_j + f_j f_i\rangle - \langle f_i\rangle\langle f_j\rangle$:

$$V = \begin{bmatrix} V_A & C \\ C^{\mathrm{T}} & V_B \end{bmatrix}, \tag{1.43}$$

with V_A, V_B and C being 2×2 matrices. $V_{A,B}$ describe individual variances of the systems A and B, whereas C stands for co-variances between those systems. Covariance matrix allows to introduce the *multimode Heisenberg uncertainty principle*, which states that if $[f_i, f_j] = i\Phi_{ij}$ then

$$V + i\Phi \geq 0 \tag{1.44}$$

holds.

Every Gaussian state can be decomposed into independent *thermal states*, which are the most fundamental Gaussian states [223] without a loss of a purity. These thermal states then represent overall amount of the classical noise globally contained in that state. The thermal state is a mixed state of harmonic oscillator which is characterized by temperature T, mean occupation number $\langle n\rangle = \frac{1}{e^{\hbar\omega/k_B T}-1}$, where k_B is the Boltzmann constant, and mean energy $E = \hbar\omega\left(\langle n\rangle + \frac{1}{2}\right)$. The density operator has the following

form in the number-state representation:

$$\rho = \sum_{i=0}^{\infty} \frac{\langle n \rangle^n}{(\langle n \rangle + 1)^{n+1}} |n\rangle\langle n|. \tag{1.45}$$

The field quadratures of the system in the thermal state have zero mean and the covariance matrix has the following form:

$$V^{\text{th}} = \left(\langle n \rangle + \frac{1}{2} \right) I, \tag{1.46}$$

where I is the 2×2 identity matrix.

In the particular case of linear dynamics of quadratures

$$f \to f' = Tf + \nu, \tag{1.47}$$

the transformations for the vector of means and covariance matrix introduced above can be expressed in a simple form:

$$\mu \to \mu' = T\mu + \langle \nu \rangle, \tag{1.48a}$$

$$V \to V' = TVT^{\text{T}} + V_\nu, \tag{1.48b}$$

where T is the matrix describing the transformations of these quadratures, ν is the vector of additive quadrature noise terms and it is assumed that the noises are not correlated with the system quadratures. Such dynamics are described by a Hamiltonian up to quadratic terms in bosonic operators, and the corresponding operations are called *Gaussian operations*. These operations transform Gaussian states to Gaussian ones.

Under some conditions two or more quantum systems can demonstrate quantum correlations, which are fundamentally different from the ones achievable by local operations and classical communication. It proves that correlated systems indeed interacted quantum mechanically. Quantum correlations exhibiting *entanglement* arise in states that can't be prepared from *separable ones* with the help of local operations and classical communication (LOCC) [96]. Separable states are the states which ca be presented in the following form:

$$\rho_{AB} = \sum_i c_i \rho_i^A \otimes \rho_i^B, \tag{1.49}$$

where $\rho_i^{A,B}$ is the density operators of systems A and B correspondingly and c_i are probabilities. However, it is not the only threshold for nonclassical correlations and different approaches are proposed to quantify non-classicality [90, 158, 159, 83, 127, 100]. From our end we will introduce several metrics ordered by gradually increasing demand on the amount of quantum correlations.

We start with *generalized squeezing* [197]. This quantity specifies the total amount of squeezing that can be extracted from the system by global passive transformations including local phase rotations and beamsplitting operations. It can be expressed as the minimal eigenvalue of the covariance matrix. Nonclassical states and quadratic nonlinearity have to be involved to reach such correlation. As the generalized squeezing upperbounds maximum of single mode squeezing extractable from the state, it is therefore broader phenomena than Gaussian entanglement.

The second measure of quantum correlations is so-called *conditional squeezing*. This squeezing is induced by measurement on one system. After the homodyne detection of the amplitude quadrature of mode B, the covariance matrix of mode A is transformed in the following way [223]:

$$V_A^{'} = V_A - \frac{1}{V_{B,11}} C \Pi C^{\mathrm{T}}, \tag{1.50}$$

where $\Pi = \mathrm{diag}(1, 0)$. We say that there is a conditional squeezing in the system A if the smallest eigenvalue of $V_A^{'}$ (so-called *conditional variance*, in the simplest case it corresponds to the variance of amplitude or phase quadrature of system A) is smaller than the shot-noise variance $1/2$, defined by the Heisenberg's uncertainty principle. The same approach holds for system B. Conditional squeezing presence shows that the generalized squeezing can be induced in the second mode. However, generalized squeezing does not always allow to observe conditional squeezing [68]. Therefore, conditional squeezing is more demanding threshold for nonclassical correlations. All these nonclassical aspects can appear even if the systems never interacted quantum mechanically, they can be provided just by local operations and classical communication.

Next characteristic, which interests us, is *Gaussian quantum entanglement* . The bipartite Gaussian state ρ_{AB} is called entangled if it is not possible to present it in the separable form (1.49) achievable by LOCC methods [56, 196]. One possible measure of quantum entanglement is *logarithmic negativity*. For bipartite Gaussian system it can be defined in the following way:

$$E_{\mathrm{N}} = \max\left(0, -\ln 2\nu_{-}\right), \tag{1.51}$$

with ν_{-} being the smallest symplectic eigenvalue of the covariance matrix of the partially transposed state:

$$\nu_{-} = \frac{1}{\sqrt{2}} \sqrt{\Sigma_V - \sqrt{\Sigma_V^2 - 4 \det V}}, \quad \Sigma_V = \det V_A + \det V_B - 2 \det C. \tag{1.52}$$

The modes A and B are considered entangled if $E_{\mathrm{N}} > 0$. Logarithmic negativity constitutes an upper bound to the distillable entanglement [169].

Last measure which we are introducing selects even smaller subset of entangled states. It is *Gaussian quantum steering*. The system is called $A \rightarrow B$ steerable if after performing measurement on the system A, it is possible to predict measurement outcome on the system B with the accuracy better than for a pure separable minimum uncertainty state such as coherent state. To quantify the the steering of bipartite Gaussian state, we use steerability [105]:

$$G_{A\rightarrow B} = \max\left(0, -\sum_{j:0<\nu_j<1} \ln \nu_j^B\right), \tag{1.53}$$

where $\{\nu_j^B\}$ are orthogonal eigenvalues of the matrix $|i\Omega M^B|$ with $\Omega = \text{antidiag}(1,-1)$ and $M^B = V_B - C^{\mathrm{T}} V_A^{-1} C$. The steerability in opposite direction can be calculated by swapping matrices V_A and V_B and substituting $C \rightarrow C^T$ and vice versa in (1.53). Similarly, as not all generalized squeezing allows conditional squeezing, not all of entangled states allow quantum steering.

CHAPTER 2

Introduction to quantum optomechanics

After introducing relevant quantum optics concepts for the Thesis, we briefly discuss basic concepts of quantum optomechanics. The interested reader can address multiple overviews of the field [147, 40, 11] for more details. We will focus here only on the parts crucial for the understanding of the Thesis.

2.1 Radiation pressure

We explain in this section the basics of the radiation-pressure interaction of electromagnetic radiation with a mechanical object. In essence, it can be reduced to the momentum exchange between them. Let us consider the simplest example of a single photon reflecting from a mechanical oscillator. We are interested in situation when the induced by interaction displacement is larger than zero-point fluctuations of the mechanical oscillator (we assume that this oscillator is in a ground state as in another case its position spread is larger) $x_{zp} = \sqrt{\hbar/2m\Omega}$, otherwise the interaction with photons cannot be resolved in presence of thermal fluctuations. The momentum of the photon with wavelength λ is h/λ, so the momentum transmitted to the mechanical oscillator after an elastic reflection is $2h/\lambda$. It is well known that equations of motion of the simplest harmonic oscillator are the following:

$$\dot{q}(t) = \frac{p(t)}{m}, \quad \dot{p}(t) = -m\Omega^2 q(t) \tag{2.1}$$

where Ω is the frequency of mechanical oscillator. It is seen from these equations that after a quarter period, the momentum kick from photon produces the displacement of $\Delta q = 8\pi x_{zp}^2/\lambda$. Condition to exceed the zero-point fluctuation of mechanical oscillator leads to inequality:

$$\frac{x_{zp}}{\lambda} > \frac{1}{8\pi}. \tag{2.2}$$

This condition is quite hard to satisfy for optical wavelength and typical micromechanical oscillators. For example, based on parameters from [143] and [58] one could estimate that the left side of (2.2) is smaller than the right side by approximately 10^9

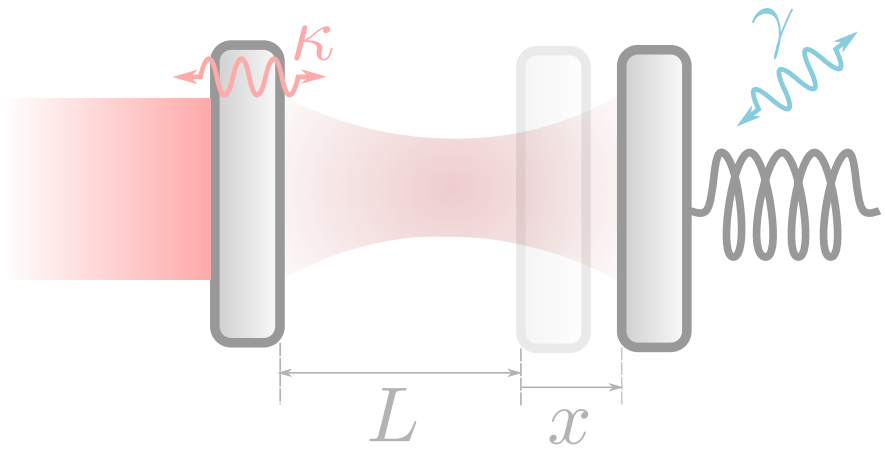

Fig. 2.1 Schematic representation of the optomechanical system: Fabry-Pérot cavity with mechanical oscillator forming the end mirror. Length of the cavity L is varying by the value x of mirror displacement, κ and γ are optical and mechanical decay rates correspondingly.

times. To reach the quantum regime of interaction some amplification methods should be used, like optical or microwave cavity. This increases the number of times the photon interacts with the oscillator, effectively allowing to enter the quantum regime of interaction.

2.2 Optomechanical coupling

A cavity optomechanical system can be presented as consisting of a large immovable mirror and smaller mirror, able to move under the radiation pressure (see Fig. 2.1). Such a Fabry-Pérot cavity configuration allows to model most of the optomechanical systems of different design [11]. In essence, an optomechanical system can be considered as two harmonic oscillators (optical and mechanical ones) coupled via radiation pressure. In this section we derive the optomechanical Hamiltonian and equations of motion of optical and mechanical modes, closely following [12, 11].

When the end mirror displaced, the resonant frequency of the optical cavity changes as well, leading to the dependence $\omega_{opt}(x)$. After expanding this dependence in Taylor series and keeping only linear term, the basic cavity-optomechanical Hamiltonian can be written in the following form:

$$H_0 = \hbar(\omega_{opt}(0) - Gx)a^\dagger a + \hbar\Omega_M b^\dagger b + i\hbar E(a^\dagger e^{-i\omega_l t} - ae^{i\omega_l t}), \tag{2.3}$$

where Ω_M is mechanical frequency, a and b are annihilation operators for optical and mechanical modes correspondingly, $G = \omega_{opt}/L$ is the optomechanical frequency shift per displacement, L is the cavity length and E describes the pump and being related to input power P as $E = \sqrt{\frac{2P}{\hbar\omega_l}}$ where ω_l is the frequency of the driving field. It is clearly

seen that smaller cavities imply larger coupling strengths. A more detailed derivation of this Hamiltonian can be found for instance in [114].

Now we can switch to the frame rotating with the pumping laser frequency. After introducing the detuning $\Delta = \omega_l - \omega_{opt}(0)$, *single photon coupling* $g_0 = Gx_{zp}$ and rewriting $x = x_{zp}(b + b^\dagger)$ we get

$$H = -\hbar\Delta a^\dagger a - \hbar g_0(b + b^\dagger)a^\dagger a + \hbar\Omega_M b^\dagger b + i\hbar E(a^\dagger - a). \tag{2.4}$$

Usually, $g_0 \ll \kappa, \Omega_M$, where κ is the cavity decay frequency. This is the reason why the strong laser pumping is needed in (2.3) - to increase the optomechanical interaction. This allows us to rewrite $a = \alpha + \delta a$, where α is the average light field amplitude and δa represents weak quantum fluctuations of electromagnetic field. Similarly, we expand $b = \beta + \delta b$ with β being the average mechanical amplitude and δb standing for quantum fluctuations of the mechanical mode. After the substitution to (2.4) and keeping only linear in α and β terms, we obtain the following linearized optomechanical Hamiltonian:

$$H = -\hbar\Delta\delta a^\dagger\delta a - \hbar g(\delta b + \delta b^\dagger)(\delta a + \delta a^\dagger) + \hbar\Omega_M\delta b^\dagger\delta b, \tag{2.5}$$

where $g = g_0\alpha$ is the enhanced optomechanical coupling strength. This Hamiltonian is a good approximation to model a large spectrum of optomechanical systems. One can notice that we consider only one optical and one mechanical mode. We can do that with optical modes because the strong laser pump drives the other cavity modes negligibly. For the mechanical mode – optomechanical cooling or amplification in the side-band resolved regime (we will talk about it later) usually affects mostly one mode, selected by the laser frequency.

From the linearized Hamiltonian (2.5) after adding dissipation and noise terms to the Heisenberg equations of motion, one can derive linearized Langevin equations [14]:

$$\delta\dot{a} = (i\Delta - \kappa/2)\delta a + ig(\delta b + \delta b^\dagger) + \sqrt{\kappa}a_{in} \tag{2.6a}$$

$$\delta\dot{b} = -(i\Omega_M + \gamma/2)\delta b + ig(\delta a + \delta a^\dagger) + \sqrt{\gamma}b_{in}, \tag{2.6b}$$

with a_{in}, b_{in} being input noise operators and γ - mechanical damping coefficient. These equations define the dynamics of the optomechanical system.

To describe the interaction of the light pulse with the optomechanical cavity, the Hamiltonian should be complemented with input-output relations for the light reflected from the Fabry-Perot cavity. According to the input-output theory of open quantum systems, this relation looks as follows:

$$\delta a_{out} = \sqrt{\kappa}\delta a - \delta a_{in}, \tag{2.7}$$

where δa_{out} describes the light leaving the optomechanical cavity.

2.2.1 Different types of interaction

In the interaction picture the interaction part of the Hamiltonian (2.5) can be rewritten in the following form:

$$H_{int} = -\hbar g(\delta b e^{-i\Omega_M t} + \delta b^\dagger e^{i\Omega_M t})(\delta a e^{i\Delta t} + \delta a^\dagger e^{-i\Delta t}) \tag{2.8}$$

Depending on the detuning Δ of the drive, three different regimes can be identified in the sideband resolved regime after *rotating-wave approximation (RWA)* applied, meaning that the terms rapidly oscillating at frequencies $\sim 2\Omega_M$ are omitted. For $\Delta = -\Omega_M$ (*red detuning*), there are two harmonic oscillators able to coherently interchange quanta - the mechanical oscillator and the cavity mode. In the RWA the interaction part of the Hamiltonian (2.5) can be rewritten in the following way:

$$H_{bs} = -\hbar g(\delta a^\dagger\, \delta b + \delta a\, \delta b^\dagger). \tag{2.9}$$

This type of interaction is often referred to as *beam-splitter* interaction. This is the case used for cooling of mechanical mode and quantum state transfer (See Introduction *Optomechanical cooling* and *Quantum communication with optomechanics*).

Another type of interaction is the *amplifier type* [11] of interaction when $\Delta = \Omega_M$ (*blue detuning*). In the RWA it can be written in the following way:

$$H_{amp} = -\hbar g(\delta a^\dagger\, \delta b^\dagger + \delta a\, \delta b). \tag{2.10}$$

When there is no dissipation in the system, it would lead to exponential growth of the energies stored in mechanical and optical modes with strong quantum correlation between the two. It can be used to entangle these modes [94, 161].

The third type of interaction is of particular interest in this thesis, and it is called *quantum non-demolition (QND)* type of interaction [29]. In the case when the strong classical pump is in resonance with the cavity $\Delta = 0$, modulated at the frequency of the mechanical oscillator and after adopting RWA, one could arrive to the QND coupling with Hamiltonian:

$$H_{QND} = \hbar g X_{opt} P_M, \quad H_{QND} = \hbar g P_{opt} X_M, \tag{2.11}$$

depending on the phase of the driving field. Here $\{X, P\}_{opt,M}$ are the optical and mechanical field quadratures correspondingly defined in the same way as (1.14a), (1.14b).

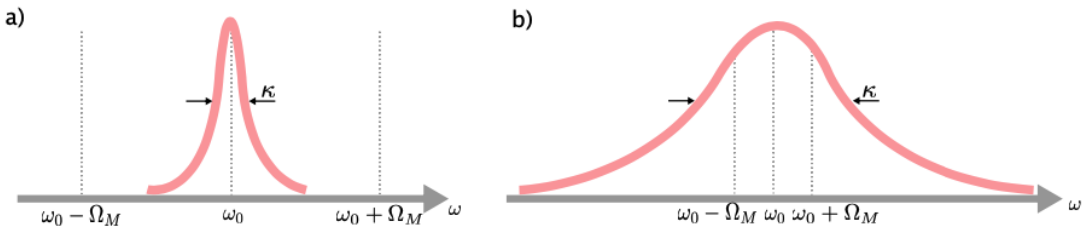

Fig. 2.2 a) Cavity resonance curve in case of the resolved sideband limit. b) Cavity resonance curve in case of the unresolved sideband limit. In both figures, ω_0 stands for the cavity resonance frequency.

2.2.2 Resolved and unresolved sideband limits

Detuning Δ is not the only parameter defining which effects can be observed in the system. There are two regimes that are defined by the relation of mechanical frequency to the optical bandwidth.

The first one is the *good cavity* or *resolved sideband limit* , when $\kappa \ll \Omega_M$ (see Fig. 2.2 (a)). The name of this limit underlines the possibility to distinguish motional sidebands from the cavity resonance. This regime is a necessary requirement to observe such effects as sideband cooling [179] or parametric heating [7] and entanglement [216]. This regime provides us with powerful tools but also has some drawbacks. For example, it is impossible to use low-frequency oscillators or tiny optical cavities (they have larger g_0 and κ). In this regime, relatively large optical powers are required to improve optomechanical coupling as the red and blue sideband are far-detuned from the resonant frequency. Also, sideband-resolved cavities impose the limit on the pulse duration, for instance, pulses with a duration close to the mechanical period will be strongly distorted, as we discuss in [173, 218].

Another limit is *bad cavity* or *unresolved sideband* one. It requires opposite inequality to be satisfied $\kappa \gg \Omega_M$ (see Fig. 2.2 (b)). In this case, mechanical sidebands are also cavity-enhanced and the cavity acts as an optical amplifier. This regime also allows for low-frequency and high-mass resonators, which was a limitation of resolved sideband regime. Bad cavity limit is of big interest among researches and a number of important achievements have been made. It is very useful for a number of applications like quantum-limited position and force sensing [1, 187]. Recently the first experiment on ground-state cooling of a macroscopic oscillator in the unresolved sideband regime was performed [41], not mentioning unrealized proposals of cooling and manipulating mechanical oscillators in the unresolved sideband regime – interference of multiple sub-period pulses [131, 130] which allows suppressing undesirable interactions, leaving only cooling ones, schemes involving variation of the detuning [121], optomechanical coupling [221], mechanical frequency [120, 63, 231] and the input power [63]. Hybrid systems are the other target of different proposals to achieve quantum control

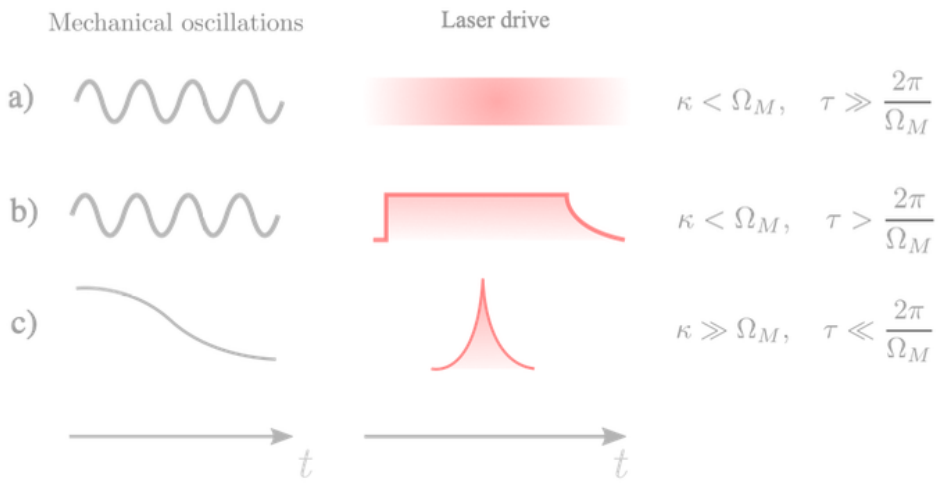

Fig. 2.3 Different temporal regimes representation. a) Continuous regime, when the pulse duration is much longer than the mechanical period b) Long pulses, the interaction happens during many of mechanical periods, but can be switched on and off c) Pulsed regime, when the interaction is much faster than mechanical period.

beyond the resolved sideband limit - superconducting circuits [73], cold atoms, ions, NV-centers [230] and others [181]. Large bandwidth κ opens the way for fast detection of mechanics, which is important for the feedback-based quantum control.

2.2.3 Different temporal interaction regimes

It is possible to determine, among others, three different temporal regimes of interaction (See Fig. 2.3). The first one is the so-called *continuous regime*. In this case, the laser drive duration is much longer comparing with the mechanical period of oscillations ($\tau \gg 2\pi/\Omega_M$) and the system is in resolved sideband regime $\kappa < \Omega_M$ (however, exceptions exists such as the Laser Interferometer Gravitational-Wave Observatory (LIGO)). The interaction happens during many of the mechanical periods. In this case, the steady-state is analyzed.

The second one is *long-pulsed regime* when $\tau > 2\pi/\Omega_M$ and $\kappa < \Omega_M$. In this regime, the interaction again proceeds for many mechanical periods, but comparing with the continuous regime, the light may be switched off, so the state of mechanics can be immediately analyzed after the interaction.

In both mentioned regimes, provided that optical decay rate κ is much smaller than the mechanical frequency Ω_M, one typically detunes driving frequency away from the cavity resonance. Based on the value and sign of the detuning, one gets either beam-splitter or amplifier types of interaction.

There is the third regime of interaction, *pulsed regime*, pioneered by Vanner [214], developed in this thesis and in [31]. In this regime $\tau \ll 2\pi/\Omega_M$ and $\kappa \gg \Omega_M$ so the

interaction is much faster than a mechanical period and the mechanical position may be considered as constant during the interaction. No distinguishable optical sidebands are produced in this regime. Regardless of the detuning, the interaction is always $H \sim X_{opt}X_M$.

CHAPTER 3

High efficiency transfer of non-classical state of light to mechanical system

One of the purposes of this thesis is to propose the physical interconnection of recent methods of quantum optics [72] with quantum optomechanics [147, 40, 11].

The first step we are considering is the key problem of efficient quantum state transfer from an electromagnetic system to a mechanical one. Coherent exchange of quantum states between different systems is a very important line of research in the area of quantum optics, which has a prominent application in quantum memory [128]. This is a non-trivial task, as, negative values of Wigner function (an indicator of quantum non-Gaussianity) are very fragile [34, 33, 238, 50], so the high-efficient interface should be developed.

To design such an interface we were inspired by several theoretical and experimental works. Among them, there is a demonstration of entanglement between pulsed radiation and mechanical system [161], which can be used for quantum state teleportation. As it was mentioned previously, quantum teleportation is not necessary for quantum state transfer when the state is not transferred on a long distance. Instead, the very basic interaction between light and mechanics, caused by radiation pressure, can be used. This coupling provides a basic continuous-variable gate - quantum non-demolition (QND) interaction. Note, that the improvement of transfer through beam-splitter or amplifier type coupling between light and mechanics will require much complex quantum processing [67]. The QND coupling is therefore the most feasible and versatile for such improvements. This interaction was studied in detail in the pulsed regime beyond the sideband resolved limit in a number of works [214, 213, 18]. Nevertheless, pulsed QND interaction in the sideband resolved limit remains attractive for a basic continuous variable gate design. One of the drawbacks of long pulses for a quantum interface is the weak coupling to the mechanics which is not enough for perfect upload. In [66] a very elegant solution was proposed - a combination of presqueezing of the input light and feedforward control can effectively enhance QND coupling between light and mechanics. As it was demonstrated that non-Gaussian states of light can be squeezed [70, 150], it was a very natural step to propose quantum interface incorporating all these achieve-

ments together.

The contribution of this thesis is the proof of the feasibility of quantum interface for efficient non-classical state transfer between light and mechanics, which exploits local Gaussian preprocessing of light to enhance optomechanical coupling. We have clearly shown that the negativity of the Wigner function is preserved. Moreover, we have demonstrated that for interfaces failing to do so, presqueezing helps to preserve Wigner function negativity. Our estimations include a range of experimental parameters that are suitable for further implementation in the laboratory.

This subject attracted an investigation of similar ideas. For example, in [95] a protocol generating entanglement of distinct states of the mechanical oscillator is proposed. This protocol relies on a sequence of three pulsed optomechanical quantum non-demolition interactions in the bad-cavity regime, and the presqueezing of optical mode is used to enhance cooling by measurement of mechanical mode. In [174] authors introduced the protocol for photon-phonon-photon transfer of highly nonclassical quantum state. In another work [113] it is shown that a particular kind of imperfect transducer that uses QND swapping of quantum states can be transformed into a perfect one-way transducer with the help of feed-forward and squeezing.

PHYSICAL REVIEW A **93**, 033813 (2016)

Squeezer-based pulsed optomechanical interface

Andrey A. Rakhubovsky,* Nikita Vostrosablin, and Radim Filip
Department of Optics, Palacký University, 17. Listopadu 12, 771 46 Olomouc, Czech Republic
(Received 24 November 2015; published 9 March 2016)

We prove feasibility of high-fidelity pulsed optomechanical interface based on all-optical presqueezing of non-Gaussian quantum states of light before they enter the optomechanical system. We demonstrate that feasible presqueezing of optical states effectively increases the low noise transfer of them to mechanical oscillator. It allows one to surpass the limit necessary to transfer highly nonclassical states with negative Wigner function. In particular, we verify that with this help single photon states of light can be efficiently turned to single phonon states of mechanical oscillator, keeping the negativity of the Wigner function. It opens the possibility to merge quantum optomechanics with the recent methods of quantum optics.

DOI: 10.1103/PhysRevA.93.033813

I. INTRODUCTION

Recent development of continuous-variable tools of quantum optics [1] and quantum optomechanics [2–4] merges these two disciplines in one unique platform. Advantageously, both these fields can mutually benefit. A necessary step for their complete merger is the high fidelity transfer of nonclassical states of light to mechanical systems. Such quantum interface should be able to transfer a broad class of highly nonclassical states of light, for example, exhibiting negative Wigner function [5–13]. It is known that negative values of Wigner function are very fragile [14–17]; they can quickly disappear under influence of damping and noise, but also vanish in an inefficient interface.

Recently, entanglement between pulsed radiation and mechanical oscillator has been demonstrated [18]. It can be used to teleport quantum state of pulsed light in cavity optomechanical systems [19]. However, teleportation strategy is not necessary for this purpose, since the state is not transferred at a distance. Instead of generating continuous-variable entanglement that is fragile under loss, we can directly use basic coupling between light and mechanical oscillator caused by a pressure of light. Advantageously, this coupling provides a basic continuous variable gate—quantum nondemolition (QND) interaction, when quantum states are strongly displaced before they start to interact with a mechanical system [4].

This nondemolition interaction in optomechanics has been already exploited in the regime of very short and intensive pulses to manipulate mechanical system without the cavity [20–23]. Very recently, the pulsed interface without the cavity based on multiple QND interactions has been proposed [24]. This platform exploits very short intensive pulses of light to reach sufficiently large optomechanical QND coupling existing beyond sideband resolved regime. However, the QND interaction in the sideband resolve regime exhibits generally attractive potential of basic continuous variable gate with the nondemolition variables. From this reason, also the pulsed cavity optomechanics [19] can advantageously use this type of interaction. Moreover, it can be simultaneously merged with cavity quantum optics, capable to produce and operate various non-Gaussian states of light [1].

The strong and coherent displacement of a quantum state, achieved from long pumping pulses, is however not sufficient for its perfect upload as the pulse containing quantum state of light cannot be arbitrarily long. Consequently, the quantum interface is seriously limited by weak and slow coupling of light pulse to mechanical object. Moreover, the interface suffers from residual thermal noise of mechanical oscillator, and additional technical noise and damping in the direct interface. Although this interface does not necessarily break entanglement, it can be very limiting for a transmission of highly nonclassical quantum states of light. In general, quantum entanglement propagating through the interface can be enhanced by quantum distillation. Quantum distillation of entanglement is only probabilistic, moreover, very demanding and practically requires quantum memories to improve the transfer of quantum states. For the continuous variable states, it moreover requires a venture beyond Gaussian operations and hence cannot be well applied here [25–27].

It was already principally recognized that QND coupling between light and matter oscillator can be enhanced by a local presqueezing of quantum states of light before the coupling [28]. Interestingly, the mutual coupling to matter is enhanced purely by a *local Gaussian* operation on light. In a fruitful combination with high-fidelity measurement of light and feedforward control of the oscillator, this allows one to achieve the optimal transfer of any, even non-Gaussian, state of light to matter oscillator. The transfer is suffering only from residual pure damping and all excess noise is in principle eliminated. Moreover, the residual damping can be made arbitrarily small as the presqueezing increases.

The squeezer-based QND interface can universally and deterministically transfer any state of light to mechanical oscillator. It is therefore different from conditional methods of preparation of non-Gaussian quantum states of mechanical systems [29–32]. Furthermore, the proposed interface is capable of transferring of arbitrary states of light, without any prior knowledge about that state, which distinguishes it from recent proposals for preparation of mechanical oscillator in nonclassical states (see [33] and references therein, and [34–36]). The ability to enhance the transfer by presqueezing makes the interface stand out from the ones relying on the beamsplitter-type optomechanical interaction [37,38].

Such the method can be extended to advanced QND scheme, which does not require the sophisticated cooling of the

*andrey.rakhubovskiy@upol.cz

mechanical oscillator [39]. These extensions are advantageous, because the procedures leading to better interface are fully deterministic and require only feasible Gaussian all-optical operations. Squeezing of single photon states and superposition of coherent states, both exhibiting negative Wigner function, have been already experimentally demonstrated [40,41].

In this paper, we investigate the application of this proof-of-principle approach to pulsed quantum optomechanics which is suitable for a merger with current optomechanical methods [19] with already demonstrated online optical squeezer operating on the non-Gaussian states of light [41]. We analyze the method beyond adiabatic elimination of the cavity mode and under the mechanical decoherence. We confirm that proof-of-principle idea can be applied to pulsed optomechanical systems. The squeezing is capable to obtain transmission of non-Gaussian states with negative Wigner function, when commonly used prolongation of coherent pulse is not helpful. We demonstrate this on a feasible example of squeezed single photon state transferred to the mechanical oscillator [42]. This study certifies feasibility of merge of current quantum optics technology [1] and developing quantum optomechanics.

II. QUANTUM NONDEMOLITION OPTOMECHANICAL COUPLING

We consider an interface allowing one to transfer quantum state encoded in an optical pulse to the mechanical oscillator of an optomechanical system. The scheme of the interface is sketched at Fig. 1 and mainly relies on the QND interaction in a cavity optomechanical system between the optical and mechanical modes comprising the system. The interaction is followed by detection on the optical side and consequent displacement of the mechanical mode based on the outcome of the detection.

The QND interaction with a macroscopic mechanical object was first proposed [43,44] to circumvent the standard quantum limit [45] of sensitivity of gravitational-wave detectors. This method was later revisited under the title of back-action evading measurement [46] and has been recently realized experimentally [47,48].

The QND interaction between the two oscillators I and II is described by the Hamiltonian of the form $H_{\rm qnd} \propto g\,Q_{\rm I}Q_{\rm II}$, with Q denoting *quadrature* amplitudes of different oscillators, and g, coupling. In the rotating frame where the quadratures Q are constants of motion the interaction of this type does not disturb them, but instead displaces the conjugate quadratures P by an amount proportional to $g\,Q$. Consequently, prior squeezing of a mode that results in expansion of Q is formally equivalent to an increase of the interaction strength. Using postsqueezing of the mode after the interaction, we can simply recover the QND with the increased interaction strength.

An optomechanical cavity can be thought of as a Fabry-Pérot resonator pumped through a semitransparent stationary mirror with another mirror being movable and perfectly reflective. The system thus comprises two harmonic oscillators (optical and mechanical modes) coupled via the radiation pressure. The Hamiltonian of the system reads [49]

$$H = \hbar\omega_c a^\dagger a + \hbar\omega_m b^\dagger b - \hbar g_0 a^\dagger a(b^\dagger + b),$$

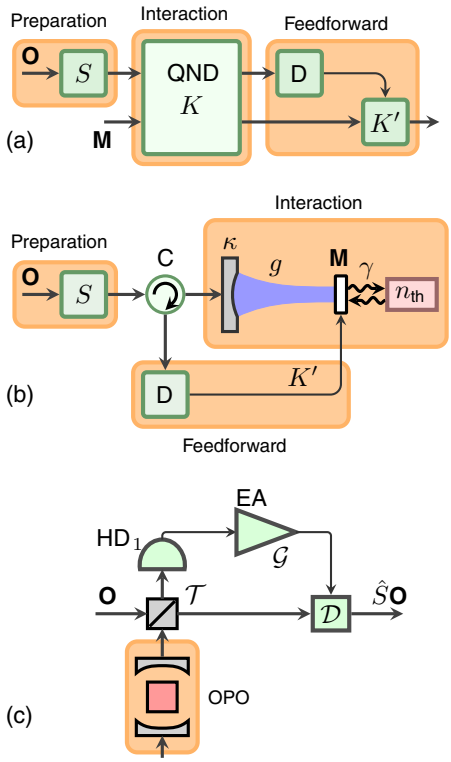

FIG. 1. (a) Simplified scheme of the interface. The optical mode (O) is prepared in the desired state, passes the squeezing operation (S), and is coupled via the QND interaction with the mechanical mode (M). The optical mode is then detected (D) and the outcome of the measurement is used to displace M. (b) A sketch of optomechanical implementation; C—circulator. (c) Principal scheme of squeezing operation (see Sec. III); OPO—optical parametric oscillator.

with a (b) standing for annihilation operator of the optical (mechanical) mode with eigenfrequency ω_c (ω_m). The optomechanical coupling is inherently nonlinear and represents a nondemolition probe of the number of intracavity photons ($a^\dagger a$) by the displacement of the mechanics. This nondemolition nature of the interaction has been proposed for instance for detection of photon number [50] or increasing precision of thermal noise measurement [51].

In experimental realizations typically the single-photon coupling strength g_0 is small and the interaction is thus very weak. In order to observe it usually the system is considered in presence of a strong classical pump. This allows to linearize the dynamics of the system and consider quantum fluctuations near the classical mean values. The Hamiltonian of the system is then written in the rotating frame defined by $H_{\rm rf} = \hbar\omega_c a^\dagger a + \hbar\omega_m b^\dagger b$ as follows:

$$H = \hbar g_0\sqrt{n_{\rm cav}}(a^\dagger e^{-i\psi} + a\,e^{i\psi})(b\,e^{-i\omega_m t} + b^\dagger e^{i\omega_m t}),$$

where we assumed the pump to be resonant with the cavity. The phase ψ is defined by the phase of the pump. The optomechanical coupling is enhanced by the mean optical amplitude proportional to the mean intracavity photon number $n_{\rm cav}$.

Assuming that the optical pump is modulated in such a way that $\sqrt{n_{\rm cav}} \to \sqrt{n_{\rm cav}}\cos(\omega_m t + \phi)$, we apply rotating wave

approximation (RWA) omitting terms rapidly oscillating at frequencies $\sim 2\omega_m$ and obtain the following Hamiltonian:

$$H = \hbar g(X\cos\psi - Y\sin\psi)(q\cos\phi - p\sin\phi), \quad (1)$$

where we defined the enhanced optomechanical coupling $g \equiv g_0\sqrt{n_{\rm cav}}$ and the optical and mechanical quadratures $X = (a^\dagger + a)$, $Y = i(a^\dagger - a)$, $q = (b^\dagger + b)$, and $p = i(b^\dagger - b)$.

A proper choice of phases ϕ and ψ transforms (1) into a particular Hamiltonian corresponding to the QND interaction, for instance putting $\psi = 0$, $\phi = \pi$ yields $H_{\rm I} = -\hbar g X q$.

Finally, to account for coupling to the environment we include viscous damping of the mechanical mode at rate γ, optical damping at rate κ, and noise terms [52] and write the Heisenberg-Langevin equations:

$$\begin{aligned}
\dot q &= -\frac{\gamma}{2}q + \sqrt{\gamma}\xi_q,\\
\dot p &= -\frac{\gamma}{2}p + gX + \sqrt{\gamma}\xi_p,\\
\dot X &= -\kappa X + \sqrt{2\kappa}X^{\rm in},\\
\dot Y &= -\kappa Y + gq + \sqrt{2\kappa}Y^{\rm in}.
\end{aligned} \quad (2)$$

Here $X^{\rm in}, Y^{\rm in}$ are the quadratures of the optical input mode, ξ is the mechanical damping force with quadratures $\xi_{q,p}$, which we assume to be Markovian and satisfy usual commutation relations $[\xi_q(t),\xi_p(t')] = 2i\delta(t - t')$.

Note that to write (1) we applied RWA at the mechanical frequency ω_m which requires the latter to exceed the rates of all the other processes taking place in the system, i.e., $\omega_m \gg \kappa, g, \gamma$. In practice it is sufficient to ensure the so-called *resolved sideband regime*, $\omega_m \gg \kappa$. The experimental platform discussed here is therefore different from the one used in Ref. [24].

The system thus effectively comprises three modes: the input optical mode that encodes the target state, the intracavity optical mode, and the mechanical mode. The former two are coupled at rate κ and the latter two are coupled at rate g. The intracavity mode thus serves as a transducer between the input optical and the mechanical modes. Under certain conditions the intracavity mode can be eliminated. In Sec. IV this elimination is performed to consider the system in a simple approximation. The system is considered without this elimination in Sec. V and the account of the mechanical bath is examined in Sec. VI.

III. PRESQUEEZING OF NON-GAUSSIAN STATES OF LIGHT

During the past decade, quantum optics has progressed in the implementation of squeezing operation on quantum states of light. It was mainly due to development of the measurement-induced operations [40], which do squeeze any quantum state of light without injecting it into the cavity-based degenerate optical parametric amplifier. The basic scheme is depicted in Fig. 1(c). The input state of light is mixed with squeezed vacuum from OPO at the variable beam splitter with transmittivity $\mathcal{T}$ and one output is measured by a high efficiency and low-noise homodyne detection $\rm HD_1$. The electric signal from the detector is amplified in the electronic amplifier EA with the variable gain $\mathcal{G}$. It can be used to directly modulate ($\mathcal{D}$) the undetected output from the beam splitter in suitable optical quadrature. After optimization of $\mathcal{G}$ to eliminate noise of the nonsqueezed variable from OPO, we can reach the transformation

$$X^{\rm in} \to \frac{1}{\sqrt{\mathcal{T}}}X^{\rm in}, \quad Y^{\rm in} \to \sqrt{\mathcal{T}}Y^{\rm in} + \sqrt{1-\mathcal{T}}Y^{\rm sq}$$

of the input operators $X^{\rm in}, Y^{\rm in}$, where $Y^{\rm sq}$ is squeezed variable at the output of the OPO. In the limit of sufficiently large squeezing produced by OPO, the input state can be intensively amplified in the variable $X^{\rm in}$ by the factor $S = 1/\sqrt{\mathcal{T}}$, as has been demonstrated, for example, for the single photon state [41]. The complementary variable $X^{\rm in}$ is squeezed by the factor S^{-1}. Recently, dynamical control of the squeezing operation has been demonstrated [53]. The purity of squeezed light from OPO is not limiting, because noise from antisqueezed quadrature can be eliminated in the feedforward loop. Recently, maximum squeezing from OPO reached -12 dB, which is sufficient to perform high-quality squeezing of non-Gaussian states of light. Moreover, recently fully optically integrated version of measurement-induced squeezer can improve phase stability and provide much higher quality of the squeezing procedure for very nonclassical states [54]. Other improvements can be expected from the recent control of quantum states in optical cavities [55]. The efficient schemes based on an optimal control of injection and extraction of non-Gaussian states in the cavity of OPO could in future substitute the measurement induced squeezers.

The feedforward strategy of all optical presqueezing can be further combined with the feedforward optomechanical interface. Instead to directly modulate light before it enters the optomechanical cavity, we can combine the results from homodyne measurement $\rm HD_1$ with other results of homodyne detection D of light leaving the optomechanical cavity and apply them together to properly displace the mechanical state. The situation simplifies even more for a transfer of given state to mechanical oscillator. In this case, it is sufficient to prepare the squeezed version of this state directly, for example, using recent high-fidelity tunable multiphoton subtraction schemes. The squeezing on the top of non-Gaussian states can be very large, up to already experimentally generated -12 dB [56]. Although this method is conditional and not universal, it can be versatile for high-quality preparation of non-Gaussian quantum state of mechanical system. The simplest testing situation appears if the highly squeezed state is transferred to the mechanical oscillator. The squeezing is then used to prepare a ground state or squeezed state of mechanical system. It can be done differently, using the projection by homodyne measurement D, than recently demonstrated squeezing in electromechanical oscillators [57,58].

IV. ADIABATIC ELIMINATION OF INTRACAVITY MODE

Before we present full analysis, we repeat the basic idea of the squeezer-based interface [28] in the simplest approximation, where the cavity mode is adiabatically eliminated and mechanical bath is not very occupied. It allows us to simply imagine the ideal performance of the squeezer-based optomechanical interface.

Typically in an optomechanical experiment $\kappa \gg \gamma/2$ holds, so if the mechanical bath is not very occupied, one could assume $\gamma = 0$. The condition $\kappa \gg g$ is commonly satisfied as well, which means that the optical mode in the cavity can respond to any changes in the input mode or the mechanical mode instantaneously [this amounts to putting $\dot{X} = \dot{Y} = 0$ in (2)].

Consequently the intracavity mode is removed and in this simple picture the QND interaction between the input optical and mechanical modes results in exchange of one of the quadratures

$$\begin{aligned} q(\tau) &= q(0), \quad p(\tau) = p(0) + K\mathbf{X}^{\rm in}, \\ \mathbf{X}^{\rm out} &= \mathbf{X}^{\rm in}, \quad \mathbf{Y}^{\rm out} = \mathbf{Y}^{\rm in} + Kq(0), \end{aligned} \tag{3}$$

with transfer coefficient

$$K = g\sqrt{2\tau/\kappa}. \tag{4}$$

To write the transformations (3) we defined the quadratures of input and output pulses as integral over the rectangular pulse

$$\mathbf{Q}^{\rm k} = \frac{1}{\sqrt{\tau}} \int_0^\tau ds\, Q^{\rm k}(s), \quad Q = X, Y, \quad {\rm k} = {\rm in,out},$$

so that $[\mathbf{X}^{\rm k}, \mathbf{Y}^{\rm k}] = 2i$, and used input-output relations $Q^{\rm out} = \sqrt{2\kappa}\, Q - Q^{\rm in}$.

To complete the state transfer to the mechanical mode we need to upload $\mathbf{Y}^{\rm in}$ to the mechanical quadrature q. This can be achieved by a feedforward displacing the mechanical mode by amount equal to $-K'\mathbf{Y}^{\rm out}$. The feedforward control of mechanical oscillator in an optomechanical cavity was realized in several setups, for instance, by means of radiation pressure or dielectric gradient force actuation [59–63].

The feedforward can in principle be implemented by a QND interaction with the second pulse via the Hamiltonian $H_{\rm II} = -\hbar g' Y p$. If the duration of the second pulse equals τ', the coupling will be analogous to (3) with transfer coefficient $K' = g'\sqrt{2\tau'/\kappa}$. After this procedure the two quadratures of the input optical mode are written to the quadratures of the mechanical mode

$$\begin{aligned} q' &= q(0)(1 - KK') - K'\mathbf{Y}^{\rm in}, \\ p' &= p(0) + K\mathbf{X}^{\rm in}. \end{aligned}$$

The quadratures of the optical pulse are transferred to the mechanical mode in two steps, one quadrature at time. Therefore, squeezing of the pulse that amplifies one of the quadratures at cost of reduction of the other one can help to transfer the amplified quadrature. Indeed, squeezing of the pulse amounts to substitution $\mathbf{X}^{\rm in} \to S\mathbf{X}^{\rm in}$; $\mathbf{Y}^{\rm in} \to S^{-1}\mathbf{Y}^{\rm in}$ in (3) and this is equivalent to replacement $K \to SK$.

The other quadrature transfer can be enhanced by increasing the feedforward gain. Or, if we think of the feedforward as of another QND interaction with limited strength, by appropriate amplification of the optical mode. Note that the squeezing of the first pulse weakens the quadrature $\mathbf{Y}^{\rm in}$ that should be transfered in the second step, so the amplification should account for it, which means, the gain of the feedforward should be replaced as $K' \to K'S$. However, since the other quadrature $\mathbf{X}^{\rm out}$ is no longer of our interest, the amplification needs not to be noiseless as long as the noises are concentrated in this other quadrature.

After the feedforward the mechanical mode contains the squeezed target state:

$$\begin{aligned} q_f &= \sqrt{\frac{K'}{KS}}[q(0)\sqrt{1-T} - \sqrt{T}\mathbf{Y}^{\rm in}], \\ p_f &= \sqrt{\frac{KS}{K'}}[p(0)\sqrt{1-T} + \sqrt{T}\mathbf{X}^{\rm in}], \end{aligned} \tag{5}$$

with transmittivity

$$T = \frac{(KS)^2}{1 + (KS)^2},$$

provided that $K' = \frac{KS}{1+(KS)^2}$.

The transfer coefficient thus depends only on the product KS and increasing this product allows to approach an ideal transfer with $T = 1$. From the definition (4) of K it follows that for a given κ the same increase in the product KS can be provided by means of equal increase of either S, g, or $\sqrt{\tau}$. Increasing coupling strength or duration of the pulse can impose difficulties in experimental optomechanical realization. At the same time stronger presqueezing of the optical pulse helps to improve the transfer by cost of additional resource of external quantum optical tools.

The equations (5) can be recast in terms of target state and added noise (we *formally* consider squeezing of the mechanical state to symmetrize the expressions)

$$q_f = -\sqrt{T}\mathbf{Y}^{\rm in} + \sqrt{1-T}X_N, \quad p_f = \sqrt{T}\mathbf{X}^{\rm in} + \sqrt{1-T}Y_N. \tag{6}$$

The transformation is effectively combining the target state with quadratures $\mathbf{X}^{\rm in}, \mathbf{Y}^{\rm in}$ and a noisy mode with quadratures X_N, Y_N on a beam splitter with the transmittivity T.

The variance of the added noise is defined as the product of the variances of quadratures of the noisy mode

$$V_N \equiv \sqrt{V_{X_N} V_{Y_N}} \tag{7}$$

and is limited (see [64]) from below by the shot noise level: $V_N \geqslant 1$. Protocol that saturates the inequality is said to realize the *excess-noise-free* upload [28]. This excess-noise-free is very advantageous for transmission of nonclassical features of non-Gaussian states, like transfer of single photon states to single phonon state. It is due to much higher robustness of quantum non-Gaussianity to loss than to the phase-insensitive noise.

The transfer defined by (5) represents mixture of the target state with the initial state of the mechanical mode and is excess-noise-free, provided the mechanical mode is initially in the ground state.

V. BEYOND ADIABATIC APPROXIMATION OF OPTOMECHANICAL COUPLING

In the previous section we demonstrated the principal possibility of an excess-noise-free transfer of a quantum state of light to mechanics that can be enhanced by optical presqueezing. The necessary condition of the transfer was the instantaneous reaction of the cavity mode to any changes. In this section we perform analysis showing that the cavity memory effects caused by the finite cavity reaction time do not

limit the interface performance. We first analyze the system assuming no mechanical decoherence ($\gamma = 0$) and then carry out the full analysis in Sec. VI.

After interacting with a presqueezed pulse, the mechanical system has quadratures

$$q(\tau) = q(0),$$
$$p(\tau) = p(0) + KS\mathbf{X}^{\rm in} + \frac{g}{\kappa}(1-e^{-\kappa\tau})X(0) - \frac{gS}{\kappa}\sqrt{1-e^{-2\kappa\tau}}\mathbf{X}^{\rm in}_{\delta}.$$

Due to the cavity memory effect, the simple transformations (3) become disturbed by the quadrature of the intracavity mode $X(0)$ and an auxiliary asymmetric mode of input field $\mathbf{X}^{\rm in}_{\delta}$, defined as

$$\mathbf{Q}^{\rm in}_{\delta} = \sqrt{\frac{2\kappa}{1-e^{-2\kappa\tau}}}\int_0^{\tau} ds\, e^{-\kappa(\tau-s)}Q^{\rm in}(s), \quad Q = X,Y, \quad (8)$$

in order to satisfy commutations $[\mathbf{X}^{\rm in}_{\delta},\mathbf{Y}^{\rm in}_{\delta}] = 2i$.

By definition the asymmetric mode is composed primarily of the values of $Q^{\rm in}(t)$ adjacent to the end of the interval of integration, which is a manifestation of memory. In the limit where the cavity mode could be eliminated, $\kappa \to +\infty$ the integration kernel approaches Dirac delta $[e^{-\kappa(\tau-s)} \sim \delta(\tau - s)]$, so $\mathbf{X}^{\rm in}_{\delta} \sim X^{\rm in}(\tau)$ up to normalization. Finally, the prefactor makes contribution of this term negligible.

The input-output transformation for the optical quadrature $\mathbf{Y}^{\rm out}$ that is of our interest reads

$$\mathbf{Y}^{\rm out} = q(0)K\left(1-\frac{1-e^{-\kappa\tau}}{\kappa\tau}\right) + S^{-1}\mathbf{Y}^{\rm in} + Y(0)\sqrt{\frac{2}{\kappa\tau}(1-e^{-\kappa\tau})} - S^{-1}\sqrt{\frac{2}{\kappa\tau}(1-e^{-2\kappa\tau})}\mathbf{Y}^{\rm in}_{\delta}.$$

We would like to note that the cavity memory effect manifests itself differently in the optical output and the mechanical modes, which makes introduction of the asymmetric mode in the form (8) necessary.

After the displacement $q(\tau) \to q(\tau) - K'S\mathbf{Y}^{\rm out}$ and *formal* postsqueezing with amplitude $\sqrt{KS/K'}$, the mechanical mode has quadratures

$$q_f = -\sqrt{T}\mathbf{Y}^{\rm in} + \sqrt{1-T}\left[q(0)\left(1+\frac{2g^2S^2}{\kappa^2}(1-e^{-\kappa\tau})\right) - Y(0)\frac{2gS^2}{\kappa}(1-e^{-\kappa\tau}) + \mathbf{Y}^{\rm in}_{\delta}\frac{2gS}{\kappa}\sqrt{1-e^{-2\kappa\tau}}\right],$$
$$p_f = \sqrt{T}\mathbf{X}^{\rm in} + \sqrt{1-T}\left[p(0) + X(0)\frac{g}{\kappa}(1-e^{-\kappa\tau}) - \mathbf{X}^{\rm in}_{\delta}\frac{gS}{\kappa}\sqrt{1-e^{-2\kappa\tau}}\right]. \quad (9)$$

The presqueezing of the incoming pulse is thus not completely equivalent to increasing coupling strength due to the fact that the squeezing changes the ratio in $\mathbf{Y}^{\rm out}$ of the uploaded and intracavity modes in favor of the latter.

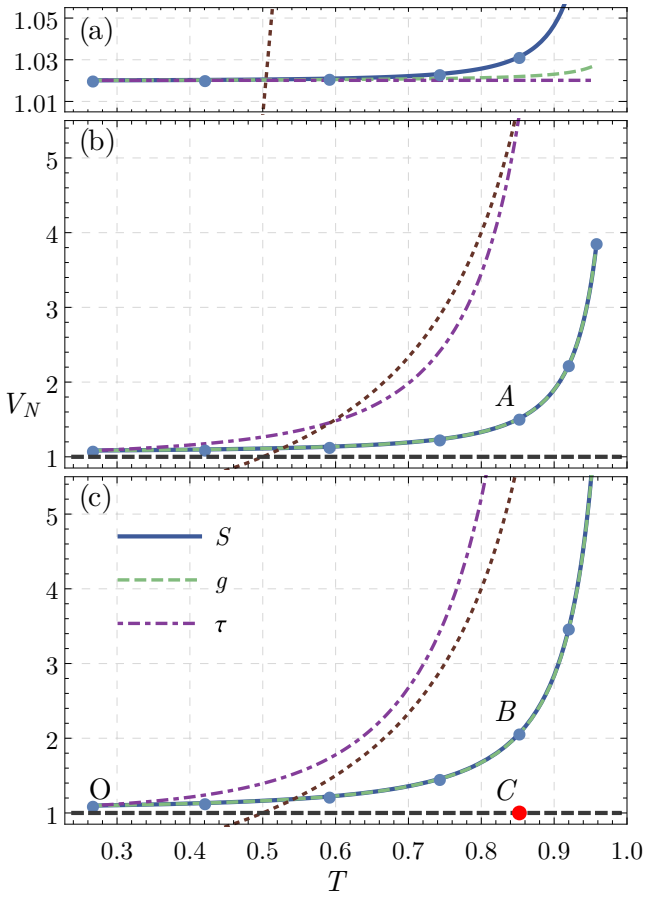

FIG. 2. Added noise variance V_N (6),(7) in shot noise units as a function of the transfer coefficient T in case of increase of squeezing S, coupling g, or pulse duration τ. (a) Solution without the mechanical bath (Sec. IV); (b) solution accounting for the mechanical bath but with adiabatically eliminated cavity mode; (c) full solution (Sec. VI). The point (O) corresponds to the initial set of parameters (10) with no presqueezing ($S = 1$). Markers denote points corresponding to sequential increase of squeezing with the step 3 dB. Dashed line marks the perfect excess-noise-free transfer $V_N = 1$. Dotted curve indicates the maximum V_N allowing transfer of the negativity of the Wigner function of a single-photon state for a given transmittivity T [$V_N^2 < T/(1-T)$].

The added noises in this scheme are provided by the initial occupation of the optical and mechanical modes of the optomechanical cavity, and the asymmetric mode caused by the finite cavity decay κ. Assuming all the noise modes in ground state, the added noise variance V_N can be approximated by

$$V_N \approx \sqrt{1+4g^2S^4/\kappa^2}.$$

Therefore, for high quality low-noise transfer we need to secure $gS^2/\kappa \ll 1$ that keeps the added noise close to the vacuum level and $gS\sqrt{\tau/\kappa} \gg 1$ for high transmittivity. Both inequalities are satisfied by making pulses longer: $\tau \gg 1/g$. This is illustrated at Fig. 2(a), where we plot the added noise variance as a function of the transmittivity of the interface for the cases of increasing squeezing, coupling, or pulse

duration. It is evident from the figure and from (9) that increasing τ allows one to increase transfer while adding little excess noise. At the same time increasing coupling or squeezing adds more noise than increasing τ. It is due to the intracavity mode which disturbs ideal dynamics observed in the adiabatic approximation. The larger τ is, however, prolonging the interaction which requires better phase stability of the transfer and, mainly, smaller decoherence potentially caused by mechanical environment of the oscillator. To make a proper conclusion on the choice of the best strategy, therefore, we need to take into account the mechanical bath.

VI. TRANSFER UNDER MECHANICAL DECOHERENCE

In this section we consider an imperfect QND interaction of a pulse with the system during which the mechanical mode is affected by its bath. Simultaneously, we keep the analysis beyond the adiabatic approximation. We still consider that highly efficient homodyne measurement is followed by a perfect instantaneous electromechanical feedforward. We first present an approximate analysis to get order-of-magnitude estimates, then sketch the steps to obtain full analytical solution, and provide its results.

In the case of small mechanical damping $\gamma \ll g,\kappa$ the simplest estimates can be easily obtained from Eqs. (9) by the substitution

$$Q(0) \to Q(0) + \sqrt{1-e^{-\gamma\tau}}\,Q_B, \quad Q = q,p,$$

where Q_B represents effective quadratures of the mechanical bath with variance $2n_{\rm th}+1$, with $n_{\rm th}$ being the average bath occupation. The corresponding contribution of the thermal noise to the variances of each of the added noise terms X_N, Y_N is $\gamma^2\tau^2(2n_{\rm th}+1)/(1-T)$.

In the region of parameters where the thermal noise from the bath dominates making other noises negligible, the added noise variance can be approximated by $V_N = 1 + 2\gamma(g\tau S)^2(2n_{\rm th}+1)/\kappa$. Despite the fact that g, τ, and S enter this expression equally, we note that $T \propto gS\sqrt{\tau}$, and hence increase in pulse length that produces the same increase in transmittivity, adds much more thermal noise then stronger coupling or squeezing.

We therefore can write several asymptotic requirements for high-transmittivity low-noise state transfer. First, to achieve high transfer gain, we need $g^2S^2\tau/\kappa \equiv \epsilon \gg 1$. Second, in order to make cavity mode induced effects negligible, $g^2S^4/\kappa^2 = S^2\epsilon/(\kappa\tau) \ll 1$. Finally, to keep the thermal noise influence moderate, $\gamma(g\tau S)^2 n_{\rm th}/\kappa = \gamma\tau n_{\rm th}\epsilon \ll 1$. The two latter combine to set the proper range for the available values of τ:

$$\frac{S^2\epsilon}{\kappa} \ll \tau \ll \frac{1}{\epsilon\gamma n_{\rm th}}.$$

Along with the simplest estimates one can perform a full analysis of the system dynamics to properly quantify the impact of different sources of the noise.

The system of dynamical equations (2) is linear and therefore has [65] a formal analytical solution that involves exponential of the matrix of its coefficients. The solution is rather complicated, and so we will present here only the expression for $p(\tau)$

$$p(\tau) = p(0)e^{-\gamma\tau/2} + \int_0^\tau ds\, e^{\gamma(s-\tau)/2}\sqrt{\gamma}\xi_p(s) + \theta(\tau)X(0) + KS\mathbf{X}^{\rm in} - \int_0^\tau ds\left[\frac{K}{\sqrt{\tau}} - \sqrt{2\kappa}\theta(\tau-s)\right]SX^{\rm in}(s),$$

$$\theta(t) \equiv \frac{g}{\kappa - \frac{\gamma}{2}}(e^{-\gamma t/2} - e^{-\kappa t}).$$

The last summand in the expression for $p(\tau)$ represents the asymmetric mode modified by mechanical decoherence. In the limit $\gamma \to 0$ this summand is reduced to $\mathbf{X}^{\rm in}_\delta$.

Using the formal solution one can write expressions for $q(\tau)$ and $\mathbf{Y}^{\rm out}$ and proceed further to obtain the beamsplitterlike transformations in the form (6). With this transformation one can analyze the added noise variance V_N (7).

Our result of estimation for the added noise variance is presented in Fig. 2(c). For estimations we used the following initial set of parameters:

$$\kappa = 221.5\ \text{MHz}, \quad g = 1\ \text{MHz}, \quad \gamma = 328\ \text{Hz}, \quad \tau = 4\times10^{-5}\ \text{s} \tag{10}$$

of a recent reported experiment with optomechanical crystal [42]. The mechanical system is very well precooled in this experiment; however, there is intensive heating of the mechanical mode by optical pump already at the level of circulating power equivalent to a few photons. We model this by setting initial mechanical occupation to $n_0 = 0.01$ and mechanical bath occupation to $n_{\rm th} = 2$.

Starting from the set (10) that is represented by the point O in the figure, we continuously increased one of the parameters S, g, or τ. Comparing Fig. 2(c) with Fig. 2(a) allows one to conclude that for the parameters we chose the main source of added noise is indeed the thermal mechanical environment. In this case, optical presqueezing is effectively equivalent to increasing the interaction strength as it follows from the simple estimate. This is as well seen from Fig. 2(c), where the curves corresponding to increase in S and g overlap.

The effect of the intracavity optical mode has two contributions. First, this mode itself produces some excess noise and, second, it serves as a memory that enhances the impact of the thermal noise. To illustrate this we analyze the transfer under the mechanical decoherence but adiabatically eliminating the cavity mode. The result of this analysis is presented at Fig. 2(b). Although the mechanical bath is the main source of noise in both Figs. 2(b) and 2(c), it is clearly seen that elimination of the cavity mode leads to underestimation of the noise impact.

The dotted lines in Fig. 2 denote the maximum variance of added noise for a given transmittivity that allows one to transfer negativity of a single-photon state. Our analysis shows that the interface we consider is capable of such a transfer. It is due to positive effect of the presqueezing, which allows one to shorten the interaction time. From this reason, the squeezer-based pulsed optomechanical interfaces in the cavities is a feasible road to achieve high-fidelity transfer of the non-Gaussian quantum states of light to mechanical oscillators. Indeed, the Wigner function of an uploaded state manifests negativity at the origin. The simplest example is transfer of a highly nonclassical single photon state to a single

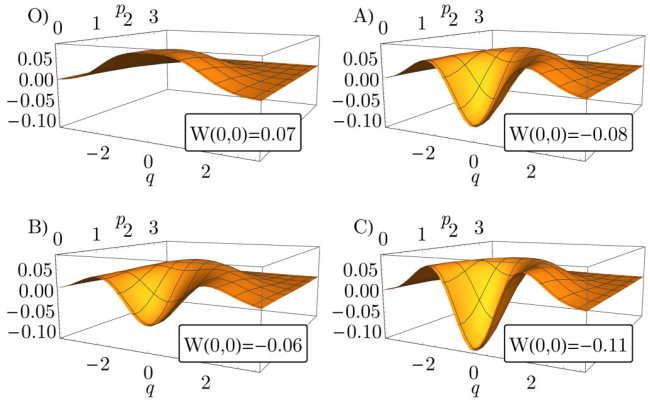

FIG. 3. Wigner function of a Fock state $|1\rangle$ transmitted to the mechanical system using the proposed protocol working in the regimes, denoted by corresponding named points at Fig. 2. O, without the presqueezing; A with 12 dB of presqueezing with intracavity mode formally eliminated; B with 12 dB of presqueezing, full solution; C, same transmittivity as in A and B, but no excess noise ($V_N = 1$). The negativity at the origin is presented at the framed insets.

phonon state. This is demonstrated in Fig. 3, where we compare the Wigner functions of a single photon state, transferred with help of the proposed protocol in regimes, denoted in Fig. 2 by the points O, A, B with the state uploaded via the excess-noise free protocol ($V_N = 1$, point C). We clearly observe a detectable preservation of negativity of the Wigner function of a single phonon state. It witnesses high-fidelity quantum transfer preserving effects which cannot be explained by stochastic mechanics. Based on this example, we can conclude that squeezed-based pulsed optomechanical interface is a feasible road to single photon-phonon transfer. Moreover, it can be used more generally to transfer other non-Gaussian states of light to mechanical systems.

We did not consider mechanical decoherence during the feedforward control of the mechanical system. This simplification is not very coarse, even if we consider a second QND interaction in place of the feedforward. In our protocol interaction gains K and K' relate to each other as $K' \propto K^{-1}$. Therefore, with increase $K \gg 1$ which is a natural condition to achieve T close to 1, the gain of the second interaction K' and consequently its duration τ' decrease. The second interaction therefore effectively approaches an instantaneous feedforward that does not suffer much from the thermal noise.

VII. CONCLUSION

We have verified feasibility and performance of the squeezer-based high-fidelity optomechanical interface for deterministic transfer of non-Gaussian highly nonclassical quantum states of light to mechanical oscillators. We observed clearly that interfaces which cannot transfer negativity of Wigner function can be improved by this method to be able to preserve it. We demonstrated importance of verification beyond the adiabatic elimination. We proved that squeezer-based interface is especially useful when the transfer is influenced by mechanical decoherence, which limits time duration of transfer. We predicted achievable quality of the interface for the experiment [42]. This interface merges developing pulsed cavity optomechanics [4] with recent state-of-the-art of continuous-variable quantum optics [1]. It opens therefore a new joint direction of cavity-based quantum optomechanics and cavity-based quantum optics. In this joint direction, the fields can be mutually fruitful and produce a united physical platform for new continuous-variable experiments with nonclassical light and mechanical oscillators.

Note added in proof. Recently, we became aware of two new relevant papers: Hof *et al.*, arXiv:1601.01663 [quant-ph] and Milburn *et al.*, arXiv:1602.01835 [quant-ph].

ACKNOWLEDGMENTS

We acknowledge Project No. GB14-36681G of the Czech Science Foundation. The research leading to these results has also received funding from the EU FP7 under Grant Agreement No. 308803 (Project BRISQ2), cofinanced by MŠMT ČR (Grant No. 7E13032). A.A.R. acknowledges support by the Development Project of Faculty of Science, Palacky University. N.V. acknowledges the support of Palacky University (IGA-PrF-2015-005).

[1] A. Furusawa and P. van Loock, *Quantum Teleportation and Entanglement* (John Wiley & Sons, New York, 2011).
[2] P. Meystre, A short walk through quantum optomechanics, Ann. Phys. (Leipzig) **525**, 215 (2013).
[3] Y. Chen, Macroscopic quantum mechanics: Theory and experimental concepts of optomechanics, J. Phys. B **46**, 104001 (2013).
[4] M. Aspelmeyer, T. J. Kippenberg, and F. Marquardt, Cavity optomechanics, Rev. Mod. Phys. **86**, 1391 (2014).
[5] A. I. Lvovsky, H. Hansen, T. Aichele, O. Benson, J. Mlynek, and S. Schiller, Quantum State Reconstruction of the Single-Photon Fock State, Phys. Rev. Lett. **87**, 050402 (2001).
[6] A. Ourjoumtsev, R. Tualle-Brouri, and P. Grangier, Quantum Homodyne Tomography of a Two-Photon Fock State, Phys. Rev. Lett. **96**, 213601 (2006).
[7] A. Ourjoumtsev, R. Tualle-Brouri, J. Laurat, and P. Grangier, Generating optical schrödinger kittens for quantum information processing, Science **312**, 83 (2006).
[8] J. S. Neergaard-Nielsen, B. M. Nielsen, C. Hettich, K. Molmer, and E. S. Polzik, Generation of a Superposition of Odd Photon Number States for Quantum Information Networks, Phys. Rev. Lett. **97**, 083604 (2006).
[9] J. S. Neergaard-Nielsen, B. M. Nielsen, H. Takahashi, A. I. Vistnes, and E. S. Polzik, High purity bright single photon source, Opt. Express **15**, 7940 (2007).
[10] A. Ourjoumtsev, H. Jeong, R. Tualle-Brouri, and P. Grangier, Generation of optical 'Schrödinger cats' from photon number states, Nature (London) **448**, 784 (2007).
[11] E. Bimbard, N. Jain, A. MacRae, and A. I. Lvovsky, Quantum-optical state engineering up to the two-photon level, Nat. Photon. **4**, 243 (2010).

[12] M. Yukawa, K. Miyata, T. Mizuta, H. Yonezawa, P. Marek, R. Filip, and A. Furusawa, Generating superposition of up-to three photons for continuous variable quantum information processing, Opt. Express **21**, 5529 (2013).
[13] M. Yukawa, K. Miyata, H. Yonezawa, P. Marek, R. Filip, and A. Furusawa, Emulating quantum cubic nonlinearity, Phys. Rev. A **88**, 053816 (2013).
[14] A. O. Caldeira and A. J. Leggett, Influence of damping on quantum interference: An exactly soluble model, Phys. Rev. A **31**, 1059 (1985).
[15] V. Bužek and P. L. Knight, Quantum Interference, Superposition States of Light, and Nonclassical Effects, in *Progress in Optics*, Vol. 34, edited by E. Wolf (Elsevier, Amsterdam, 1995), pp. 1–158.
[16] W. H. Zurek, Decoherence, einselection, and the quantum origins of the classical, Rev. Mod. Phys. **75**, 715 (2003).
[17] S. Deléglise, I. Dotsenko, C. Sayrin, J. Bernu, M. Brune, J.-M. Raimond, and S. Haroche, Reconstruction of non-classical cavity field states with snapshots of their decoherence, Nature (London) **455**, 510 (2008).
[18] T. A. Palomaki, J. D. Teufel, R. W. Simmonds, and K. W. Lehnert, Entangling mechanical motion with microwave fields, Science **342**, 710 (2013).
[19] S. G. Hofer, W. Wieczorek, M. Aspelmeyer, and K. Hammerer, Quantum entanglement and teleportation in pulsed cavity optomechanics, Phys. Rev. A **84**, 052327 (2011).
[20] M. R. Vanner, I. Pikovski, G. D. Cole, M. S. Kim, Č Brukner, K. Hammerer, G. J. Milburn, and M. Aspelmeyer, Pulsed quantum optomechanics, Proc. Natl. Acad. Sci. (USA) **108**, 16182 (2011).
[21] S. Machnes, J. Cerrillo, M. Aspelmeyer, W. Wieczorek, M. B. Plenio, and A. Retzker, Pulsed Laser Cooling for Cavity Optomechanical Resonators, Phys. Rev. Lett. **108**, 153601 (2012).
[22] M. R. Vanner, J. Hofer, G. D. Cole, and M. Aspelmeyer, Cooling-by-measurement and mechanical state tomography via pulsed optomechanics, Nat. Commun. **4**, 2295 (2013).
[23] J. Li, S. Gröblacher, and M. Paternostro, Enhancing non-classicality in mechanical systems, New J. Phys. **15**, 033023 (2013).
[24] J. S. Bennett, K. Khosla, L. S. Madsen, M. R. Vanner, H. Rubinsztein-Dunlop, and W. P. Bowen, A Quantum Optomechanical Interface Beyond the Resolved Sideband Limit, arXiv:1510.05368 [quant-ph].
[25] J. Eisert, S. Scheel, and M. B. Plenio, Distilling Gaussian States with Gaussian Operations is Impossible, Phys. Rev. Lett. **89**, 137903 (2002).
[26] J. Fiurášek, Gaussian Transformations and Distillation of Entangled Gaussian States, Phys. Rev. Lett. **89**, 137904 (2002).
[27] G. Giedke and J. Ignacio Cirac, Characterization of Gaussian operations and distillation of Gaussian states, Phys. Rev. A **66**, 032316 (2002).
[28] R. Filip, Excess-noise-free recording and uploading of nonclassical states to continuous-variable quantum memory, Phys. Rev. A **78**, 012329 (2008).
[29] F. Khalili, S. Danilishin, H. Miao, H. Müller-Ebhardt, H. Yang, and Y. Chen, Preparing a Mechanical Oscillator in Non-Gaussian Quantum States, Phys. Rev. Lett. **105**, 070403 (2010).
[30] H. Mueller-Ebhardt, H. Rehbein, C. Li, Y. Mino, K. Somiya, R. Schnabel, K. Danzmann, and Y. Chen, Quantum state preparation and macroscopic entanglement in gravitational-wave detectors, Phys. Rev. A **80**, 043802 (2009).
[31] H. Mueller-Ebhardt, H. Miao, S. Danilishin, and Y. Chen, Quantum-state steering in optomechanical devices, arXiv:1211.4315 [quant-ph].
[32] U. Akram, W. P. Bowen, and G. J. Milburn, Entangled mechanical cat states via conditional single photon optomechanics, New J. Phys. **15**, 093007 (2013).
[33] K. Hammerer, C. Genes, D. Vitali, P. Tombesi, G. Milburn, C. Simon, and D. Bouwmeester, Nonclassical States of Light and Mechanics, in *Cavity Optomechanics*, Quantum Science and Technology, edited by M. Aspelmeyer, T. J. Kippenberg, and F. Marquardt (Springer, Berlin, 2014), pp. 25–56.
[34] M. Paternostro, Engineering Nonclassicality in a Mechanical System Through Photon Subtraction, Phys. Rev. Lett. **106**, 183601 (2011).
[35] P. Sekatski, M. Aspelmeyer, and N. Sangouard, Macroscopic Optomechanics from Displaced Single-Photon Entanglement, Phys. Rev. Lett. **112**, 080502 (2014).
[36] C. Galland, N. Sangouard, N. Piro, N. Gisin, and T. J. Kippenberg, Heralded Single-Phonon Preparation, Storage, and Readout in Cavity Optomechanics, Phys. Rev. Lett. **112**, 143602 (2014).
[37] T. A. Palomaki, J. W. Harlow, J. D. Teufel, R. W. Simmonds, and K. W. Lehnert, Coherent state transfer between itinerant microwave fields and a mechanical oscillator, Nature (London) **495**, 210 (2013).
[38] J. Zhang, K. Peng, and S. L. Braunstein, Quantum-state transfer from light to macroscopic oscillators, Phys. Rev. A **68**, 013808 (2003).
[39] P. Marek and R. Filip, Noise-resilient quantum interface based on quantum nondemolition interactions, Phys. Rev. A **81**, 042325 (2010).
[40] R. Filip, P. Marek, and U. L. Andersen, Measurement-induced continuous-variable quantum interactions, Phys. Rev. A **71**, 042308 (2005).
[41] Y. Miwa, J.-i. Yoshikawa, N. Iwata, M. Endo, P. Marek, R. Filip, P. van Loock, and A. Furusawa, Exploring a New Regime for Processing Optical Qubits: Squeezing and Unsqueezing Single Photons, Phys. Rev. Lett. **113**, 013601 (2014).
[42] S. M. Meenehan, J. D. Cohen, G. S. MacCabe, F. Marsili, M. D. Shaw, and O. Painter, Pulsed Excitation Dynamics of an Optomechanical Crystal Resonator near Its Quantum Ground State of Motion, Phys. Rev. X **5**, 041002 (2015).
[43] C. M. Caves, K. S. Thorne, R. W. P. Drever, V. D. Sandberg, and M. Zimmermann, On the measurement of a weak classical force coupled to a quantum-mechanical oscillator. I. Issues of principle, Rev. Mod. Phys. **52**, 341 (1980).
[44] V. B. Braginsky, Y. I. Vorontsov, and K. S. Thorne, Quantum nondemolition measurements, Science **209**, 547 (1980).
[45] V. B. Braginsky and F. Y. Khalili, *Quantum Measurement* (Cambridge University Press, Cambridge, UK, 1995).
[46] A. A. Clerk, F. Marquardt, and K. Jacobs, Back-action evasion and squeezing of a mechanical resonator using a cavity detector, New J. Phys. **10**, 095010 (2008).
[47] J. Suh, A. J. Weinstein, C. U. Lei, E. E. Wollman, S. K. Steinke, P. Meystre, A. A. Clerk, and K. C. Schwab, Mechanically detecting and avoiding the quantum fluctuations of a microwave field, Science **344**, 1262 (2014).

[48] F. Lecocq, J. B. Clark, R. W. Simmonds, J. Aumentado, and J. D. Teufel, Quantum Nondemolition Measurement of a Nonclassical State of a Massive Object, Phys. Rev. X **5**, 041037 (2015).

[49] C. K. Law, Interaction between a moving mirror and radiation pressure: A Hamiltonian formulation, Phys. Rev. A **51**, 2537 (1995).

[50] K. Jacobs, P. Tombesi, M. J. Collett, and D. F. Walls, Quantum-nondemolition measurement of photon number using radiation pressure, Phys. Rev. A **49**, 1961 (1994).

[51] B. C. Buchler, M. B. Gray, D. A. Shaddock, T. C. Ralph, and D. E. McClelland, Suppression of classical and quantum radiation pressure noise via electro-optic feedback, Opt. Lett. **24**, 259 (1999).

[52] C. Gardiner and P. Zoller, *Quantum Noise: A Handbook of Markovian and Non-Markovian Quantum Stochastic Methods with Applications to Quantum Optics* (Springer Science & Business Media, New York, 2004).

[53] K. Miyata, H. Ogawa, P. Marek, R. Filip, H. Yonezawa, J.-i. Yoshikawa, and A. Furusawa, Experimental realization of a dynamic squeezing gate, Phys. Rev. A **90**, 060302 (2014).

[54] G. Masada, K. Miyata, A. Politi, T. Hashimoto, J. L. O'Brien, and A. Furusawa, Continuous-variable entanglement on a chip, Nat. Photon. **9**, 316 (2015).

[55] J.-i. Yoshikawa, K. Makino, S. Kurata, P. van Loock, and A. Furusawa, Creation, Storage, and On-Demand Release of Optical Quantum States with a Negative Wigner Function, Phys. Rev. X **3**, 041028 (2013).

[56] M. Mehmet, S. Ast, T. Eberle, S. Steinlechner, H. Vahlbruch, and R. Schnabel, Squeezed light at 1550 nm with a quantum noise reduction of 12.3 dB, Opt. Express **19**, 25763 (2011).

[57] E. E. Wollman, C. U. Lei, A. J. Weinstein, J. Suh, A. Kronwald, F. Marquardt, A. A. Clerk, and K. C. Schwab, Quantum squeezing of motion in a mechanical resonator, Science **349**, 952 (2015).

[58] J.-M. Pirkkalainen, E. Damskägg, M. Brandt, F. Massel, and M. A. Sillanpää, Squeezing of Quantum Noise of Motion in a Micromechanical Resonator, Phys. Rev. Lett. **115**, 243601 (2015).

[59] P. F. Cohadon, A. Heidmann, and M. Pinard, Cooling of a Mirror by Radiation Pressure, Phys. Rev. Lett. **83**, 3174 (1999).

[60] O. Arcizet, P.-F. Cohadon, T. Briant, M. Pinard, and A. Heidmann, Radiation-pressure cooling and optomechanical instability of a micromirror, Nature (London) **444**, 71 (2006).

[61] D. Kleckner and D. Bouwmeester, Sub-kelvin optical cooling of a micromechanical resonator, Nature (London) **444**, 75 (2006).

[62] M. Poggio, C. L. Degen, H. J. Mamin, and D. Rugar, Feedback Cooling of a Cantilever's Fundamental Mode Below 5 mK, Phys. Rev. Lett. **99**, 017201 (2007).

[63] G. I. Harris, U. L. Andersen, J. Knittel, and W. P. Bowen, Feedback-enhanced sensitivity in optomechanics: Surpassing the parametric instability barrier, Phys. Rev. A **85**, 061802 (2012).

[64] C. M. Caves, Quantum limits on noise in linear amplifiers, Phys. Rev. D **26**, 1817 (1982).

[65] G. A. Korn and T. M. Korn, *Mathematical Handbook for Scientists and Engineers: Definitions, Theorems, and Formulas for Reference and Review* (Courier Corporation, New York, 2000).

CHAPTER 4

Quantum non-demolition interaction between two mechanical oscillators

In the previous Chapter we have shown that methods of quantum optics can be effectively applied to the quantum state transfer in optomechanics. The next step in this direction would be a demonstration of the efficiency of a similar approach to another challenging problem, namely coupling two mechanical systems at the quantum level. Many interesting and promising experimental works in the domain of coupling different systems to mechanical oscillators, like continuous-variable cold-atom ensembles [86, 35, 99], individual atoms [86, 217], superconducting qubits [156, 167], solid-state systems [8, 106, 203, 160] and semiconductor systems [232, 152], have been performed. Despite these achievements and the fact that current experimental techniques allow to make two mechanical systems, mediated with light or microwave filed, interact with each other – no such result has been demonstrated at that time. Even more, no quantum entanglement-generating coupling between two mechanical systems outside the single cavity has been demonstrated.

Our goal was to complement the recent experiment on coupling quantized mechanical oscillations of trapped ions [30]. We wanted to establish QND coupling between two mechanical systems, using the methods proved their efficiency before [173] - Gaussian local operation on input light (presqueezing) together with feedforward control on the mechanical system. We also wanted to show that these mechanical oscillators can be efficiently entangled, indicating the quantum nature of the interaction.

The contribution of this thesis is the demonstration of the feasibility and robustness of the QND type coupling and of the ways to achieve maximum entanglement for optomechanical and electromechanical setups in the pulsed regime under the influence of transmission losses and mechanical thermal bath. This work potentially allows pulsed studies of quantum synchronization of mechanical objects [136, 233, 225], it is also important for research of the connection with quantum thermodynamics [55, 237, 60, 32] and can be extended to the coupling of more mechanical systems by different types of Gaussian and non-Gaussian interactions.

Following our publication, new proposals emerged for the state teleportation and

quantum state transfer between distant mechanical resonators [65] and for the generation of mechanical and optomechanical entanglement outside the resolved-sideband regime using the precooling and local optical squeezers for performance improvement [42]. This topic is under active exploration and recently the entanglement between two mechanical oscillators has been experimentally demonstrated in several works. In [177] authors used a set up with two on-chip based micromechanical oscillators made of nanostructured silicon beams and demonstrated entanglement at the distance of 20 cm. Light-matter entanglement between the vibrational motion of two silicon optomechanical oscillators was achieved in the setup for the optomechanical Bell test [137]. The entanglement of two massive micromechanical oscillators comprising of 10^{12} atoms and coupled through a microwave-frequency cavity which stabilized the entanglement of the centers of mass of mechanical motion was demonstrated [154]. And finally, in [220] the superposition state $|0\rangle + |1\rangle$ of mechanical excitations was created in the tool designed for quantum memory at telecom wavelength.

Pulsed quantum interaction between two distant mechanical oscillators

Nikita Vostrosablin,* Andrey A. Rakhubovsky, and Radim Filip
Department of Optics, Palacký University, 17 Listopadu 12, 771 46 Olomouc, Czech Republic
(Received 20 May 2016; revised manuscript received 26 October 2016; published 1 December 2016)

Feasible setup for pulsed quantum nondemolition interaction between two distant mechanical oscillators through an optical or microwave mediator is proposed. The proposal uses homodyne measurement of the mediator and feedforward control of the mechanical oscillators to reach the interaction. To verify the quantum nature of the interaction, we investigate the Gaussian entanglement generated in the mechanical modes. We evaluate it under influence of mechanical bath and propagation loss for the mediator and propose ways to optimize the interaction. Finally, both currently available optomechanical and electromechanical platforms are numerically analyzed. The analysis shows that implementation is already feasible with current technology.

DOI: 10.1103/PhysRevA.94.063801

I. INTRODUCTION

Quantum optomechanics and electromechanics connecting light and microwaves with mechanical motion at the quantum level is an emerging field of quantum physics and technology [1–3]. Recently, Gaussian quantum entanglement between mechanical oscillator and microwave field [4] and between nonclassical photon-phonon correlation of mechanical membrane and optical pulse [5] have been experimentally demonstrated. Both experiments used modern pulsed optomechanics [6–10]. They open new possibilities to experimentally connect other physical platforms with mechanical oscillator, like continuous-variable cold-atom ensembles [11–13], and further many discrete systems like individual atoms [11,14], superconducting qubits [15,16], solid-state systems [17–20], and semiconductor systems [21,22]. Together with these interesting and challenging interdisciplinary experiments, state-of-the-art of laboratory techniques could currently allow us to let two mechanical oscillators mediated by light or microwave field interact. It is another interesting step forward; two similar mechanical oscillators coupled at the quantum level have not been demonstrated yet. It can be very stimulating especially because the connection between two mechanical systems can physically connect quantum optomechanics to classical thermodynamics. If two similar quantum mechanical oscillators will be interfaced by the quantum version of the coupling typically used in classical mechanics, they can naturally generate entanglement. It is a simple witness that they were coupled quantum mechanically. Additionally, the mechanical-mechanical interaction can be of quantum nondemolition type, which is required for basic continuous-variable quantum gates [23], which are useful for specific features for both gate-based [24] and cluster-state-based [25] quantum computing. Recently, the nonlocal optical QND gate was demonstrated [26] following the theoretical proposals in Refs. [27,28]. Such a QND coupling was already broadly exploited between two atomic ensembles [29]. It is therefore much more important for the future to achieve such well-defined quantum interaction of mechanical oscillators, not only the generation of an entangled state of two mechanical systems.

Generation of entanglement between two mechanical systems has already been proposed in three different configurations. In the first type of proposed setup, two mechanical oscillators have been placed in a single optical cavity [30–38]. In this case, the continuous generation of steady-state entanglement appears because the mechanical oscillators interact with join optical intracavity field. This configuration has been extensively used to discuss continuous-time quantum synchronization [39–41]. In the second kind of proposal, two entangled beams of light were used to entangle two mechanical systems without the necessity of measuring them [42–44]. In the third kind of proposed setups, two continuous-wave beams of light, leaving two continuously pumped optomechanical cavities, are jointly detected in Bell measurement and photocurrent is used to correct the mechanical oscillators [45–47]. These schemes can generate entanglement at a distance; however, it is very limited because of instabilities in the blue-detuned continuous-wave regime. Advanced time-continuous quantum measurement and control has been suggested to prepare mechanical entanglement [48]. Recently, theoretical investigation of optomechanical crystals has offered many other ways to obtain mechanical entanglement [49,50]. Our goal is to propose a currently feasible scheme with potential to use the power of quantum optical tools to complement a recent experimental test of coupled quantized mechanical oscillations of trapped ions [51].

In this paper, we propose a currently feasible way to build basic *pulsed* quantum nondemolition (QND) interaction between two mechanical oscillators at a distance, connected by light or microwave field. The scheme is depicted in Fig. 1. Using homodyne detection of light or microwave field and feedforward control, means of both mechanical oscillators precisely follow the QND interaction. To generate significant entanglement of mechanical oscillators, coherent light is sufficient, and the entanglement can be very well estimated when intracavity field can be adiabatically eliminated. On the other hand, squeezed light is advantageous to approach ideal QND interaction between two mechanical systems. Feasible squeezing of light is capable to enhance entangling power of the QND interaction. However, for larger optomechanical coupling strength and larger squeezing, nonadiabatic methods taking the intracavity field fully into account are required. Importantly, the nonadiabatic calculations predict a decrease of the entanglement power for larger squeezing. It is due to

*nikita.vostrosablin@upol.cz

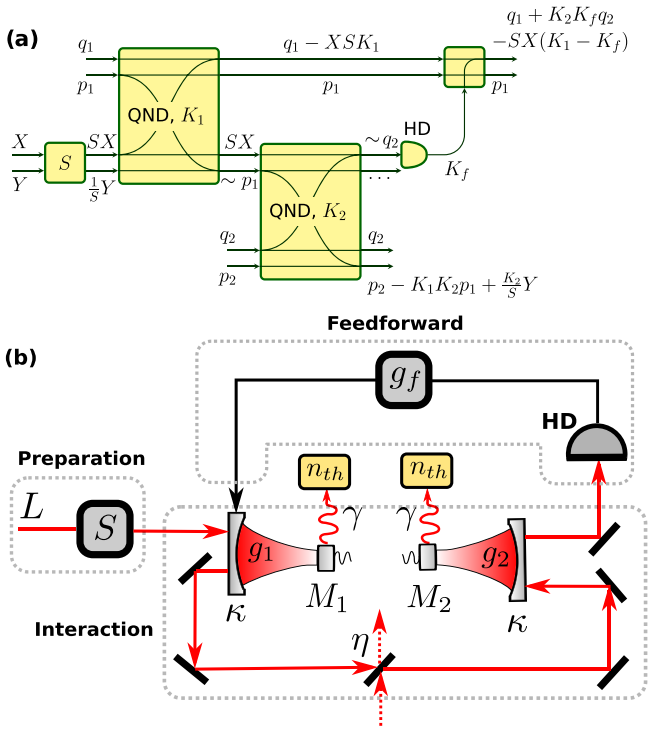

FIG. 1. The protocol of QND interaction between two mechanical modes. (a) Simplified scheme: S, squeezing operation; HD, homodyne detector. (b) Possible experimental implementation with the imperfections: η, optical losses between the cavities; n_{th}, thermal mechanical environment.

presence of the intracavity field and the squeezing has to be therefore optimized to get maximum of entangling power. We prove sufficient stability of the QND interaction under the influence of mechanical bath and transmission loss between two separated cavities. Finally, we verified that it is feasible to build the mechanical QND interaction for both current optomechanical [52] and electromechanical [53] setups.

The paper is organized in the following way. We begin by mathematical definition of quantum-nondemolition interaction and principal description of the experimental setup. First, in Sec. III we carry out a simple principal analysis of the physics of the setup. To do so we start from a brief derivation of equations of motion for an optomechanical system in Sec. III A and solve those in Sec. III B, ignoring for a while the decoherence and eliminating intracavity modes. We quantify the interaction between the mechanical modes, analyzing the transfer of first moments of quadratures and for the strength of the interaction we employ the entanglement between the modes. We use logarithmic negativity [54] as a measure of entanglement. We show principal possibility of the protocol performance and derive the simplest conditions on the experimental parameters.

Second, in Sec. IV we perform a full numerical analysis of the system allowing for the imperfections. Those include impact of the intracavity modes that mediate the interaction between the traveling light pulse and the mechanical modes and the thermal bath causing decoherence of the latter. We as well investigate the impact of the optical loss between the cavities. We show that with currently available parameters the protocol can establish a QND interface between the two distant mechanical modes.

II. SETUP FOR PULSED QND INTERACTION BETWEEN MECHANICAL OSCILLATOR

In this paper, we propose a feasible way of implementation of quantum nondemolition (QND) interaction between mechanical modes of two distant optomechanical cavities. The QND interaction of two harmonic oscillators may be described by Hamiltonian $\mathcal{H}_{\text{int}} = \hbar g Q_1 Q_2$ with $Q_{1,2}$ being the position or momentum of the corresponding oscillator and g, interaction strength. After the interaction both the variables Q_1 and Q_2 remain unperturbed (not demolished), whereas the complementary ones to Q_1 (Q_2) become linearly displaced by a value proportional to gQ_2 (gQ_1). The nondemolition interaction has been demonstrated in a few electromechanical experiments recently [55,56].

The proposed scheme is presented in the Fig. 1. It is the simplest setup for generation of QND coupling between two mechanical systems. It is basically a serial scheme which does not require multiple pass of optical pulse through single optomechanical cavity. Moreover, it exploits the advantage of squeezed light and homodyne detection, which are very efficient resources of quantum optics. The feedforward correction on mechanics can be done simply at any time by classical pulses of laser light. The modes of two mechanical oscillators M_1 and M_2 interact by turns with an optical (or microwave) pulse L via opto- (electro-)mechanical coupling. The pulse is then detected and the result of the detection is used to linearly displace the mechanical mode of the first cavity (if needed, in the second one is displaced as well). In principle this feedforward is not necessary to achieve entanglement, as the latter could be created conditional on the results of the detection. A similar method was used recently for conditional state preparation in optomechanics [57].

The optical pulse can be prepared in a squeezed intensive coherent state and sent into the optomechanical cavity. The latter in essence comprises an optical mode coupled via radiation pressure to a mechanical harmonic oscillator [58]. We follow the standard approach [1,59,60] and assume that the optical pulse is displaced with a strong classical component that is modulated at mechanical frequency. This ensures that the effective interaction within the cavity is the nondemolition type.

The QND interaction allows a partial exchange of the variables between the mechanical mode M_1 and the traveling pulse [see Fig. 1(a)]. The latter is then redirected to the second cavity with mechanical oscillator M_2, which we assume to be identical to the M_1. The QND interaction within the second cavity allows us to transmit a variable of the mode M_1 carried by the pulse to the mode M_2 and in turn to transmit a variable of the mode M_2 to the light. The pulse is then detected and the result of detection is used to displace the mode M_1 to complete transfer of the M_2 variable. A proper strong presqueezing of the light pulse and the feedforward correction allow us to eliminate all variables from the final transformation of the mechanical modes that consequently approach an ideal QND interaction between them.

III. PERFORMANCE OF SETUP FOR QND INTERACTION

A. Optomechanical quantum nondemolition interaction

Let us first consider a single optomechanical cavity that in essence embodies an optical mode and a mechanical one. The two modes are coupled by radiation pressure with the Hamiltonian [58] $H_{\rm rp} = -\hbar g_0 n_{\rm cav} x/x_{\rm zp}$, where $n_{\rm cav}$ stands for intracavity photon number, x, mechanical displacement from equilibrium, and g_0, so-called single-photon coupling strength. The mechanical zero-point fluctuation amplitude, denoted by $x_{\rm zp}$, for a mechanical oscillator with mass m and eigenfrequency ω_m equals $x_{\rm zp} = \sqrt{\hbar/2m\omega_m}$.

In order to enhance the radiation pressure coupling, a strong coherent field is used as the pump. This allows us to linearize the dynamics around a steady classical state and solve for quantum corrections. Moreover, we assume this strong classical field is resonant with the cavity and modulated at the frequency of the mechanical oscillator [59]. In this case if the mechanical frequency ω_m exceeds all other characteristic frequencies of the system, one can perform averaging to get rid of the terms at $2\omega_m$ (i.e., adopt the rotating wave approximation, RWA) to obtain the nondemolition coupling. The latter condition is usually equivalent to the requirement that the optical decay rate κ of the cavity be smaller with respect to ω_m., known as resolved-sideband regime.

After the linearization and averaging out the rapid oscillating terms we arrive to the QND coupling within the optomechanical cavity with Hamiltonian that reads (depending on the phase of the pump)

$$\mathcal{H} = \hbar g X p \quad \text{or} \quad \mathcal{H} = \hbar g Y q, \tag{1}$$

where $g = g_0\sqrt{\langle n_{\rm cav}\rangle}$ is the enhanced optomechanical coupling strength, X and Y, and q and p are quadratures of, respectively, the optical and mechanical modes which obey usual commutation relations ($[X,Y] = i$; $[q,p] = i$). The mechanical displacement x can be expressed in terms of quadratures as $x/x_{\rm zp} = q\cos\omega_m t + p\sin\omega_m t$ and a similar expression holds for the optical quadratures.

The counter-rotating terms at $2\omega_m$ could provide additional back action. In Appendix B we analyze this back action and prove that for typical experimental parameters it is sufficient to consider the system within RWA.

To describe the interaction of the propagating light pulse with the optomechanical cavity we complement the Hamiltonian of the optomechanical interaction $\mathcal{H}_1 = -\hbar g_1 X_1 p_1$ with input-output relations [61] (henceforth we denote with index "1" or "2" quantities corresponding to the respective cavity). The system is thus described by the following set of equations:

$$\begin{aligned}
\dot q_1 &= -\frac{\gamma}{2} q_1 - g_1 X_1 + \xi_{q1}, \quad \dot X_1 = -\kappa X_1 + \sqrt{2\kappa} X^{\rm in},\\
\dot p_1 &= -\frac{\gamma}{2} p_1 + \xi_{p1}, \quad \dot Y_1 = -\kappa Y_1 + \sqrt{2\kappa} Y^{\rm in} + g_1 p_1,\\
Q^{\rm out} &= \sqrt{2\kappa} Q - Q^{\rm in}, \quad Q = X,Y.
\end{aligned} \tag{2}$$

Here $X^{\rm in}, Y^{\rm in}$ are the quadratures of the pulse with commutator $[X^{\rm in}, Y^{\rm in}(t')] = i\delta(t-t')$, $\xi_{q,p}$ are the quadratures of mechanical noise. κ and γ are respectively optical and viscous mechanical damping coefficients.

B. Adiabatic regime

As a first approximation we consider the system in adiabatic regime. Given that optical decay rate exceeds the other rates in (2) (which is typically the case in experiments), one can assume that the optical mode reacts to any changes instantaneously, which is equivalent to putting $\dot X = \dot Y = 0$ in Eqs. (2). Formally this corresponds to replacement of all the functions of time with their own versions averaged over the interval with duration τ_* such that $\kappa \gg 1/\tau_* \gg \gamma, g$.

Lastly, in this section we leave out the mechanical decoherence, setting $\gamma = 0$, $\xi_{q1} = \xi_{p1} = 0$.

With these assumptions the solution of Eqs. (2) reads

$$\begin{aligned}
q_1(\tau) &= q_1(0) - SK_1\mathcal{X}^{\rm in}, \quad \mathcal{X}_1^{\rm out} = S\mathcal{X}^{\rm in},\\
p_1(\tau) &= p_1(0), \quad \mathcal{Y}_1^{\rm out} = \frac{1}{S}\mathcal{Y}^{\rm in} + K_1 p_1(0).
\end{aligned}$$

We have introduced the squeezing magnitude S and the effective interaction strength $K_1 = g_1\sqrt{2\tau/\kappa}$. We also have defined the input and output quadratures of the cavity as

$$\mathcal{Q}^{\rm k} = \frac{1}{\sqrt{\tau}}\int_0^\tau Q^{\rm k}(s)ds, \quad Q = X,Y, \quad {\rm k} = {\rm in, out}.$$

The quadratures are normalized to obey $[\mathcal{X}^{\rm k}, \mathcal{Y}^{\rm k}] = i$.

The output field from the first cavity is then delivered to the input of the second one through a purely lossy channel that performs an admixture of vacuum to the signal; therefore

$$Q_2^{\rm in} = \sqrt{\eta} Q_1^{\rm out} + \sqrt{1-\eta} Q_{\rm ls}, \quad Q = X,Y.$$

Here $Q_{\rm ls}$ are the quadratures of vacuum mode.

The optomechanical interaction within the second cavity is described by the Hamiltonian $\mathcal{H}_2 = \hbar g_2 Y_2 q_2$ and starts at time $t = \tau$. One can obtain the input-output relations for the second cavity in a similar fashion. For simplicity we assume the parameters of the second cavity (except the coupling g_2) to replicate the parameters of the first one.

The optical output quadrature $\mathcal{X}_2^{\rm out}$ is measured and the position of the mechanical mode of the first cavity is displaced so that the final value equals $q_1 = q_1(\tau) + K_f\mathcal{X}_2^{\rm out}$:

$$\begin{aligned}
q_1 &= q_1(0) + K_2 K_f q_2(\tau)\\
&\quad - S\mathcal{X}^{\rm in}(K_1 - K_f\sqrt{\eta}) + \mathcal{X}_{\rm ls} K_f\sqrt{1-\eta},\\
p_1 &= p_1(0),\\
q_2 &= q_2(\tau),\\
p_2 &= p_2(\tau) - K_1 K_2 p_1(0)\sqrt{\eta}\\
&\quad - \mathcal{Y}^{\rm in}\frac{K_2\sqrt{\eta}}{S} - K_2\sqrt{1-\eta}\mathcal{Y}_{\rm ls}.
\end{aligned} \tag{3}$$

Similarly, we have introduced $K_2 = g_2\sqrt{\frac{2\tau}{\kappa}}$ here.

To approach the ideal QND interaction of the two mechanical modes with Hamiltonian $\mathcal{H}_{\rm QND} = \hbar K_1 K_2 \tau^{-1} p_1 q_2$ one needs to fulfill a few conditions. First, ensure low loss ($\eta \to 1$) to get rid of the noisy mode $Q_{\rm ls}$. Second, pick a proper feedforward gain $K_f = K_1/\sqrt{\eta}$ and provide high squeezing $S \gg 1$ to suppress the optical mode $\mathcal{Q}^{\rm in}$.

To quantify the strength of the interaction we estimate the entanglement between the two mechanical modes, namely the logarithmic negativity [54] (see Appendix A for details).

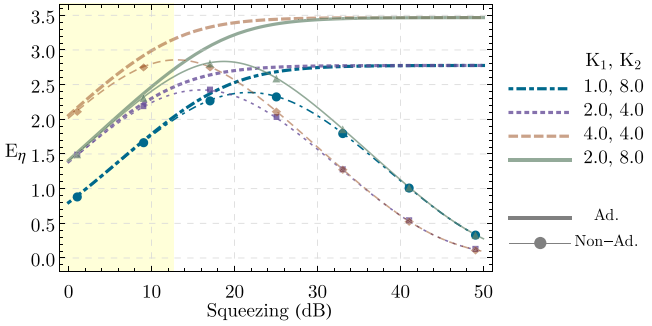

FIG. 2. Entanglement between the two mechanical modes as a function of optical presqueezing. Thick lines correspond to adiabatic solution; thin lines with markers to solution with cavity mode. Different colors and dashes are used for different ratio of the gains K_1 and K_2. Losses are absent: $\eta = 1$. Highlighted is the region of squeezing magnitudes not exceeding the value of 12.7 dB reported in Ref. [62].

In the lossless case, the optimal value of squeezing yielding maximum of entanglement is given by $S = |K_2/(K_1 - K_f)|$. Therefore, for the feedforward $K_f = K_1$ the entanglement increases with squeezing infinitely. In the limit of moderately strong coupling ($K_{1,2} \gtrsim 1$) the following approximation holds:

$$E_\eta \approx -\ln \frac{1}{2K_1K_2}\sqrt{1+\frac{K_2^2}{S^2}}. \tag{4}$$

From this expression follows that although increase of both S and $K_{1,2}$ leads to stronger entanglement, it is more efficient to increase K_1. This can be seen from the latter equation in (3), where the noisy mediator quadrature $\mathcal{Y}^{\rm in}$ enters with a multiplier $\propto K_2$.

The LN for this simple model is presented as a function of the presqueezing S in Fig. 2 (solid lines). The parameters used for simulation are $\kappa/2\pi = 221.5$ MHz, $\gamma/2\pi = 328$ Hz, $\tau = 4.5\,\mu$s that correspond to a recent optomechanical experiment [52] with increased pulse duration τ.

From the Fig. 2 is is clear that for low squeezing the LN is mostly defined by the interaction strength K_1 in the first cavity as it follows from (4). In the limit of high squeezing the LN saturates to the value that is defined by the product of gains K_1K_2, again in agreement with (4).

IV. ROBUSTNESS TO IMPERFECTIONS

There are two sources of hindrance that we left out for the previous section. First is the intracavity modes that mediate interaction between the propagating pulse and the mechanical modes of interest. In addition, the intracavity modes produce unwanted memory effects that disturb the desired QND interaction. Second is the interaction of mechanical modes with the thermal environment.

In this section we first study these two sources independently and finally provide a full solution, taking both into account simultaneously.

A. Impact of the intracavity modes

To consider the effect of the intracavity modes on the QND interface, we solve the set of dynamical equations (2) without the mechanical decoherence ($\gamma = 0$, $\xi_{q,p} = 0$). The solution reads (for compactness we write the solution for the lossless case, $\eta = 1$)

$$\begin{aligned}
q_1 &= q_1(0) + q_2(\tau)K_2K_f\left(1-\frac{1-e^{-\kappa\tau}}{\kappa\tau}\right)\\
&\quad - S(K_1-K_f)\frac{1}{\sqrt{\tau}}\int_0^\tau X_1^{\rm in}(s)ds\\
&\quad + SK_1\int_0^\tau X_1^{\rm in}(s)\left\{e^{-\kappa(\tau-s)}\left[1-4\kappa(\tau-s)\frac{K_f}{K_1}\right]\right\}ds\\
&\quad + X_1(0)\left\{\frac{2g_f}{\kappa}[(1-e^{-\kappa\tau})-2\kappa\tau e^{-\kappa\tau}]-\frac{g_1}{\kappa}[1-e^{-\kappa\tau}]\right\}\\
&\quad + X_2(0)\frac{2g_f}{\kappa}(1-e^{-\kappa\tau}),\\
p_1 &= p_1(0),\\
q_2 &= q_2(\tau),\\
p_2 &= p_2(\tau) - p_1(0)K_1K_2\left(1+e^{-\kappa\tau}-\frac{2}{\kappa\tau}(1-e^{-\kappa\tau})\right)\\
&\quad - \frac{K_2}{S}\frac{1}{\sqrt{\tau}}\int_0^\tau\{1-e^{-\kappa(\tau-s)}[2\kappa(\tau-s)+1]\}Y_1^{\rm in}(s)ds\\
&\quad - Y_1(0)\frac{2g_2}{\kappa}[1-e^{-\kappa\tau}(1+\kappa\tau)]-Y_2(0)\frac{g_2}{\kappa}(1-e^{-\kappa\tau}),
\end{aligned} \tag{5}$$

where we defined $g_f \equiv K_f\sqrt{\kappa/2\tau}$.

These equations deviate from the idealized set (3) by presence of the initial intracavity quadratures $Q_{1,2}(0)$. In addition, the pulse quadratures $Q^{\rm in}$ can no longer be eliminated completely by a proper choice of K_f and high squeezing S. Moreover, in this case high squeezing amplifies the noisy summand with $X^{\rm in}$ degrading the interface. The impact of this summand can be reduced by redefining the temporal mode of the output pulse (applying optimal time filter at the detection). This, however, cannot cancel the noisy summand completely as the optical quadratures that are written during the first pass ($X^{\rm in}$) and second pass ($Y^{\rm in}$) are distorted in different manner; see Eq. (5).

From the Eqs. (5) follows that in the limit $\kappa \gg g_{1,2,f}$ and $\kappa\tau \gg 1$ these equations reduce to the pure QND transformations (3). Furthermore, from the first equation it follows that the effect of the unwanted summand $\propto SX^{\rm in}$ can be reduced by decreasing K_1. This is illustrated in Fig. 2 where we plot the LN for solution including the cavity modes as a function of squeezing for different couplings. At high squeezing the full solution deviates from the adiabatic one; however, the curves with lower K_1 show this deviation at higher squeezing than the curves with higher K_1.

The proper choice of the coupling thus allows us to approach the performance of the idealized adiabatic regime. Note that in order to increase the LN it is more efficient to increase K_1 than K_2. To increase the LN staying close to the preferred adiabatic regime (and therefore a pure QND interface

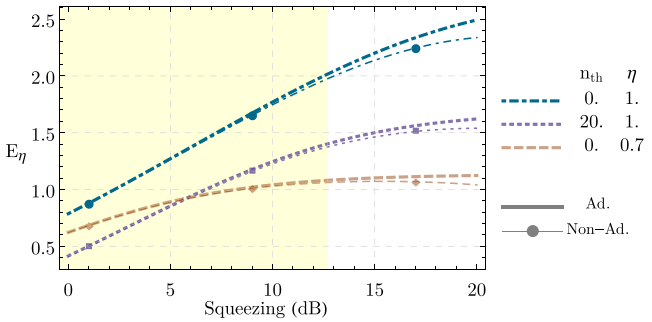

FIG. 3. Entanglement as a function of squeezing in the presence of a mechanical bath with mean number of phonons $n_{\rm th}$ and optical losses with transmittivity η. The optomechanical gains equal $K_1 = 1$, $K_2 = 8$, the same as for the blue dot-dashed line in Fig. 2.

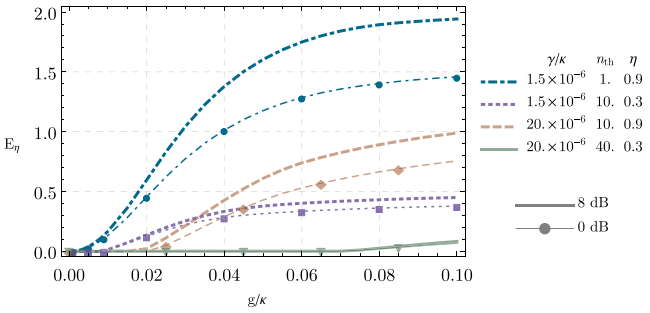

FIG. 4. Maximal entanglement achievable with the coupling rate g (in units of κ), for optomechanical parameters [52] (blue dot-dashed and violet dotted lines) and electromechanical [53] (brown dashed and green solid).

between the mechanical modes), on the contrary it is preferable to increase K_2.

B. Mechanical thermal bath

Finally we consider the system in the presence of the thermal mechanical environment.

We assume that each of the mechanical modes is coupled at rate γ to its own environment that is in a thermal state with occupation $n_{\rm th}$ (see Fig. 1). The coupling for both modes takes place during the interaction with the pulse. Moreover, the first mode remains coupled to the environment during the interaction of the second system with the pulse. Before the interaction with the pulse the mechanical modes are in the ground state (the possibility to precool the mechanical oscillator close to the ground state has been demonstrated for a number of setups [5,63,64]).

The thermal bath is represented in Eqs. (2) by Langevin force quadratures $\xi_{\rm q,p}$. These quadratures are assumed Markovian so that

$$\langle \xi_a(t)\xi_a(t') + \xi_a(t')\xi_a(t)\rangle = \gamma(2n_{\rm th}+1)\delta(t-t'),\ a = q,p;$$
$$\langle \xi_q(t)\xi_p(t') + \xi_p(t')\xi_q(t)\rangle = 0.$$

The LN in adiabatic regime with intracavity modes eliminated is approximately given by (here $K_1 = K_2 = K$)

$$E_\eta \approx -\ln\frac{1}{2K^2}\sqrt{1+\Gamma K^4+\frac{K^2}{S^2}(1+\Gamma K^4)},\quad \Gamma = 2\gamma\tau n_{\rm th}. \tag{6}$$

In the case of zero mechanical damping the expression is reduced to (4).

The LN corresponding to the full solution with all the imperfections is plotted as a function of the squeezing S in Fig. 3 for a set of different parameters.

The main means of how the mechanical environment affects the entanglement is by adding the thermal noise to the mechanical quadratures. Besides this, the environment also creates a small imbalance that prohibits the perfect cancellation of the optical mediator mode in q_1 by feedforward. The magnitude of this imbalance is, however, almost negligible.

We as well plot the LN as a function of the squeezing for nonzero loss ($1-\eta \neq 0$). Figure 3 shows that at higher squeezing the entanglement between the mechanical modes is more tolerant to the mechanical bath than to the optical loss. Nevertheless, even with realistic loss parameters the entanglement does not vanish. We observe that adiabatic elimination is capable of fitting very well the results for a wide range of feasible squeezing of radiation.

Numerical analysis shows that the nonzero occupation of the mechanical bath creates a threshold for the coupling that allows the entanglement. At the same time, nonzero optical loss only decreases the value of the LN, so in the case of zero occupation of the bath, the entanglement can tolerate any finite loss.

C. Coupling optimization for experiments [52,53]

In prior sections we focused on approaching a pure QND interaction between the two mechanical modes. Therefore we assumed the feedforward to be adjusted in a way that helps to cancel most of the optical mediator quadrature $X^{\rm in}$, i.e., $K_f = K_1/\sqrt{\eta}$. Now we aim for maximization of the entanglement between the two modes. We waive the constraint on K_f and numerically optimize the logarithmic negativity with respect to the optomechanical gains $K_{1,2}$, feedforward strength K_f, and the pulse duration τ given a limitation on the coupling strength.

The results of the numerical optimization are presented in Fig. 4. The optimal regime to achieve maximal entanglement appears to be very close to the regime of pure QND between the mechanical oscillators with long pulses $\kappa\tau \gg 1$ and $K_f = K_1/\sqrt{\eta}$.

A squeezed source of radiation apparently helps to improve entanglement in both opto- and electromechanical scheme for large η close to perfect transmission and smaller $n_{\rm th}$. Simultaneously, the threshold for g/κ to observe entanglement is lowered as well for higher η and lower $n_{\rm th}$. On the other hand, for larger $n_{\rm th}$ and lower η, the squeezing of radiation is not important; however, we can still observe entanglement of mechanical systems if γ/κ is not too large and g/κ is sufficiently large. Our analysis (see Appendix B) shows that under these conditions and for moderate squeezing the rotating-wave approximation standardly employed in the theory of optomechanics is well justified. It is therefore fully feasible to generate entanglement with state-of-the-art systems.

The optomechanical setup noticeably outperforms the electromechanical one due to higher eigenfrequency of the mechanical oscillator and consequently lower bath occupation. The high occupation of the mechanical thermal bath in the electromechanical setup places a constraint on the available pulse durations, which in turn limits the QND gain K.

V. CONCLUSION

We have proposed feasible way of the simplest pulsed implementation of entangling quantum nondemolition coupling between two distant but very similar mechanical oscillators, implementable with both current electromechanical and optomechanical setups. The method exploits squeezed light and microwave radiation and highly efficient homodyne detection to induce maximal entanglement for this purely mechanical coupling. We verified robustness of the procedure under small transmission loss between the oscillators and under mechanical thermal baths. We realized that both current optomechanical [52] and electromechanical [53] setups are sufficient for the implementation of an extended version of multiple QND interaction. It will allow pulsed studies of quantum synchronization of mechanical objects [39–41]. Afterwards, a detailed study of quantum interaction of possibly very different mechanical systems is important for development of physical connection with quantum thermodynamics [65–68]. The method can be further extended to controllably couple more mechanical systems in the future by different types of Gaussian interactions and possibly challenging non-Gaussian transformations.

ACKNOWLEDGMENTS

We acknowledge Project No. GB14-36681G of the Czech Science Foundation. A.A.R. acknowledges support by the Development Project of Faculty of Science, Palacky University. N.V. acknowledges the support of Palacky University (IGA-PrF-2016-005).

APPENDIX A: LOGARITHMIC NEGATIVITY

The mechanical modes in our system are initially in thermal states and the optical modes are all in vacuum, and the linear dynamic preserves the Gaussianity of the states of mechanical modes. A Gaussian state of a two-mode system with quadratures $f = [q_1, p_1, q_2, p_2]^T$ is fully determined by a vector of means $\langle f \rangle$ and a covariance matrix (CM) with elements defined as

$$V_{ij} = \tfrac{1}{2} \langle \Delta f_i \Delta f_j + \Delta f_j \Delta f_i \rangle.$$

Here angular brackets denote the averaging over the quantum state, and $\Delta f_i \equiv f_i - \langle f_i \rangle$.

The covariance matrix may be divided into 2×2 blocks such that

$$V = \begin{bmatrix} \mathcal{V}_1 & \mathcal{V}_c \\ \mathcal{V}_c^T & \mathcal{V}_2 \end{bmatrix},$$

where $\mathcal{V}_1$ and $\mathcal{V}_2$ characterize internal correlations in mechanical subsystems. The matrix $\mathcal{V}_c$ stands for the correlations between the first and second mechanical modes. The diagonalization of the CM leads to symplectic eigenvalues $\nu_\pm$ [54],

$$\nu_\pm = \sqrt{\tfrac{1}{2}(\Sigma(V) \pm \sqrt{\Sigma(V)^2 - 4 \det V})},$$

with

$$\Sigma(V) = \det \mathcal{V}_1 + \det \mathcal{V}_2 - 2 \det \mathcal{V}_c.$$

Logarithmic negativity is defined then as $E_\eta = \max[0, -\ln 2\nu_-]$ and we use it as the measure of the entanglement of the system under the consideration.

APPENDIX B: BEYOND ROTATING WAVE APPROXIMATION

The rotating wave approximation (RWA) is usually adopted for considerations of the optomechanical systems working in the resolved-sideband regime ($\kappa \ll \omega_m$). In this appendix we consider our protocol without this approximation. We outline here the main steps that lead to an analytical expression for the covariance matrix of the mechanical modes. The covariance matrix contains additional terms from back action compared to the case of RWA. We show that these terms do not impact the entanglement of the modes much. For the sake of simplicity we do not consider in this appendix thermal environments of mechanics and optical losses between the cavities. Both these effects can be easily taken into account.

The equations of motion for the first system read

$$\dot{q}_1 = g_1 X_1 (\cos 2\omega_m t - 1), \tag{B1}$$

$$\dot{p}_1 = g_1 X_1 \sin 2\omega_m t, \tag{B2}$$

$$\dot{X}_1 = \sqrt{2\kappa} X_1^{\text{in}} - \kappa X_1, \tag{B3}$$

$$\dot{Y}_1 = \sqrt{2\kappa} Y_1^{\text{in}} - \kappa Y_1 + g_1 p_1 (1 - \cos 2\omega_m t) + g_1 q_1 \sin 2\omega_m t. \tag{B4}$$

As is easily seen, this system of equations allows an analytical solution. First, Eq. (B3) has the solution

$$X_1(t) = e^{-\kappa t} \left[X_1(0) + \sqrt{2\kappa} \int_0^t ds\, e^{\kappa s} X_1^{\text{in}}(s) \right]. \tag{B5}$$

We then plug this expression into Eqs. (B1) and (B2) to solve for q_1 and p_1. The solution for p_1 reads

$$\begin{aligned} p_1(\tau) - p_1(0) &= X_1(0) g_1 \int_0^\tau dt\, e^{-\kappa t} \sin 2\omega_m t \\ &\quad + g_1 \sqrt{2\kappa} \int_0^\tau dt\, e^{-\kappa t} \sin 2\omega_m t \\ &\quad \times \int_0^t ds\, e^{\kappa s} X^{\text{in}}(s) \\ &= X_1(0) g_1 \mathcal{I}(0) + g_1 \sqrt{2\kappa} \int_0^\tau ds e^{\kappa s} X^{\text{in}}(s) \mathcal{I}(s), \end{aligned} \tag{B6}$$

where

$$\mathcal{I}(s) \equiv \int_s^\tau dt\, e^{-\kappa t} \sin 2\omega_m t. \tag{B7}$$

Notice that we swapped the order of integration when going to the last line in (B6) in order to have $X^{\rm in}$ in the outermost integration. We do a similar swap with the consequent expressions.

The solution for q_1 can be written in a similar fashion. This with (B6) can then be substituted into Eq. (B4) to obtain the solution for Y_1.

The very same procedure repeatedly applied to the equations of motion for the second cavity and input-output relations allows us to obtain a full analytical solution for the vector of quadratures of the mechanical modes. The solution itself is rather cumbersome so we do not present it here.

Having the solution, we proceed to compute the covariance matrix. To demonstrate the method of calculation we use Eq. (B6) to compute the element $V_{2,2} = \langle p_1(\tau)^2\rangle$:

$$\begin{aligned} V_{2,2} &= \langle p_1^2(0)\rangle + \langle X_1^2(0)\rangle g_1^2 \mathcal{I}^2(0) \\ &\quad + 2\kappa g_1^2 \iint_0^\tau ds ds' \left\langle X_1^{\rm in}(s) \circ X_1^{\rm in}(s')\right\rangle e^{\kappa(s+s')} \mathcal{I}(s)\mathcal{I}(s') \\ &= \langle p_1^2(0)\rangle + \langle X_1^2(0)\rangle g_1^2 \mathcal{I}^2(0) + V_{\rm X} 2\kappa g_1^2 \int_0^\tau ds\, e^{2\kappa s} \mathcal{I}^2(s), \end{aligned} \tag{B8}$$

where we used

$$\left\langle X_1^{\rm in}(s) \circ X_1^{\rm in}(s')\right\rangle = V_{\rm X}\delta(s-s'). \tag{B9}$$

It is illustrative to estimate the difference between the full solution (B8) and the straightforward solution $V_{2,2}^{\rm RWA} = \langle p_1^2(0)\rangle$ obtained with advantage of RWA. The quantity $\mathcal{I}$ defined above serves as a measure of this divergence. One can make estimations:

$$[g_1\mathcal{I}(0)]^2 \sim \left(\frac{g_1}{2\omega_m}\right)^2 = \left(\frac{g_1}{\kappa}\right)^2\left(\frac{\kappa}{2\omega_m}\right)^2 \ll 1,$$

$$2\kappa g_1^2 \int_0^\tau ds\, e^{2\kappa s}\mathcal{I}^2(s) \sim \cos^2 2\omega_m\tau \left(\frac{g_1}{2\omega_m}\right)^2 \ll 1.$$

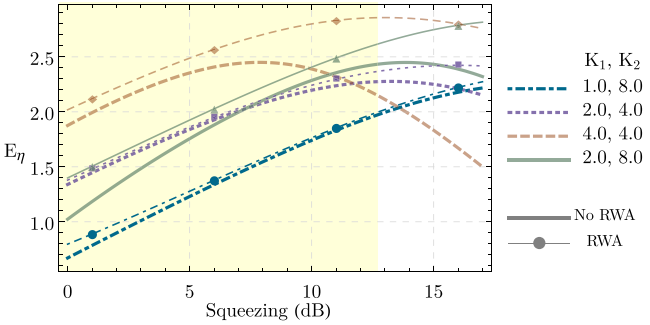

FIG. 5. Entanglement (logarithmic negativity) as a function of squeezing of the input state computed from the full solution (thick lines) and with help of RWA (thin lines with markers). For details, see the caption of Fig. 2.

Besides these simple estimates, we present the computed logarithmic negativity of the mechanical modes in Fig. 5. One can see that the adoption of RWA leads to an overestimation of entanglement due to the back action that comes from the counter-rotating terms in the Hamiltonian. However, for appropriate parameters, the full solution without RWA still approaches rather closely the idealized adiabatic one provided that the optomechanical coupling is not too strong (cf. blue dot-dashed lines in Figs. 2 and 5). We use the sideband-resolution parameter $\kappa/\omega_m = 0.04$, which is a conservative estimate for a number of current experimental setups [4,52].

We became aware recently of another publication [69] that deals with a QND interaction beyond RWA.

[1] M. Aspelmeyer, T. J. Kippenberg, and F. Marquardt, Cavity optomechanics, Rev. Mod. Phys. **86**, 1391 (2014).

[2] M. Aspelmeyer, T. J. Kippenberg, and F. Marquardt, *Cavity Optomechanics* (Springer Verlag, Berlin, 2014).

[3] W. P. Bowen and G. J. Milburn, *Quantum Optomechanics* (Taylor & Francis, Boca Raton, London, New York, 2015).

[4] T. A. Palomaki, J. D. Teufel, R. W. Simmonds, and K. W. Lehnert, Entangling mechanical motion with microwave fields, Science **342**, 710 (2013).

[5] R. Riedinger, S. Hong, R. A. Norte, J. A. Slater, J. Shang, A. G. Krause, V. Anant, M. Aspelmeyer, and S. Gröblacher, Non-classical correlations between single photons and phonons from a mechanical oscillator, Nature (London) **530**, 313 (2016).

[6] S. G. Hofer, W. Wieczorek, M. Aspelmeyer, and K. Hammerer, Quantum entanglement and teleportation in pulsed cavity optomechanics, Phys. Rev. A **84**, 052327 (2011).

[7] M. R. Vanner, I. Pikovski, G. D. Cole, M. S. Kim, Č. Brukner, K. Hammerer, G. J. Milburn, and M. Aspelmeyer, Pulsed quantum optomechanics, Proc. Natl. Acad. Sci. USA **108**, 16182 (2011).

[8] M. R. Vanner, J. Hofer, G. D. Cole, and M. Aspelmeyer, Cooling-by-measurement and mechanical state tomography via pulsed optomechanics, Nat. Commun. **4**, 2295 (2013).

[9] J.-Q. Liao and C. K. Law, Cooling of a mirror in cavity optomechanics with a chirped pulse, Phys. Rev. A **84**, 053838 (2011).

[10] J.-Q. Liao and C. K. Law, Parametric generation of quadrature squeezing of mirrors in cavity optomechanics, Phys. Rev. A **83**, 033820 (2011).

[11] K. Hammerer, M. Aspelmeyer, E. S. Polzik, and P. Zoller, Establishing Einstein-Poldosky-Rosen Channels between Nanomechanics and Atomic Ensembles, Phys. Rev. Lett. **102**, 020501 (2009).

[12] S. Camerer, M. Korppi, A. Jockel, D. Hunger, T. W. Hansch, and P. Treutlein, Realization of an Optomechanical Interface between Ultracold Atoms and a Membrane, Phys. Rev. Lett. **107**, 223001 (2011).

[13] A. Jockel, A. Faber, T. Kampschulte, M. Korppi, M. T. Rakher, and P. Treutlein, Sympathetic cooling of a membrane oscillator

in a hybrid mechanical-atomic system, Nat. Nanotechnol. **10**, 55 (2015).

[14] B. Vogell, T. Kampschulte, M. T. Rakher, A. Faber, P. Treutlein, K. Hammerer, and P. Zoller, Long distance coupling of a quantum mechanical oscillator to the internal states of an atomic ensemble, New J. Phys. **17**, 043044 (2015).

[15] A. D. O'Connell, M. Hofheinz, M. Ansmann, R. C. Bialczak, M. Lenander, E. Lucero, M. Neeley, D. Sank, H. Wang, M. Weides, J. Wenner, J. M. Martinis, and A. N. Cleland, Quantum ground state and single-phonon control of a mechanical resonator, Nature (London) **464**, 697 (2010).

[16] J. M. Pirkkalainen, S. U. Cho, J. Li, G. S. Paraoanu, P. J. Hakonen, and M. A. Sillanpaa, Hybrid circuit cavity quantum electrodynamics with a micromechanical resonator, Nature (London) **494**, 211 (2013).

[17] O. Arcizet, V. Jacques, A. Siria, P. Poncharal, P. Vincent, and S. Siedelin, A single nitrogen-vacancy defect coupled to a nanomechanical oscillator, Nat. Phys. **7**, 879 (2011).

[18] S. Kolkowitz, A. C. Bleszynski Jayich, Q. P. Unterreithmeier, S. D. Bennett, P. Rabl, J. G. E. Harris, and M. D. Lukin, Coherent sensing of a mechanical resonator with a single-spin qubit, Science **335**, 1603 (2012).

[19] J. Teissier, A. Barfuss, P. Appel, E. Neu, and P. Maletinsky, Strain Coupling of a Nitrogen-Vacancy Center Spin to a Diamond Mechanical Oscillator, Phys. Rev. Lett. **113**, 020503 (2014).

[20] P. Ovartchaiyapong, K. W. Lee, B. A. Myers, and A. C. Bleszynski Jayich, Dynamic strain-mediated coupling of a single diamond spin to a mechanical resonator, Nat. Commun. **5**, 4429 (2014).

[21] I. Yeo, P.-L. de Assis, A. Gloppe, E. Dupont-Ferrier, P. Verlot, N. S. Malik, E. Dupuy, J. Claudon, J.-M. Gerard, A. Auffeves, G. Nogues, S. Seidelin, J.-P. Poizat, O. Arcizet, and M. Richard, Strain-mediated coupling in a quantum dot–mechanical oscillator hybrid system, Nat. Nanotechnol. **9**, 106 (2014).

[22] M. Montinaro, G. Wust, M. Munsch, Y. Fontana, E. Russo-Averchi, M. Heiss, A. Fontcuberta i Morral, R. J. Warburton, and M. Poggio, Quantum dot opto-mechanics in a fully self-assembled nanowire, Nano Lett. **14**, 4454 (2014).

[23] S. D. Bartlett, B. C. Sanders, S. L. Braunstein, and K. Nemoto, Efficient Classical Simulation of Continuous Variable Quantum Information Processes, Phys. Rev. Lett. **88**, 097904 (2002).

[24] J.-i. Yoshikawa, Y. Miwa, A. Huck, U. L. Andersen, P. van Loock, and A. Furusawa, Demonstration of a Quantum Nondemolition Sum Gate, Phys. Rev. Lett. **101**, 250501 (2008).

[25] Y. Miwa, R. Ukai, J. I. Yoshikawa, R. Filip, P. van Loock, and A. Furusawa, Demonstration of cluster state shaping and quantum erasure for continuous variables, Phys. Rev. A **82**, 032305 (2010).

[26] S. Yokoyama, R. Ukai, J. I. Yoshikawa, P. Marek, R. Filip, and A. Furusawa, Nonlocal quantum gate on quantum continuous variables with minimal resources, Phys. Rev. A **90**, 012311 (2014).

[27] R. Filip, Continuous-variable quantum nondemolishing interaction at a distance, Phys. Rev. A **69**, 052313 (2004).

[28] R. Filip, P. Marek, and U. L. Andersen, Measurement-induced continuous-variable quantum interactions, Phys. Rev. A **71**, 042308 (2005).

[29] K. Hammerer, A. S. Sørensen, and E. S. Polzik, Quantum interface between light and atomic ensembles, Rev. Mod. Phys. **82**, 1041 (2010).

[30] S. Mancini, V. Giovannetti, D. Vitali, and P. Tombesi, Entangling Macroscopic Oscillators Exploiting Radiation Pressure, Phys. Rev. Lett. **88**, 120401 (2002).

[31] M. J. Hartmann and M. B. Plenio, Steady State Entanglement in the Mechanical Vibrations of Two Dielectric Membranes, Phys. Rev. Lett. **101**, 200503 (2008).

[32] A. Xuereb, C. Genes, and A. Dantan, Strong Coupling and Long-Range Collective Interactions in Optomechanical Arrays, Phys. Rev. Lett. **109**, 223601 (2012).

[33] M. J. Woolley and A. A. Clerk, Two-mode back-action-evading measurements in cavity optomechanics, Phys. Rev. A **87**, 063846 (2013).

[34] H. Seok, L. F. Buchmann, E. M. Wright, and P. Meystre, Multimode strong-coupling quantum optomechanics, Phys. Rev. A **88**, 063850 (2013).

[35] H. Tan, G. Li, and P. Meystre, Dissipation-driven two-mode mechanical squeezed states in optomechanical systems, Phys. Rev. A **87**, 033829 (2013).

[36] M. J. Woolley and A. A. Clerk, Two-mode squeezed states in cavity optomechanics via engineering of a single reservoir, Phys. Rev. A **89**, 063805 (2014).

[37] H. Flayac and V. Savona, Heralded Preparation and Readout of Entangled Phonons in a Photonic Crystal Cavity, Phys. Rev. Lett. **113**, 143603 (2014).

[38] Ch.-J. Yang, J.-H. An, W. Yang, and Y. Li, Generation of stable entanglement between two cavity mirrors by squeezed-reservoir engineering, Phys. Rev. A **92**, 062311 (2015).

[39] A. Mari, A. Farace, N. Didier, V. Giovannetti, and R. Fazio, Measures of Quantum Synchronization in Continuous Variable Systems, Phys. Rev. Lett. **111**, 103605 (2013).

[40] L. Ying, Y.-Ch. Lai, and C. Grebogi, Quantum manifestation of a synchronization transition in optomechanical systems, Phys. Rev. A **90**, 053810 (2014).

[41] T. Weiss, A. Kronwald, and F. Marquardt, Noise-induced transitions in optomechanical synchronization, New J. Phys. **18**, 013043 (2016).

[42] J. Zhang, K. Peng, and S. L. Braunstein, Quantum-state transfer from light to macroscopic oscillators, Phys. Rev. A **68**, 013808 (2003).

[43] M. Pinard, A. Dantan, D. Vitali, O. Arcizet, T. Briant, and A. Heidmann, Entangling movable mirrors in a double-cavity system, Europhys. Lett. **72**, 747 (2005).

[44] L. Mazzola and M. Paternostro, Activating optomechanical entanglement, Sci. Rep. **1**, 199 (2011).

[45] S. Pirandola, D. Vitali, P. Tombesi, and S. Lloyd, Macroscopic Entanglement by Entanglement Swapping, Phys. Rev. Lett. **97**, 150403 (2006).

[46] K. Børkje, A. Nunnenkamp, and S. M. Girvin, Proposal for Entangling Remote Micromechanical Oscillators via Optical Measurements, Phys. Rev. Lett. **107**, 123601 (2011).

[47] M. Abdi, S. Pirandola, P. Tombesi, and D. Vitali, Entanglement Swapping with Local Certification: Application to Remote Micromechanical Resonators, Phys. Rev. Lett. **109**, 143601 (2012).

[48] S. G. Hofer and K. Hammerer, Entanglement-enhanced time-continuous quantum control in optomechanics, Phys. Rev. A **91**, 033822 (2015).

[49] M. Schmidt, M. Ludwig, and F. Marquardt, Optomechanical circuits for nanomechanical continuous variable quantum state processing, New J. Phys. **14**, 125005 (2012).

[50] H. Flayac, M. Minkov, and V. Savona, Remote macroscopic entanglement on a photonic crystal architecture, Phys. Rev. A **92**, 043812 (2015).

[51] K. R. Brown, C. Ospelkaus, Y. Colombe, A. C. Wilson, D. Leibfried, and D. J. Wineland, Coupled quantized mechanical oscillators, Nature (London) **471**, 196 (2011).

[52] S. M. Meenehan, J. D. Cohen, G. S. MacCabe, F. Marsili, M. D. Shaw, and O. Painter, Pulsed Excitation Dynamics of an Optomechanical Crystal Resonator near its Quantum Ground State of Motion, Phys. Rev. X **5**, 041002 (2015).

[53] C. F. Ockeloen-Korppi, E. Damskägg, J.-M. Pirkkalainen, T. T. Heikkilä, F. Massel, and M. A. Sillanpää, Low-Noise Amplification and Frequency Conversion with a Multiport Microwave Optomechanical Device, Phys. Rev. X **6**, 041024 (2016).

[54] A. Serafini, F. Illuminati, and S. De Siena, Symplectic invariants, entropic measures and correlations of Gaussian states, J. Phys. B **37**, L21 (2004).

[55] E. E. Wollman, C. U. Lei, A. J. Weinstein, J. Suh, A. Kronwald, F. Marquardt, A. A. Clerk, and K. C. Schwab, Quantum squeezing of motion in a mechanical resonator, Science **349**, 952 (2015).

[56] J.-M. Pirkkalainen, E. Damskägg, M. Brandt, F. Massel, and M. A. Sillanpää, Squeezing of Quantum Noise of Motion in a Micromechanical Resonator, Phys. Rev. Lett. **115**, 243601 (2015).

[57] W. Wieczorek, S. G. Hofer, J. Hoelscher-Obermaier, R. Riedinger, K. Hammerer, and M. Aspelmeyer, Optimal State Estimation for Cavity Optomechanical Systems, Phys. Rev. Lett. **114**, 223601 (2015).

[58] C. K. Law, Interaction between a moving mirror and radiation pressure: A Hamiltonian formulation, Phys. Rev. A **51**, 2537 (1995).

[59] V. B. Braginsky, Y. I. Vorontsov, and K. S. Thorne, Quantum nondemolition measurements, Science **209**, 547 (1980).

[60] A. A. Clerk, F. Marquardt, and K. Jacobs, Back-action evasion and squeezing of a mechanical resonator using a cavity detector, New J. Phys. **10**, 095010 (2008).

[61] D. F. Walls and Gerard J. Milburn, *Quantum Optics* (Springer Science & Business Media, 2007).

[62] T. Eberle, S. Steinlechner, J. Bauchrowitz, V. Händchen, H. Vahlbruch, M. Mehmet, H. Müller-Ebhardt, and R. Schnabel, Quantum Enhancement of the Zero-Area Sagnac Interferometer Topology for Gravitational Wave Detection, Phys. Rev. Lett. **104**, 251102 (2010).

[63] J. Chan, T. P. Mayer Alegre, A. H. Safavi-Naeini, J. T. Hill, A. Krause, S. Groeblacher, M. Aspelmeyer, and O. Painter, Laser cooling of a nanomechanical oscillator into its quantum ground state, Nature (London) **478**, 89 (2011).

[64] J. D. Teufel, T. Donner, Dale Li, J. W. Harlow, M. S. Allman, K. Cicak, A. J. Sirois, J. D. Whittaker, K. W. Lehnert, and R. W. Simmonds, Sideband cooling of micromechanical motion to the quantum ground state, Nature (London) **475**, 359 (2011).

[65] Y. Dong, K. Zhang, F. Bariani, and P. Meystre, Work measurement in an optomechanical quantum heat engine, Phys. Rev. A **92**, 033854 (2015).

[66] K. Zhang, F. Bariani, and P. Meystre, Theory of an optomechanical quantum heat engine, Phys. Rev. A **90**, 023819 (2014).

[67] C. Elouard, M. Richard, and A. Auffèves, Reversible work extraction in a hybrid opto-mechanical system, New J. Phys. **17**, 055018 (2015).

[68] M. Brunelli, A. Xuereb, A. Ferraro, G. De Chiara, N. Kiesel, and M. Paternostro, Out-of-equilibrium thermodynamics of quantum optomechanical systems, New J. Phys. **17**, 035016 (2015).

[69] D. Malz and A. Nunnenkamp, Exact solution of optomechanical dual-beam backaction-evading measurement, Phys. Rev. A **94**, 053820 (2016).

CHAPTER 5

Quantum opto- and electromechanical transducers

The next logical step in our exploration of quantum interaction of different systems would be a quantum transducer between different electromagnetic fields mediated by the mechanical system. Such a transducer allows entangling two directly non-interacting radiation modes and thus – quantum state transfer, which is of our high interest as it is an important milestone for the development of unified quantum technology [104].

There was sufficient progress in the development of different types of transducers interconnecting optical and microwave fields – both theoretical proposals and experimental realizations, together with transducers coupling optical fields. These works present a wide range of different hybrid designs. The interested reader can address a short overview of the main achievements in this field in the introduction of our paper presented in this section.

However, most of these transducers have two main drawbacks. Firstly, they cannot operate in the time-resolved quantum regime, when the quantum states are defined in a short time interval and, secondly – they are very restricted by a performance by the mechanical noise of the mediator.

Being inspired by [69], we propose a new kind of opto- and electromechanical transducer, based on geometric phase effect [20], which allows establishing robust entanglement between directly non-interacting systems with a noisy mechanical mediator. Moreover, by optimization of system parameters, we establish a particular type of quantum interaction between radiation modes - a quantum non-demolition (QND) type of interaction.

The impact of this thesis is the theoretical development of symmetric (optical field to optical field) transducer and study of the influence of optical losses and mechanical bath on the performance of such a setup. The same analysis is performed for asymmetric transducer for mechanical mode shared across two opto(electro-)mechanical cavities. This analysis has been performed for state-of-the-art experimental parameters. It was shown that the optimization of parameters of individual interactions allows getting sufficient entanglement in the domain of parameters where this entanglement wouldn't be possible otherwise. The research opens a way for further study of pulsed transducers and their implementation with other physical platforms.

Our work might be very relevant as we witness a growing interest in the topic of quantum optomechanical transducers. New approaches have emerged in the last years. A mechanically mediated microwave–optical converter with 47% conversion efficiency using a feed-forward protocol [92] has been shown. In [9] authors demonstrated the conversion of microwave and telecom photons in a setup based on silicon photonics, cavity optomechanics, and superconducting circuits. And finally, efficient microwave-to-optics conversion using a mechanical oscillator in its quantum ground state was demonstrated in [71].

Research Article | Vol. 25, No. 16 | 7 Aug 2017 | OPTICS EXPRESS 18974
Optics EXPRESS

Pulsed quantum continuous-variable optoelectromechanical transducer

NIKITA VOSTROSABLIN,* ANDREY A. RAKHUBOVSKY, AND RADIM FILIP

Department of Optics, Palacký University, 17. Listopadu 12, 771 46 Olomouc, Czech Republic
*nikita.vostrosablin@upol.cz

Abstract: We propose a setup allowing to entangle two directly non-interacting radiation modes applying four sequential pulsed quantum resonant interactions with a noisy vibrational mode of a mechanical oscillator which plays the role of the mediator. We analyze Gaussian entanglement of the radiation modes generated by the transducer and confirm that the noisy mechanical mode can mediate generation of entanglement. The entanglement, however, is limited if the interaction gains are not individually optimized. We prove the robustness of the transducer to optical losses and the influence of the mechanical bath and propose the ways to achieve maximal performance through the individual optimization.

OCIS codes: (270.0270) Quantum optics; (120.4880) Optomechanics.

References and links

1. H. J. Kimble, "The quantum internet," Nature **453**, 1023–1030 (2008).
2. J. Verdú, H. Zoubi, Ch. Koller, J. Majer, H. Ritsch, and J. Schmiedmayer, "Strong magnetic coupling of an ultracold gas to a superconducting waveguide cavity," Phys. Rev. Lett. **103**, 043603 (2009).
3. D. Marcos, M. Wubs, J. M. Taylor, R. Aguado, M. D. Lukin, and A. S. Sørensen, "Coupling nitrogen-vacancy centers in diamond to superconducting flux qubits," Phys. Rev. Lett. **105**, 210501 (2010).
4. M. Hafezi, Z. Kim, S. L. Rolston, L. A. Orozco, B. L. Lev, and J. M. Taylor, "Atomic interface between microwave and optical photos," Phys. Rev. A **85**, 020302 (2012).
5. C. A. Regal and W. Lehnert, "From cavity electromechanics to cavity optomechanics," Journal of Physics: Conference Series **264**, 012025 (2011).
6. S. Takeda, T. Mizuta, M. Fuwa, P. van Loock, and A. Furusawa, "Determenistic quantum teleportation of photonic quantum bits by a hybrid technique", Nature **500**, 315–318 (2013).
7. L. Tian, "Optoelectromechanical transducer: Reversible conversion between microwave and optical photons," Annalen der Physik **527**, 1–14 (2015).
8. H. Ogawa, H. Ohdan, K. Miyata, M. Taguchi, K. Makino, H. Yonezawa, J. Yoshikawa, and A. Furusawa, "Real-time quadrature measurement of a single-photon wave packet with continuous temporal-mode matching," Phys. Rev. Lett. **116**, 233602 (2016).
9. K. Makino, Y. Hashimoto, J. Yoshikawa, H. Ohdan, T. Toyama, P. van Loock, and A. Furusawa, "Synchronization of optical photons for quantum information processing," Science Advances **2**, e1501772 (2016).
10. T. A. Palomaki, J. D. Teufel, R. W. Simmonds, and K. W. Lehnert, "Entangling mechanical motion with microwave fields," Science **342**, 710–713 (2013).
11. T. A. Palomaki, J. W. Harlow, J. D. Teufel, R. W. Simmonds, and K. W. Lehnert, "Coherent state transfer between itinerant microwave fields and a mechanical oscillator," Nature **495**, 210–214 (2013).
12. S. G. Hofer, W. Wieczorek, M. Aspelmeyer, and K. Hammerer, "Quantum entanglement and teleportation in pulsed cavity optomechanics," Phys. Rev. A. **84**, 052327 (2011).
13. M. V. Berry, "The adiabatic phase and Pancharatnam's phase for polarized light," J. Mod. Opt. **34**, 1401–1407 (1987).
14. V. Kupčík and Radim Filip, "Continous-variable entanglement mediated by a thermal oscillator," Phys. Rev. A **92**, 022346 (2015).
15. M. Aspelmeyer, T. J. Kippenberg, and F. Marquardt, "Cavity optomechanics," Rev. Mod. Phys. **86**, 1391 (2014).
16. M. Metcalfe, "Applications of cavity optomechanics," Appl. Phys. Rev. **1**, 031105 (2014).
17. Sh. Barzanjeh, M. Abdi, G. J. Milburn, P. Tombesi, and D. Vitali, "Reversible Optical-to-Microwave Quantum Interface," Phys. Rev. Lett. **109**, 130503 (2012).
18. Y-D Wang and A. A. Clerk, "Using interference for high fidelity quantum state transfer in optomechanics," Phys. Rev. Lett. **108**, 153604 (2012).
19. L. Tian, "Adiabatic state conversion and pulse transmission in optomechanical system," Phys. Rev. Lett. **108**, 153604 (2012).
20. Y-D Wang and A. A. Clerk, "Using dark modes for high-fidelity optomechanical quantum state transfer," New. J. Phys. **14**, 105010 (2012).

#292878 https://doi.org/10.1364/OE.25.018974
Journal © 2017 Received 14 Apr 2017; revised 22 Jun 2017; accepted 24 Jun 2017; published 28 Jul 2017

Optics EXPRESS

21. S. A. McGee, D. Meiser, C. A. Regal, K. W. Lehnert, and M. J. Holland, "Mechanical resonators for storage and transfer of electrical and optical quantum states," Phys. Rev. A **87**, 053818 (2013).
22. K. Xia, M. R. Vanner, and J. Twamley, "An opto-magneto-mechanical quantum interface between distant superconducting qubits," Sci. Rep. **4**, 5571 (2014).
23. M. Winger, T. D. Blasius, T. P. Mayer Alegre, A. H. Safavi-Naeini, S. Meenehan, J. Cohen, S. Stobbe, and O. Painter, "A chip-scale integrated cavity-electro-optomechanics platform," Opt. Express **19**, 24905–24921 (2011).
24. J. Bochmann, A. Vainsencher, D. D. Awschalom, and A. N. Cleland, "Nanomechanical coupling between microwave and optical photons," Nature Physics **9**, 712–716 (2013).
25. R. W. Andrews, R. W. Peterson, T. P. Purdy, K. Cicak, R. W. Simmonds, C. A. Regal, and K. W. Lehnert, "Bidirectional and efficient conversion between microwave and optical light," Nature Physics **10**, 321–326 (2014).
26. T. Bagci, A. Simonsen, S. Schmid, L. G. Villanueva, E. Zeuthen, J. Appel, J.M. Taylor, A. S. Sørensen, K. Usami, A. Schliesser, and E. S. Polzik, "Optical detection of radio waves through a nanomechanical transducer," Nature **507**, 81–85 (2014).
27. T. Menke, P. S. Burns, A. P. Higginbotham, N. S. Kampel, R. W. Peterson, K. Cicak, R. W. Simmonds, C. A. Regal, and K. W. Lehnert, "Reconfigurable re-entrant cavity for wireless coupling to an electro-optomechanical device," https://arxiv.org/abs/1703.06470.
28. M. Asjad, S. Zippilli, P. Tombesi, and D. Vitali, "Large distance continuous variable communication with concatenated swaps," Physica Scripta **90**, 7 (2015).
29. M. Asjad, P. Tombesi, and D. Vitali, "Feedback control of two-mode output entanglement and steering in cavity optomechanics," Phys. Rev. A **94**, 052312 (2016).
30. L. Tian and H. Wang, "Optical wavelength conversion of quantum states with optomechanics," Phys. Rev. A. **82**, 053806 (2010).
31. C. Dong, V. Fiore, M. C. Kuzyk, L. Tian, and H. Wang, "Optical wavelength conversion via optomechanical coupling in a silica resonator," Ann. Phys. (Berlin) **527**, 100 (2015).
32. J. T. Hill, A. H. Safavi-Naeini, J. Chan, and O. Painter, "Coherent optical wavelength conversion via cavity optomechanics," Nat. Commun. **3** 1196 (2012).
33. Y. Liu, M. Davanco, V. Aksyuk, and K. Srinivasan, "Electromagnetically induced transparency and wideband wavelength conversion in silicon nitride microdisk optomechanical resonators," Phys. Rev. Lett. **110**, 223603 (2013).
34. F. Q. Lecocq, J. B. Clark, R. W. Simmonds, J. A. Aumentado, and J. D. Teufel, "Mechanically mediated microwave frequency conversion in the quantum regime," Phys. Rev. Lett. **116**, 043601 (2016).
35. Y. Miwa, J.-I. Yoshikawa, N. Iwata, M. Endo, P. Marek, R. Filip, P. van Loock, and A. Furusawa, "Exploring a New Regime for Processing Optical Qubits: Squeezing and Unsqueezing Single Photons," Phys. Rev. Lett. **113**, 013601 (2014).
36. P. Treutlein, C. Genes, K. Hammerer, M. Poggio, and P. Rabl, "Hybrid Mechanical Systems," in *Cavity Optomechanics*, M. Aspelmeyer, T. J. Kippenberg, F. Marquardt, eds., (Springer, 2014)
37. M. Wallquist, K. Hammerer, P. Rabl, M. Lukin, and P. Zoller, "Hybrid quantum devices and quantum engineering," Phys. Scr. **2009**, 014001 (2009).
38. V. B. Braginsky, Y. I. Vorontsov, and K. S. Thorne, "Quantum Nondemolition Measurements," Science **209**, 547-557 (1980).
39. A. A. Clerk, F. Marquardt, and K. Jacobs, "Back-action evasion ans squeezing of a mechanical resonator using a cavity detector," New J. Phys. **10**, 095010 (2008).
40. P. Marek and R. Filip, "Noise-resilient quantum interface based on quantum nondemolition interactions," Phys. Rev. A **81**, 042325 (2010).
41. A. S. Sørensen and K. Mølmer, "Entanglement and quantum computation with ions in thermal motion," Phys. Rev. A. **62**, 022311 (2000).
42. G. J. Milburn, S. Schneider, and D. F. V. James, "Ion trap quantum computing with warm atoms," Fortschr. Phys. **48**, 801–810 (2000).
43. D. Leibfried, B. DeMarco, V. Meyer, D. Lucas, M. Barett, J. Britton, W. M. Itano, B. Jelenković, C. Lange, T. Rosenband, and D. J. Wineland, "Experimental demonstration of a robust high-fidelity geometric two ion-qubit phase gate," Nature **422**, 412–415 (2003).
44. G. Vacanti, R. Fazio, M. S. Kim, G. M. Palme, M. Paternostro, and V. Vedral, "Geometric phase kickback in a mesoscopic qubit-oscillator system," Phys. Rev. A **85**, 022129 (2012).
45. I. Pikovsky, M. R. Vanner, M. Aspelmeyer, M. S. Kim, and Č. Brukner, "Probing Planck-scale physics with quantum optics," Nature Phys. **8**, 393–397 (2012).
46. K. E. Khosla, M. R. Vanner, W. P. Bowen, and G. J. Milburn, "Quantum state preparation of a mechanical resonator using an optomechanical geometric phase," New. J. Phys. **15**, 043025 (2013).
47. C. K. Law, "Interaction between a moving mirror and radiation pressure: A Hamiltonian formulation," Phys. Rev. A **51**, 2537–2541 (1995).
48. V. B. Braginsky, Y. I. Vorontsov, F. Y. Khalili, "Optimal quantum measurement in detectors of gravitational radiation," JETP Lett **27**, 276 (1978).
49. M. R. Vanner, I. Pikovsky, G. D. Cole, M. S. Kim, Č. Brukner, K. Hammerer, G. J. Milburn, and M. Aspelmeyer, "Pulsed Quantum Optomechanics," PNAS **108**, 16182 (2011).
50. M. R. Vanner, J. Hofer, G. D. Cole, and M. Aspelmeyer, "Cooling-by-measurement and mechanical state tomography

Optics EXPRESS

via pulsed optomechanics," Nature Communications **4**, 2295 (2013).
51. J. S. Bennett, K. Khosla, L. S. Madsen, M. R. Vanner, H. Rubinsztein-Dunlop, and W. P. Bowen, "A quantum optomechanical interface beyond the resolved sideband regime," New J. Phys. **18**, 053030 (2016).
52. V. Giovannetti and D. Vitali, "Phase-noise measurement in a cavity with a movable mirror undergoing quantum Brownian motion," Phys. Rev. A **63**, 023812 (2001).
53. A. A. Rakhubovsky, N. Vostrosablin, and R. Filip, "Squeezer-based pulsed optomechanical interface," Phys. Rev. A **93**, 033813 (2016).
54. L.-M.Duan, G. Giedke, J. I. Cirac, and P. Zoller, "Inseparability criterion for continuous variable systems," Phys. Rev. Lett. 84(12), 2722—2725 (2000).
55. R. Simon, "Peres-Horodecki separability criterion for continuous variable systems," Phys. Rev. Lett. **84(12)**, 2726-–2729 (2000).
56. C. Weedbrook, S. Pirandola, R. García-Patrón, N. J. Cerf, T. C. Ralph, J. H. Shapiro, and S. Lloyd, "Gaussian quantum information," Rev. Mod. Phys. **84**, 621–669 (2012).
57. W. P. Bowen and G. J. Milburn, *Quantum Optomechanics* (CRC Press, 2015), Appendix A "Linear detection of optical fields".
58. A. I. Lvovsky, H. Hansen, T. Aichele, O. Benson, J. Mlynek, S. Schiller, "Quantum state reconstruction of the single-photon Fock state," Phys. Rev. Lett. **87**, 050402 (2001).
59. J. Suh, A. J. Weinstein, C. U. Lei, E. E. Wollman, S. K. Steinke, P. Meystre, A. A. Clerk, and K. C. Schwab, "Mechanically detecting and avoiding the quantum fluctuations of a microwave field," Science **344 (6189)**, 1262–1265 (2014).
60. F. Lecocq, J. B. Clark, R. W. Simmonds, J. Aumentado, and J. D. Teufel, "Quantum nondemolition measurement of a nonclassical state of a massive object," Phys. Rev. X **5**, 041037 (2015)
61. S. M. Meenehan, J. D. Cohen, G. S. MacCabe, F. Marsili, M. D. Shaw, and O. Painter, "Pulsed excitation dynamics of an optomechanical crystal resonator near its quantum ground state of motion," Phys. Rev. X **5**, 041002 (2015).
62. K. Hammerer, M. Aspelmeyer, E. S. Polzik, and P. Zoller, "Establishing Einstein-Poldosky-Rosen Channels between Nanomechanics and Atomic Ensembles," Phys. Rev. Lett. **102**, 020501 (2009).
63. K. Hammerer, M. Wallquist, C. Genes, M. Ludwig, F. Marquardt, P. Treutlein, P. Zoller, J. Ye, and H. J. Kimble, "Strong Coupling of a Mechanical Oscillator and a Single Atom," Phys. Rev. Lett. **103**, 063005 (2009).
64. P. C. Maurer, G. Kucsko, C. Latta, L. Jiang, N.Y. Yao, S. D. Bennett, F. Pastawski, D. Hunger, N. Chisholm, M. Markham, D. J. Twitchen, J. I. Cirac, and M. D. Lukin, "Room-Temperature Quantum Bit Memory Exceeding One Second," Science **336**, 1283–1286 (2012).
65. A. Huck, S. Kumar, A. Shakoor, and U. L. Andersen, "Controlled Coupling of a Single Nitrogen-Vacancy Center to a Silver Nanowire," Phys. Rev. Lett. **106**, 096801 (2011).

1. Introduction

Quantum transducers are hybrid quantum systems important for development of unified quantum technology [1]. They practically demonstrate ability to universally entangle even very different quantum systems [2–4] and therefore, exchange quantum states between them. The transducer in principle connects two different systems A and B that otherwise are not interacting [5]. For an example, the systems A and B individually interact only in the pairs $A-M$ and $B-M$ with a mediating system M. The latter is however also a quantum system, therefore it can introduce quantum noise to the transducer. Moreover, M is typically open to an environment, which is noisy and lossy and limitedly measurable. It is therefore important to take this connection into account to propose a feasible quantum transducer. Continuous-variable (CV) quantum transducers are capable to quantum mechanically couple two different oscillators A and B by a mediating oscillator M. They can generate Gaussian CV entanglement, which can be used, for example, to teleport states between A and B [6]. Advantageously, they can be built, without any nonlinearity, from the most common linearized interactions $A-M$, $B-M$ of the oscillators. First type of transducers use simultaneously running linearized couplings $A-M$ and $B-M$ towards a steady state where $A-B$ coupling can be of a high quality and sufficient strength [7]. Ideally, the mediator M should be completely eliminated and not influence the coupling $A-B$. Nontrivial optimization of the $A-M$ and $B-M$ coupling strengths over time can improve the transducer quality.

These transducers, however, cannot operate in time-resolved quantum regime, with nonclassical states defined within a shorter time interval, used in modern optical [8, 9] and microwave experiments [10, 11]. To solve this problem, pulsed CV quantum transducers operating with

Optics EXPRESS

optical and microwave pulses are required. The pulsed regime was already used to generate entanglement [10] and propose for quantum teleportation [12]. Complementary to previous approach, the pulsed transducers individually control the interactions $A - M$ and $B - M$ by time non-overlapping pump pulses. The main idea is to use twice a sequence of the interactions $A - M$ and $B - M$ and exploit power of geometric phase effect [13] for CVs to eliminate the mediator M regardless of its noisy initial state. Recently, a principal robustness of such the proof-of-principle pulsed transducer between arbitrary quantum oscillators has been proven theoretically and temporal optimization of pulse control beyond the geometric phase effect has been suggested to reach the robust regime [14]. It opens a way to propose the pulsed transducers for various experimental platforms, for example, quantum optomechanics and electromechanics, what is the subject of our investigation. In this approach authors were considering short-time interactions $A - M$ and $B - M$. This allowed them to drop the decoherence of the mediator during the interactions and model all the damping processes by beam-splitting-type interaction with the environment between the unitary interactions of the system M with the systems A and B. As it will be discussed further, we consider longer interactions what pushes us to study the mechanical damping during the interactions with the mediator. It brings our system closer to real pulsed optomechanical experiments with long pulses.

Rapid development of quantum optomechanics [15, 16] puts forward a mechanical oscillator as a suitable mediator for the construction of the pulsed transducers. A lot of progress is done in the direction of optoelectromechanical transducers. The reversible optoelectromechanical transducer which used the effective source of two-mode squeezing between optical idler and a microwave signal to transfer quantum states between optical and microwave fields via quantum teleportation was proposed in [17]. High-fidelity quantum state conversion between microwave and optical fields may be performed through the excitation of the mechanical dark mode [5, 18–21]. This approach allows significant suppression of the mechanical noise from the mediator. An opto-magneto-mechanical system was proposed in [22] to interconnect microwave-to-optical quantum information. In this device the optical field was coupled to the mechanical degree of freedom which was, from its part, coupled to the magnetic field of the superconducting flux qubit. This scheme was also analyzed to transfer quantum information between distant superconducting qubits. Several experimental works were performed in the direction of quantum state transfer. In [23] an integrated optomechanical and electromechanical nanocavity was used to efficiently interconvert microwave and optical signals. In this device a photonic crystal defect cavity and an electrical circuit were both coupled to the same mechanical degree of freedom. In [24] a piezoelectric optomechanical crystal was used for coherent signal transfer between itinerant microwave and optical fields. In another experimental work [25] a mechanically compliant silicon nitride membrane was used to realize a high-fidelity conversion between optical light and microwave. In [26] a transducer utilizing a high-Q nanomembrane to interconvert radio-frequency waves with optical light was demonstrated. Very recently a new experimental work [27] considering the device capable for microwave-to-optics conversion by placing all components inside a re-entrant microwave cavity was performed. This design allows the wireless coupling to the transmission line with the possibility to vary the strength of this coupling without affecting the performance of the setup. There was also sufficient progress in the domain of transducers interconnecting optical fields. Optomechanical device entangling two optical fields was proposed in [28]. This setup was also considered to be used for quantum state teleportation of light signals over long distances, mediated by concatenated swap operations. The scheme containing two-mode optical cavity and the closed-loop feedback control was studied in [29]. This setup allowed to entangle the outputs and to coherently teleport quantum states between them. Coherent quantum state transfer between optical fields by the sequence of optomechanical pulses was studied theoretically [30]. In the experiment [31] a conversion of optical fields between two different frequencies by coupling them to a mechanical mode of a

Optics EXPRESS

silica resonator was demonstrated. It was also the first experimental observation of a mechanical dark mode for the optomechanical transducer. Another experimental setup for optical wavelength conversion was demonstrated in [32] with a silicon optomechanical crystal nanocavity. The optical frequency up- and down-conversion was also demonstrated in [33] for silicon nitride microdisk resonators. There were also observations of low-noise frequency conversion between two microwave fields as, for instance, in [34] where two microwave fields were coupled to a single mechanically compliant capacitor. Despite this remarkable progress in the field of opto- and electromechanical transducers, there is still one sufficient limitation — mechanical noise which restricts the performance of aforementioned setups. Our approach, based on the geometric phase effect allows to bypass this limitation. This method requires a pulsed control of mechanical systems, which is simultaneously advantageously compatible with modern quantum optics [8, 9, 35].

In this paper, we propose a pulsed CV quantum transducer with a noisy mechanical system as a mediator and analyze its feasibility for optoelectromechanical experiment. We study the influence of radiation losses and mechanical bath and we show that optimization of parameters allows high performance of the proposed transducer even for very noisy mediator. To demonstrate the feasibility of the proposed setup we firstly consider the symmetrical transducer which connects optical field to optical field. Such scheme is a good demonstration of the viability of the proposed concept and does not require involved modifications of the state-of-the-art experimental platforms for near-future implementation. Only then we consider more general case of the asymmetrical transducer coupling optical to microwave fields. This case is very important since it follows the trend to connect different quantum systems which is crucial for the future development of hybrid quantum systems [36, 37].

2. Pulsed CV quantum symmetrical transducer

2.1. Setup description

The basic idea of the setup which we consider is depicted in Fig. 1. The two radiation modes A and B are coupled to the same mechanical oscillator M but do not interact directly. The quantum states of the modes A and B are defined in flat-top temporal pulses with duration τ_A and τ_B correspondingly (see Fig. 1(a)). We discuss the timescales of the pulses in Sec. 2.3. Each pulse interacts with the mechanical mediator M twice during the protocol. After the interaction of the first pulse with the mechanical mode is complete, the former is sent to the delay line (see Fig. 1(a)) while the second pulse enters its cavity to interact with the mechanical mode. The operation is then repeated until the four interactions are performed. The block scheme of the protocol is depicted on Fig. 1(b). Note that the transducer between two optical modes requires only one one-sided optomechanical cavity, to which the pulses are directed in turns.

The mechanical mediator is coupled to the radiation modes by the means of four sequential quantum non-demolition (QND) interactions [38, 39]. The nondemolition interactions preserve always one quadrature variable (generalized position or momentum) of the single oscillator and perform therefore a partial quadrature exchange between the two oscillators. Only a single non-demolition variable is transferred between two systems during an individual interaction. This type of interaction was demonstrated to be a good candidate for constructing quantum interfaces between light and matter in purpose, for instance, to transfer a quantum state of light, what was proposed to realize with the help of two QND interactions [40]. The appropriate combination of such QND interactions of the modes A and B with mechanical mediator M allows driving the latter around a closed path in the phase space in such a way that the geometric phase appears. The geometric phase effect has been already used in quantum optics [41–43] and optomechanics where mechanical oscillator was coupled to a qubit [44] or light [45, 46]. As a result of the geometric phase imparted to the mechanical system the modes A and B appear to be coupled to each other but not to the mediator M that is brought back to the initial state. This result is

Optics EXPRESS

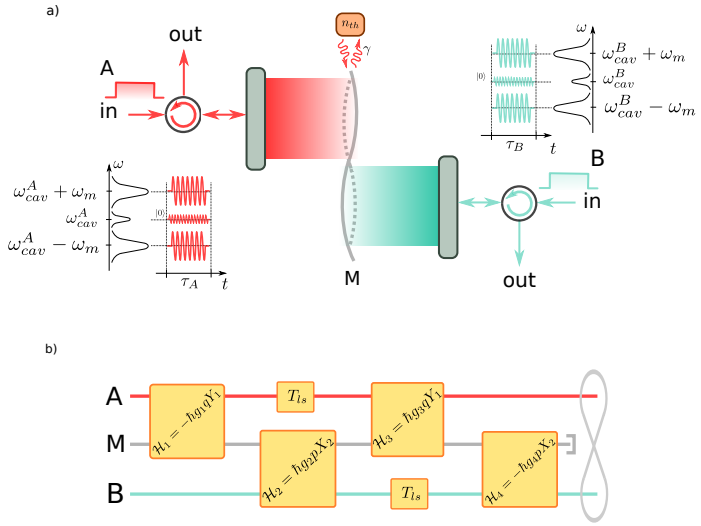

Fig. 1. (a) Schematic representation of the pulsed transducer interconnecting two radiation modes A and B which may be both optical as well as optical and microwave fields. The first amplitude-modulated pulse A (red) containing classical Stokes and anti-Stokes sidebands on $\omega^A_{\rm cav} \pm \omega_m$ and quantum fluctuations, which are in the vacuum state $|0\rangle$, on $\omega^A_{\rm cav}$, is sent to the first cavity to interact with mechanical mode M during the time τ_A . After the interaction is complete the pulse is sent to the delay line whereas the second pulse B (blue), being in the vacuum state $|0\rangle$ as well, interacts with M during τ_B within the second cavity. The interactions of the two pulses are then repeated one more time and both pulses are released to the outputs. The pulses do not overlap during the protocol. Radiation pulses are subject to losses $T_{\rm ls}$ and the mechanical mode is coupled at rate γ to the mechanical bath with mean occupation number $n_{\rm th}$. (b) Block-diagram of the sequence of the interactions between the pulses of modes A and B with the mechanical mediator M.

achievable due to specific character of the QND interaction, which qualify it to be a basic CV quantum gate. The transducer can therefore principally work for any initial state, even a very noisy one, of the mediator M.

In [14], it has been observed that the transducer can be stable against the small in-coupling and out-coupling losses of the radiation modes and losses in the delay lines, if the interaction gains of all four QND coupling are optimized. To reach sufficiently high gain of individual interactions with mediator and overall gain of the transducer, the enhancement by a high-Q cavity is necessary. The intracavity field is continuously leaking out the cavity. Simultaneously, the mechanical mode is also continuously damped to its noisy environment. Considerations of these imperfections go far beyond the basic stability check in [14]. In more realistic setup with the cavities and noisy mechanical environment, we therefore need to carefully analyze the performance of quantum transducer through noisy mediator and compare it to realistic parameters of the experimental schemes.

2.2. *Optomechanical interaction*

In a basic case an optomechanical system may be modeled as a single cavity mode of the optical resonator interacting with a single one of a mechanical oscillator via the radiation pressure (see Fig. 1(a)). The Hamiltonian of the optomechanical system may thus be written as [47]:

$$\mathcal{H} = \frac{\hbar\omega_c}{4}\left(X^2 + Y^2\right) + \frac{\hbar\omega_m}{4}\left(p^2 + q^2\right) - \frac{\hbar g_0}{4} q \left(X^2 + Y^2\right),$$

Optics EXPRESS

with X, Y and q, p being the quadratures of optical and mechanical modes correspondingly, with eigenfrequencies ω_c and ω_m. These quadratures satisfy commutation relations $[X, Y] = 2i$, $[q, p] = 2i$. The single-photon coupling rate g_0 is usually very small and thus the optomechanical interaction is very weak. To further enhance this interaction the cavity is pumped by a strong classical field. This approach allows to linearize the dynamics of the system and consider small quantum corrections to the mean classical values of the quadratures. The CV transducer is capable to generate Gaussian entanglement correlating these corrections.

To obtain a QND interaction we consider each pump to be resonant with the cavity and properly modulated at the mechanical resonant frequency which is assumed to exceed the corresponding cavity decay rates $\omega_m \gg \kappa_A, \kappa_B$ (the resolved sideband condition). After using a rotating wave approximation where we get rid of terms oscillating at $2\omega_m$, in terms of the quantum corrections defined at linearization, we obtain the following QND interaction Hamiltonian depending on the phase of the pump:

$$\mathcal{H}_i = \hbar \varkappa_i q Y_A \quad \text{or} \quad \mathcal{H}_j = \hbar \varkappa_j p X_B, \tag{1}$$

where $i = \{1, 3\}$, $j = \{2, 4\}$ denotes the interaction number, $\varkappa_1 = -g_1$, $\varkappa_2 = g_2$, $\varkappa_3 = g_3$, $\varkappa_4 = -g_4$ are individual interaction strengths of radiation modes with the mechanical one. The change of the sign of interaction strength can be obtained by a suitable adjustment of pump phase. The large intracavity photon number $n_{\mathrm{cav},i}$ corresponding to i-th interaction enhances the optomechanical coupling strength so that $g_i = g_0\sqrt{n_{\mathrm{cav},i}}$. See Fig. 1(b) for our choice of the sequence of the QND interactions. This sequence of interactions leads to the closed rectangular path in the phase space of mediator's variables q and p. Due to this the mediator becomes uncoupled from the radiation modes at the end of the protocol and does not affect its efficiency.

It is worth noting that another type of QND interaction in which the interaction time is very short compared to the mechanical period is possible. It was firstly introduced by Braginsky and coworkers [48] within the context of sensitive force detecting. This approach was studied within other optomechanical systems [49–51] and might be used to improve the robustness of the setup under consideration against thermal excitations.

In the Heisenberg picture the system of quantum Langevin Eqs. [52] describing the dynamics of the first and second QND interactions may be written as follows:

$$\begin{aligned}
\dot{X}_A &= -\kappa_A X_A + \sqrt{2\kappa_A} X_A^{\mathrm{in}} + \varkappa_1 q, & \dot{X}_B &= -\kappa_B X_B + \sqrt{2\kappa_B} X_B^{\mathrm{in}}, \\
\dot{Y}_A &= -\kappa_A Y_A + \sqrt{2\kappa_A} Y_A^{\mathrm{in}}, & \dot{Y}_B &= -\kappa_B Y_B + \sqrt{2\kappa_B} Y_B^{\mathrm{in}} - \varkappa_2 p, \\
\dot{q} &= -\frac{\gamma}{2} q + \sqrt{\gamma}\xi_{x1}, & \dot{q} &= -\frac{\gamma}{2} q + \sqrt{\gamma}\xi_{x2} + \varkappa_2 X_B, \\
\dot{p} &= -\frac{\gamma}{2} p + \sqrt{\gamma}\xi_{p1} - \varkappa_1 Y_A, & \dot{p} &= -\frac{\gamma}{2} p + \sqrt{\gamma}\xi_{p2},
\end{aligned} \tag{2}$$

where $\kappa_{A,B}$ are cavity decay rates of two corresponding cavities, γ is the mechanical damping coefficient, $X^{\mathrm{in}}, Y^{\mathrm{in}}$ are the optical (microwave) input quadratures, and $\xi_{xi,pi}$ are mechanical noise quadratures. Note, here the mechanical decoherence is present during whole the time of the entangling process, differently to simplified analysis in [14].

2.3. Adiabatic elimination and the entanglement generation

As it was mentioned previously we firstly consider symmetrical transducer putting equal decay rates $\kappa_A = \kappa_B = \kappa$ and assuming that κ is much larger than other rates in the dynamical Eqs. (2). The latter condition gives us a possibility to adiabatically eliminate the influence of the intracavtiy field by setting the derivatives of field quadratures equal to zero [12]. To find theoretical upper bound for generated entanglement, we assume here the mechanical mode decoherence-free putting $\gamma = 0$ and $\xi_{xi,pi} = 0$. Previous studies [53] show that the optomechanical QND interaction can be degraded by cavity memory effects due to finite linewidth κ and mechanical

Optics EXPRESS

bath. The consideration when these effects are eliminated therefore allows to estimate the ultimate performance of our transducer that we will later use to evaluate the realistic regimes. We refer to this adiabatic lossless and noiseless regime as the ideal one.

Using Langevin Eqs. and the input-output relations in the form

$$Q^{\text{out}}(t) = \sqrt{2\kappa}Q(t) - Q^{\text{in}}(t), \tag{3}$$

where $Q = \{X, Y\}$, we can show that the scheme depicted in Fig. 1 is equivalent to the QND interaction between modes A and B (see Appendix A for the rigorous derivation):

$$\begin{aligned} \mathcal{X}_A^{\text{out}} &= \mathcal{X}_A^{\text{in}} - \eta^2 \mathcal{X}_B^{\text{in}}, \quad & \mathcal{X}_B^{\text{out}} &= \mathcal{X}_B^{\text{in}}, & q &= q(0), \\ \mathcal{Y}_A^{\text{out}} &= \mathcal{Y}_A^{\text{in}}, & \mathcal{Y}_B^{\text{out}} &= \mathcal{Y}_B^{\text{in}} + \eta^2 \mathcal{Y}_A^{\text{in}}, & p &= p(0), \end{aligned} \tag{4}$$

where we have introduced effective QND coupling strength $\eta = g\sqrt{\frac{2\tau}{\kappa}}$, new quadratures $\mathcal{Q} = \{\mathcal{X}, \mathcal{Y}\}$, $\mathcal{Q} = \frac{1}{\sqrt{\tau}} \int_o^\tau Q(t)dt$ integrated over rectangular pulses, pulse duration time τ (at this point we assumed identical pulses $\tau_A = \tau_B = \tau$) and we have put all optomechanical couplings equal to each other and equal to g. As we can see from (4) the mechanical mode is completely traced out from these transformations due to geometric phase effect discussed in the Section 2.1 and 2.2.

Let us now discuss the main assumptions that led us to the Eqs. (4). First, in order to achieve the QND-type optomechanical interaction we use the rotating wave approximation, that requires the resolved-sideband condition ($\omega_m \gg \kappa$) and rather long pulses $\omega_m \tau \gg 1$. Second, to avoid the dispersion and justify the adiabatic elimination of the cavity modes we assume the pulses long enough compared to the inverse cavity bandwidth: $\kappa\tau \gg 1$. Finally, we assume the pulses to be shorter than the mechanical decoherence time: $n_{\text{th}}\gamma\tau \ll 1$. These inequalities could be combined into a single chain inequality

$$\omega_m \gg \kappa \gg \tau^{-1} \gg \gamma n_{\text{th}}.$$

Provided these conditions are fulfilled by a certain experimental setup we could expect of this setup the performance close to the desired one, described by the Eqs. (4).

We choose the entanglement of the modes A and B as the measure of the efficiency of the proposed transducer. Our consideration is limited to zero-mean Gaussian states as the initial states of the three modes are such (the vacuum states for the radiation ones and the thermal state for the mechanical mode) and the nondemolition interaction due to its linearity preserves the Gaussianity of the quantum states. Any zero-mean Gaussian state $\hat{\rho}$ of two modes A and B with quadratures $f = [\mathcal{X}_A, \mathcal{Y}_A, \mathcal{X}_B, \mathcal{Y}_B]^T$ can be fully described by the covariance matrix [54, 55] with elements $V_{ij} = \frac{1}{2}\text{Tr}\left[\hat{\rho}\left(f_i f_j + f_j f_i\right)\right]$. To numerically characterize the Gaussian entanglement we use logarithmic negativity defined as

$$E_{\text{N}} = \max\left[0, -\log_2 \nu_-\right], \tag{5}$$

with ν_- being the smallest symplectic eigenvalue of the partially transposed covariance matrix [56] that can be computed as follows:

$$\nu_- = \frac{1}{\sqrt{2}}\sqrt{\Sigma(V) - \sqrt{\Sigma(V)^2 - 4\det V}},$$

where

$$\Sigma(V) = \det\mathcal{V}_1 + \det\mathcal{V}_2 - 2\det\mathcal{V}_c,$$

Optics EXPRESS

with $\mathcal{V}_{1,2}$, $\mathcal{V}_c$ being 2×2 block-matrices composing the covariance matrix:

$$V = \begin{bmatrix} \mathcal{V}_1 & \mathcal{V}_c \\ \mathcal{V}_c^T & \mathcal{V}_2 \end{bmatrix}.$$

In the ideal case of adiabatic elimination of the intracavity modes and the absence of decoherence processes the symplectic eigenvalue for the two radiation modes A and B may be expressed in the following form:

$$\nu_-^0 = \sqrt{1 - 2\eta^4 \left[\sqrt{1 + \eta^{-4}} - 1\right]}. \tag{6}$$

The corresponding logarithmic negativity is nonzero for arbitrary $\eta > 0$ and monotonically increases regardless of the state of the mechanical mediator since in (4) the mechanical quadratures appear to be traced out of the transformations of the radiation modes. The dependence of the entanglement on the coupling strength is illustrated in Fig. 2 (solid purple curve). The main question is how close the realistic transducer can be to this idealized case.

3. Decoherence processes for the symmetrical transducer

In this section we consider the radiation loss and mechanical decoherence during whole time of the transducer operation. First we include radiation losses in the delay lines, then we study the influence of the mechanical bath and finally we combine both to explore their joint contribution. In each case we start with Eqs. (2) in adiabatic regime, from which we obtain the input-output relations, equivalent to (4) that in turn are used to analyze the coupling of the two radiation modes. These procedures allow a detailed analysis of decoherence in the quantum transducer.

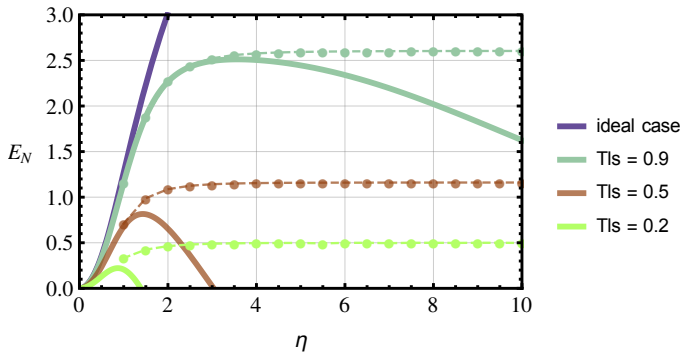

Fig. 2. Logarithmic negativity E_{N} as the function of QND coupling strength $\eta = g\sqrt{\frac{2\tau}{\kappa}}$ in the lossless adiabatic case (top purple curve) and in the case of radiation losses T_{ls} present (lower solid curves). See definition of T_{ls} in (7). Dotted lines correspond to the case of the optimal combination of the strengths of individual interactions. It demonstrates that radiation losses only partially limit generation of entanglement from the transducer. The optimization of gains is efficient only for large loss.

3.1. The influence of radiation losses

In the state-of-the-art cavity optomechanical systems the dominant cause of photon loss is the imperfect coupling of the cavity to the detection channel [15]. The ineffective in- and out-coupling can be modelled [57] as a beamsplitter admixing a part of vacuum to the signal. The other optical (microwave) imperfections including photon losses, imperfect mode matching, dark counts can be modelled by another beamsplitter [58]. Since all these photon leakage processes

Optics EXPRESS

are linear, they can all be combined and characterized by a single virtual beamsplitter with a given transmittance.

Finally, the imperfections preceding the very first and following the very last optomechanical interactions can be attributed to an imperfect, respectively, state preparation and detection, and can be left out for the analysis of the scheme. Therefore the only losses that are crucial for the performance of the protocol, are the ones taking place between the two sequential interactions of each of the radiation modes with the mechanical mode.

As explained above, we model the radiation losses by a virtual beamsplitter with the transmittance $T_{\rm ls}$ (so that $T_{\rm ls} = 1$ corresponds to the lossless case). After a mode with quadratures Q passes this beamsplitter the quadratures are transformed in the following way:

$$Q \to \sqrt{T_{\rm ls}} Q + \sqrt{1 - T_{\rm ls}} Q_{\rm ls} \tag{7}$$

with $Q_{\rm ls}$ being noise quadratures of vacuum.

To qualitatively allow for losses, we use the adiabatic consideration of the Sec. 2.3 and introduce these beamsplitters after the first and the second QND interactions (see Fig. 1(b)). For the sake of simplicity we assume damping coefficients $T_{\rm ls}$ to be the same for both modes. We consider the initial mechanical state to be in the ground state within this section.

The radiation losses break the entanglement monotonicity for increased interaction gain η. Instead, the maximal value of logarithmic negativity is reached for a finite coupling. This effect is obviously more pronounced at larger losses as may be seen from Fig. 2. For higher η smaller amounts of losses are sufficient to break the entanglement. In the limit of small losses $T_{\rm ls} \sim 1$ and weak coupling $\eta \ll 1$ the symplectic eigenvalue may be approximated in the following form:

$$\nu_- \simeq 1 - \frac{1}{2} \left(1 + T_{\rm ls}\right) \eta^2. \tag{8}$$

Losses therefore do not impose a threshold on the value of η — for any transmittance $T_{\rm ls}$ there is entanglement for arbitrarily low values of η. The coupling strength η however becomes bounded from above as shown in Fig. 2. We also see from this figure that the entanglement behavior near the origin is defined by the losses value — the approximated value of the derivative of the logarithmic negativity reads:

$$\left.\frac{\partial E_{\rm N}}{\partial \eta}\right|_{\eta \to 0} \simeq \frac{2}{\ln 2} \sqrt{T_{\rm ls}} \eta. \tag{9}$$

In the ideal case without any losses we compensate for the influence of the noisy mechanical mediator setting strengths of each interaction equal to each other. This makes the mechanical system to go along the closed path in the phase space. Losses lead to the imbalance in the system what destroys the closed form of the trajectory and makes it opened. This phase-space representation explains well why the behavior of the logarithmic negativity is non-monotonous with respect to g: in the presence of losses larger optomechanical coupling values lead to the larger imbalance of the phase-space trajectory what increases the coupling with the mediator. The imbalance can be corrected by making the strengths of individual QND interactions non-equal. We numerically find the optimal combination of gains η_i that brings the phase-space trajectory to be as close to the ideal closed one as possible and thus provides the maximum of the achievable entanglement given the constraint on coupling strengths $0 < \eta_i < \eta$. The coupling strength can be manipulated by change of interaction time or pumping. They are equivalent at this point. The result of the numerical optimization is presented in Fig. 2. The maximal logarithmic negativity $E_{\rm N}$ is plotted as a function of the upper boundary of the region over which we optimize. As we can see from this figure the optimization helps to restore high values of entanglement especially in case of high losses. In the case of small losses and small η non-optimized logarithmic negativity is close to the maximally achievable value (6).

Optics EXPRESS

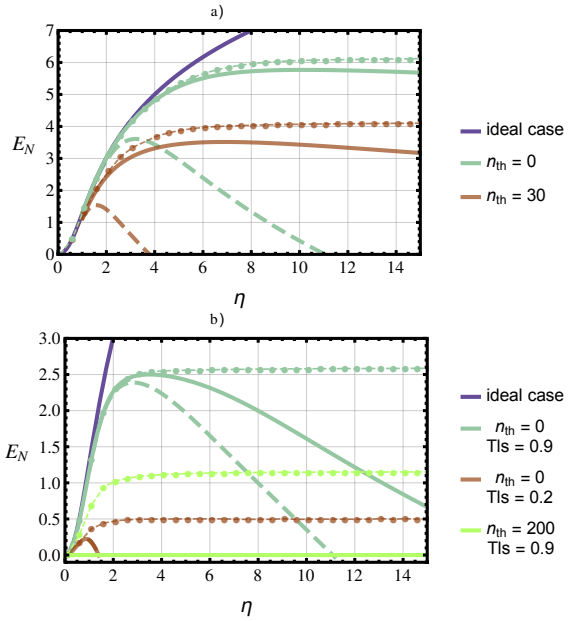

Fig. 3. Logarithmic negativity E_{N} as the function of the QND coupling $\eta = g\sqrt{\frac{2\tau}{\kappa}}$. For both top and bottom figures solid and dashed lines correspond to the non-optimized case with respectively g or τ varied, dotted lines with markers show the result of optimization. For the plots we used $\gamma = 1.5\times10^{-6}\,\kappa$. (a) Lossless case in presence of mechanical bath. Parameters are varied in the following regions: $0 \le g \le 0.4\kappa$ (for fixed $\tau = 687/\kappa$); $7\times10^2/\kappa \le \tau \le 9\times10^4/\kappa$ (for fixed $g = 0.03\kappa$). This plot demonstrates that mechanical bath does not affect the entanglement drastically and the optimization is efficient for larger mechanical bath occupation numbers. (b) Mechanical bath and radiation losses. Parameters here are varied in the following regions: $0 \le g \le 0.4\kappa$ (for fixed $\tau = 687/\kappa$); $7\times10^2/\kappa \le \tau \le 9\times10^4/\kappa$ (for fixed $g = 0.03\kappa$). This plot demonstrates that the performance of the proposed transducer may be quite high. Even for large bath occupation $n_{\mathrm{th}} = 200$ the optimization helps to reach significant values of the entanglement.

3.2. *The influence of the thermal environment*

Now we explore the proposed setup with the presence of the thermal mechanical environment and investigate its influence on the protocol performance. We consider the mechanical bath to be in the thermal state with mean occupation number n_{th}, being coupled to the mechanical mode at rate γ and we model it by the noisy quadratures $\xi_{xi,pi}$ in (2). We then solve the Eqs. (2) in adiabatic approximation and analyze the solution.

We assume that the damping force in (2) is the Markovian one, that the noisy quadratures satisfy commutation relations:

$$[\xi_{xi,pi}(t), \xi_{xi,pi}(t')] = 2i\delta(t-t'),$$

and in the high-temperature limit ($\hbar\omega \ll 2k_{\mathrm{B}}T$) they have the following property:

$$\langle \xi_{xi,pi}(t)\xi_{xi,pi}(t')\rangle = (2n_{\mathrm{th}}+1)\delta(t-t').$$

In the idealised adiabatic case each of interactions is parametrized by a single coupling parameter η_i, upper-bounded by maximal η. In presence of the mechanical bath the entanglement

Optics EXPRESS

changes differently with respect to changes in optomechanical coupling g and pulse duration τ even if those result in equal coupling parameter η. It is reflected in Fig. 3(a). Increasing of g causes deviation from the monotonic increase of entanglement which is seen more clearly for large values of g. If we instead increase the temporal duration of pulses τ to achieve same interaction gain η the entanglement is suppressed stronger because the influence of the mechanical bath is obviously more significant for longer interaction times. It is worth noting that for any thermal occupation arbitrarily low coupling η generates entanglement. We also note that in contrast to previous section, the derivatives near the origin are the same in this case, so in the limit $\eta \ll 1$ all curves coincide.

To reach maximal entanglement we again optimize the logarithmic negativity with respect to the four unequal optomechanical couplings g_i and different interaction times τ. In other words, we numerically find maximum of the function $E_{\mathrm{N}}(g_i, \tau_i)$ given the constraint that the corresponding effective couplings $\eta_i \equiv g_i\sqrt{2\tau_i/\kappa} < \eta$. The result of this optimization is presented in Fig. 3(a). The optimization proves especially useful for larger values of mean occupation number n_{th}: in contrast to the non-optimal case of equal couplings, in the optimized regime entanglement monotonically increases with η.

We would like to note that in the region of small values of the mean bath occupation number n_{th} and QND coupling η the entanglement values are close to the ones of the ideal adiabatic case. On the other hand, in the case of large n_{th}, which is of our interest, the entanglement increases at different rate than in the adiabatic regime.

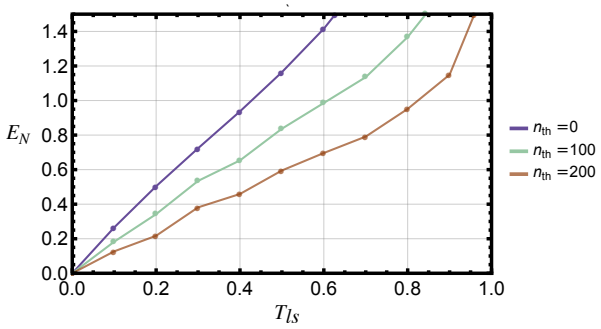

Fig. 4. Optimized logarithmic negativity as the function of the radiation losses T_{ls} for different values of the initial occupation number n_{th}. This figure reflects the fact that the influence of the radiation losses on the performance of the setup is more significant than the one of the thermal state of the mechanical mediator. For high value of losses ($T_{\mathrm{ls}} \ll 1$), independently from the value of initial occupation, the optimization does not help sufficiently.

3.3. *Joint influence of radiation losses and mechanical bath*

To complete the full analysis we consider the joint impact of the radiation losses and mechanical bath on the protocol performance which is reflected in Fig. 3(b). Apparently, joint influence of the radiation losses and mechanical bath is not critical. The transducer still keeps possibility to generate detectable entanglement, especially for low η. The figure shows that including radiation losses in addition to mechanical bath depresses the curves more for larger interaction strength in agreement with results of Section 3.1. The figure shows as well that the influence of the radiation losses is more drastic than the mechanical bath impact when both are present simultaneously. It is therefore important to keep the delay lines lossless.

We once again optimize the interaction parameters η_i by varying simultaneously optomechanical couplings g_i and the pulse durations τ_i to achieve maximum of entanglement (finding numerically maximum of the function $E_{\mathrm{N}}(g_i, \tau_i)$). We see that in the case of joint influence of

Optics EXPRESS

both mechanical bath and radiation losses the optimization helps sufficiently, especially for larger values of mean occupation number n_{th} and radiation losses. In particular, for high $n_{\mathrm{th}} = 200$ (and non zero losses) where for the non-optimized case the entanglement is not generated at all, the optimal regime shows sufficient values of logarithmic negativity which is a very promising result. In agreement with Section 3.1 the optimal entanglement saturates to a finite value apparently set by the value of losses and thermal noise. This can be regarded as a proof that the maximum achievable entanglement is as high as close the trajectory of the mechanical mode in the phase space can approach the closed one. It clearly demonstrates advantage of the optimization beyond the basic idea of geometric phase effect in the real pulsed cavity quantum transducer.

The optimization helps us as well to prove that the radiation losses have more dramatic negative impact on the transducer performance than the mechanical bath occupation. To confirm this point we also plot Fig.4 where the optimized logarithmic negativity as the function of radiation losses for different values of the initial occupation of the mechanical mode is presented. For small amount of losses the optimal logarithmic negativity has remarkable values even for quite high n_{th} whereas for small n_{th} and high losses the value of the maximal entanglement is significantly lower.

Since along this section we consider all main decorence processes, what brings us closer to the experiment, and the QND interaction is the basis of the proposed scheme, we would like to mention few experimental works related with the implementation of the QND interaction. In [59] the two-tone QND measurement in a superconducting electromechanical device was performed to detect back-action forces, reduce the quantum noise and the measurement imprecision. In another experiment [60] authors coupled a mechanical resonator to two microwave cavities and demonstrated the ability to perform a QND measurement of a single mechanical quadrature. This kind of measurement was further used to verify the preparation of a squeezed state in the mechanical oscillator. Despite the fact that these experiments weren't pulsed ones we made estimations about the QND coupling η available within them and found that it ranges from ~ 0.3 for the first one to ~ 0.6 for the second one. This demonstrates that state-of-the-art experimental possibilities allow to implement proposed device in the laboratory.

4. Asymmetrical transducer

Up to this moment we considered a symmetric transducer that could in principle be implemented with two radiation modes entering in turns a same optomechanical cavity. Now we switch to a principally different case, where a common mechanical mode is shared across two opto(electro-)mechanical cavities. This type of transducer allows coupling physically different modes of radiation, for instance, optical and microwave fields and was implemented in continuous wave regime in [25,26]. The performance of the transducer has been proven [25] to be partially limited by mechanical environment occupation. We show that our scheme is capable of reasonable performance at relatively high temperatures.

To characterize the system performance we introduce new effective QND coupling parameter $\eta' = \sqrt{2g_A g_B \sqrt{\frac{\tau_A \tau_B}{\kappa_A \kappa_B}}}$, where subscripts A and B denote optical and microwave systems correspondingly. We take into account losses in both modes and the mechanical bath.

Our analysis shows that in the case of small radiation losses and low mechanical bath occupation the optoelectromechanical transducer demonstrates very small deviations from maximally achievable performance even without optimization of the individual interactions what is reflected in Fig. 5. For the numerical parameters of the analysis we were inspired by two experimental works. The first one reported in [61] considers a nanoscale silicon optomechanical crystal and the second one [10] explores pulsed entanglement in an electromechanical system. Both these setups are operating in the pulsed regime what suits well our analysis and allows to estimate the feasibility of the future experimental implementation.

Optics EXPRESS

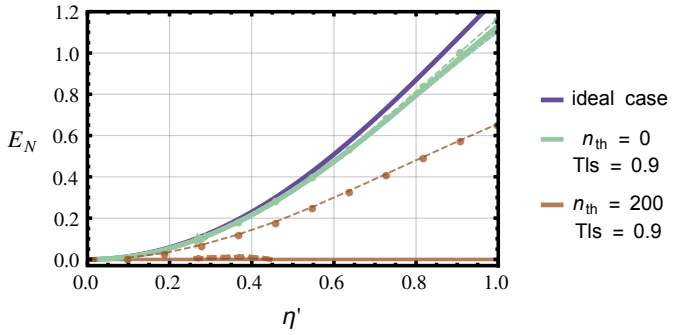

Fig. 5. Logarithmic negativity E_{N} as the function of QND coupling $\eta' = \sqrt{2g_A g_B \sqrt{\frac{\tau_A \tau_B}{\kappa_A \kappa_B}}}$ in the presence of mechanical bath and radiation losses for the case of asymmetric transducer. Solid lines correspond to the non-optimized cases with $g_{A,B}$ varied (for fixed $\tau_A = 690/\kappa_A$ and $\tau_B = 80/\kappa_B$), dashed lines — for the same case with $\tau_{A,B}$ increased (for fixed $g_A = 0.03\kappa_A$ and $g_B = 0.03\kappa_B$), dotted lines with markers stand for the optimized cases. Parameters are varied in the following regions: $0 \leq g_A \leq 0.07\kappa_A$; $0 \leq g_B \leq 0.1\kappa_B$; $2.2 \times 10^2/\kappa_A \leq \tau_A \leq 4.4 \times 10^3/\kappa_A$; $2.3/\kappa_B \leq \tau_B \leq 113/\kappa_B$ with $\kappa_B = 0.01 \times \kappa_A$ and $\gamma = 1.5 \times 10^{-4}\kappa_B$. Brown dashed line is responsible for the changes in τ_B while changes in τ_A in the corresponding region does not lead to any entanglement appearance thus demonstrating the asymmetry of the system. This figure demonstrates that the proposed transducer is feasible to entangle optical and microwave fields with the state of the art experimental possibilities.

To achieve maximum of entanglement we performed the same optimization of parameters as we did previously unless this time the coupling strengths $g_{A,B}$ and pulse durations $\tau_{A,B}$ for the two modes were bounded in individual regions in order to reflect the difference between the two modes. It means that we numerically maximized the function $E_{\mathrm{N}}(g_A, g_B, \tau_A, \tau_B)$ over the region $0 \leq g_A \leq 0.07\kappa_A$, $0 \leq g_B \leq 0.1\kappa_B$, $2.2 \times 10^2/\kappa_A \leq \tau_A \leq 4.4 \times 10^3/\kappa_A$, $2.3/\kappa_B \leq \tau_B \leq 113/\kappa_B$. In the case of small losses and low occupations this optimization does not help sufficiently (See Fig. 5 where green lines virtually overlap). However for the case of high thermal occupation $n_{\mathrm{th}} = 200$ where the entanglement is not observable (solid brown line on Fig. 5) the optimized curve demonstrates significant values of the logarithmic negativity (brown dotted line with markers).

It is worth noting that variation of τ_A and τ_B leads to different results in the entanglement behavior. As you may see for the case of $n_{\mathrm{th}} = 200$ variation of τ_B (dashed brown curve) leads to a region of non-zero entanglement, whereas variation of τ_A in the region of realistic parameters does not produce any entanglement. This is related to the fact that at large bath occupation number the individual subsystems are very sensitive to the changes in the pulse duration thus the asymmetry of the transducer becomes more apparent.

5. Conclusion

In this paper we explored pulsed optomechanical transducer which entangles two directly non-interacting radiation modes with assistance of a noisy mechanical mediator. We considered this system in the adiabatic regime for the case of symmetrical transducer interconnecting optical fields and we explored the realistic performance of this system in the presence of decoherence for both symmetrical and asymmetrical (allowing to connect optical to microwave radiation) cases. We have shown that the appropriate choice of parameters and their numerical optimization over controllable interaction time and pumping power allow promising performance of such

Optics EXPRESS

device for experiment. It goes beyond simple understanding based on the geometric phase effect [14]. Particularly, for the case of very high bath occupation number $n_{\rm th} = 200$ where the entanglement is not generated in the non-optimal case, the optimization shows significant values of achievable logarithmic negativity. It is apparently measurable value of the entanglement detectable in the experiments. This result is a good demonstration of potential efficiency of proposed pulsed transducer and a stimulation for the experimental teams. It opens the way for further exploration of pulsed transducers combining them with other physical platforms, like for example atoms [62, 63] or solid-state systems like NV centers [64, 65].

A. Derivation of the input-output relations in the adiabatic lossless regime

In this Appendix we derive in details the input-output relations for a single pulsed optomechanical interaction and outline the steps necessary to obtain the Eqs. (4). For simplicity we assume all the parameters to be equal for all pulsed interactions (e.g., $\kappa_A = \kappa_B = \kappa$, $\varkappa_i = \varkappa$).

In the adiabatic regime when $\kappa \gg \{\varkappa, \gamma\}$ the Eqs. of motion for the quadratures read in absence of the mechanical environment

$$\begin{aligned} 0 &= -\kappa X_A + \sqrt{2\kappa} X_A^{\rm in} + \varkappa q; & \dot{q} &= 0; \\ 0 &= -\kappa Y_A + \sqrt{2\kappa} Y_A^{\rm in}; & \dot{p} &= -\varkappa Y_A. \end{aligned}$$

The solution for the intracavity quadratures is straightforward

$$X_A(t) = \sqrt{\frac{2}{\kappa}} X_A^{\rm in}(t) + \frac{\varkappa}{\kappa} q(t), \qquad Y_A(t) = \sqrt{\frac{2}{\kappa}} Y_A^{\rm in}(t).$$

The solution for the mechanical quadratures is then

$$q(\tau) = q(0); \qquad p(\tau) = p(0) - \varkappa \int_0^\tau Y_A(t)dt = p(0) - \varkappa \sqrt{\frac{2}{\kappa}} \int_0^\tau Y_A^{\rm in}(t)dt \equiv p(0) - \varkappa \sqrt{\frac{2\tau}{\kappa}} \mathcal{Y}_A^{\rm in},$$

where we used the solution for $Y_A(t)$ and defined the new quadrature of the input noise $\mathcal{Y}_A^{\rm in}$. With help of the input-output relations (3) we can write the output quadratures of the leaking field corresponding to the first pulse, i.e., for $0 \le t \le \tau$:

$$X_A^{\rm out}(t) = X_A^{\rm in}(t) + \varkappa \sqrt{\frac{2}{\kappa}} q(0), \qquad Y_A^{\rm out}(t) = Y_A^{\rm in}(t). \tag{10}$$

In a fully similar fashion, for the second pulse the expressions for the quadratures read (for $\tau \le t \le 2\tau$)

$$X_B^{\rm out}(t) = X_B^{\rm in}(t), \quad Y_B^{\rm out}(t) = Y_B^{\rm in}(t) - \varkappa \sqrt{\frac{2}{\kappa}} p(\tau), \quad q(2\tau) = q(\tau) + \varkappa \sqrt{\frac{2\tau}{\kappa}} \mathcal{X}_B^{\rm in}, \quad p(2\tau) = p(\tau).$$

The second interaction of the the mode A with the optomechanical cavity is described by the Eqs. in the left column of (2) with substitution $\varkappa \to -\varkappa$. Furthermore, since the pulse of the mode A is sent back to the cavity to participate in the pulsed interaction during $2\tau \le t \le 3\tau$, the input field quadratures $\{X, Y\}_A^{\rm in}$ are defined by the output quadratures $\{X, Y\}_A^{\rm out}$ of the first pulse:

$$X_A^{\rm in}(t) = X_A^{\rm out}(t - 2\tau), \quad Y_A^{\rm in}(t) = Y_A^{\rm out}(t - 2\tau), \qquad \text{for } 2\tau \le t \le 3\tau.$$

Therefore, by advantage of (10)

$$Y_A(t) = \sqrt{\frac{2}{\kappa}} Y_A^{\rm in}(t) = \sqrt{\frac{2}{\kappa}} Y_A^{\rm out}(t - 2\tau) = \sqrt{\frac{2}{\kappa}} Y_A^{\rm in}(t - 2\tau), \qquad \text{for } 2\tau \le t \le 3\tau,$$

Optics EXPRESS

and consequently

$$p(3\tau) = p(2\tau) + \varkappa \int_{2\tau}^{3\tau} Y_A(t)dt = p(0) - \varkappa\sqrt{\frac{2}{\kappa}}\left[\int_0^{\tau} Y_A^{\mathrm{in}}(t)dt - \int_{2\tau}^{3\tau} Y_A^{\mathrm{in}}(t-2\tau)dt\right] = p(0).$$

Moreover, for $2\tau \le t \le 3\tau$

$$X_A^{\mathrm{out}}(t) = X_A^{\mathrm{in}}(t) - \varkappa\sqrt{\frac{2}{\kappa}}q(2\tau) = X_A^{\mathrm{in}}(t-2\tau) + \varkappa\sqrt{\frac{2}{\kappa}}q(0) - \varkappa\sqrt{\frac{2}{\kappa}}\left(q(0) + \varkappa\sqrt{\frac{2\tau}{\kappa}}\mathcal{X}_B^{\mathrm{in}}\right)$$
$$= X_A^{\mathrm{in}}(t-2\tau) - \frac{2\varkappa^2\sqrt{\tau}}{\kappa}\mathcal{X}_B^{\mathrm{in}}.$$

The other quadratures read after the third pulsed interaction (for $2\tau \le t \le 3\tau$)

$$q(3\tau) = q(2\tau), \quad Y_A^{\mathrm{out}}(t) = Y_A^{\mathrm{in}}(t-2\tau).$$

Integrating the expressions for $\{X, Y\}_A^{\mathrm{out}}(t)$ over the duration of the third pulsed interaction allows to write the final input-output relations for the mode A, as in (4):

$$\mathcal{X}_A^{\mathrm{out}} \equiv \frac{1}{\sqrt{\tau}}\int_{2\tau}^{3\tau} dt X_A^{\mathrm{out}}(t) = \frac{1}{\sqrt{\tau}}\int_0^{\tau} dt X_A^{\mathrm{in}}(t) - \frac{2\varkappa^2\tau}{\kappa}\mathcal{X}_B^{\mathrm{in}} \equiv \mathcal{X}_A^{\mathrm{in}} - \eta^2\mathcal{X}_B^{\mathrm{in}},$$
$$\mathcal{Y}_A^{\mathrm{out}} \equiv \frac{1}{\sqrt{\tau}}\int_{2\tau}^{3\tau} dt Y_A^{\mathrm{out}}(t) = \mathcal{Y}_A^{\mathrm{in}}.$$

Carefully analyzing the fourth pulsed interaction in a similar way one can show that $p(4\tau) = p(0)$, $q(4\tau) = q(0)$ and

$$\mathcal{X}_B^{\mathrm{out}} \equiv \frac{1}{\sqrt{\tau}}\int_{3\tau}^{4\tau} dt X_B^{\mathrm{out}}(t) = \mathcal{X}_B^{\mathrm{in}},$$
$$\mathcal{Y}_B^{\mathrm{out}} \equiv \frac{1}{\sqrt{\tau}}\int_{3\tau}^{4\tau} dt Y_B^{\mathrm{out}}(t) = \mathcal{Y}_B^{\mathrm{in}} + \eta^2\mathcal{Y}_A^{\mathrm{in}}.$$

Funding

Czech Science Foundation (GAČR) (GB14-36681G); Institutional Support of Palacký University (IGA-PřF-2017-008).

CHAPTER 6

Optomechanical transducer with ultrashort pulses

Next iteration in our study of possibilities to connect different quantum systems is the exploration of another parameter region - *bad cavity* or *unresolved sideband* regime [214].

This regime is of big interest among researchers now. In many of the optomechanical applications, like the construction of quantum information networks, interconnecting different systems (see the overview of opto- and electromechanical transducers in the previous section) or proposals to prepare massive mechanical oscillators in non-classical states, which can be of use for probing of quantum-to-classical transition [40] or mass sensing [124] and accelerometry [109], it is beneficial to use a low-frequency mechanical oscillator [148].

State-of-the-art technologies allow to cool mechanical oscillator to near its ground state in the unresolved sideband limit, like optical measurement-based feedback cooling [170] or with other techniques, to mention a few – methods of dissipative optomechanics [61], optomechanically-induced transparency [157] or using hybrid quantum systems [19, 99, 39]. However, an alternative approach is to engineer quantum non-demolition (QND) interactions between short pulses and mechanics [214]. QND interactions are frequently used for upload of quantum states [66, 135, 101] and can be considered as some sort of "basis" for this kind of tasks.

In this work, we extended our previous results for the quantum transducer, based on the geometric phase effect to the so-called *stroboscopic regime*. The contribution of this thesis is the demonstration of potential good performance of such a system under the influence of different decoherence processes and, what is important, for an almost arbitrary noisy mechanical mediator. We analyze different measures of quantum correlations between radiation modes – generalized and conditional squeezing, entanglement, and steering (See Sec.1.8 for a brief introduction of these metrics) at different levels of protocol's build-up. We also performed the same analysis for the system without a cavity. This work was done in close collaboration with the experimental group of Prof. Ulrik Andersen from Denmark Technical University and there is an expectation of the experimental realization of this scheme and further researches in the area of quantum transducers. Our exploration fits well to the current trend of development of

optomechanics, as the stroboscopic approach is very promising direction that continues to develop fast today [175, 42, 31].

New Journal of Physics
The open access journal at the forefront of physics

Deutsche Physikalische Gesellschaft DPG IOP Institute of Physics

PAPER • OPEN ACCESS

Quantum optomechanical transducer with ultrashort pulses

To cite this article: Nikita Vostrosablin *et al* 2018 *New J. Phys.* **20** 083042

New Journal of Physics
The open access journal at the forefront of physics

Deutsche Physikalische Gesellschaft DPG
IOP Institute of Physics

Published in partnership with: Deutsche Physikalische Gesellschaft and the Institute of Physics

OPEN ACCESS

RECEIVED
30 May 2018

REVISED
13 August 2018

ACCEPTED FOR PUBLICATION
21 August 2018

PUBLISHED
30 August 2018

PAPER

Quantum optomechanical transducer with ultrashort pulses

Nikita Vostrosablin[1], Andrey A Rakhubovsky[1,3], Ulrich B Hoff[2], Ulrik L Andersen[2] and Radim Filip[1]

[1] Department of Optics, Palacký University, 17 Listopadu 12, 771 46 Olomouc, Czechia
[2] Center for Macroscopic Quantum States (bigQ), Department of Physics, Technical University of Denmark, Fysikvej, D-2800 Kgs. Lyngby, Denmark
[3] Author to whom any correspondence should be addressed.

E-mail: nikita.vostrosablin@gmail.com, andrey.rakhubovsky@gmail.com, ulrich.hoff@fysik.dtu.dk, ulrik.andersen@fysik.dtu.dk and filip@optics.upol.cz

Keywords: quantum information, quantum optics, optomechanics

Abstract

We propose an optomechanical setup allowing quantum mechanical correlation, entanglement and steering of two ultrashort optical pulses. The protocol exploits an indirect interaction between the pulses mediated optomechanically by letting both interact twice with a highly noisy mechanical system. We prove that significant entanglement can be reached in the bad cavity limit, where the optical decay rate exceeds all other damping rates of the optomechanical system. Moreover, we demonstrate that the protocol generates a quantum non-demolition interaction between the ultrashort pulses which is the basic gate for further applications.

1. Introduction

According to the rules of quantum theory, a quantum state can be swapped between physical systems of the same dimension without any limitation. Such transduction between different physical platforms opens the full operation space for quantum technology [1]. Many different systems, however, do not interact directly and transduction can be realized only through a mediator. Mechanical systems are very good candidates for such mediators, interconnecting electromagnetic radiation of different or same frequencies and building universal transducers [2–5], as they can couple to various quantum systems including spins, cold atoms, Bose–Einstein condensates and photons of a wide range of frequencies. The interaction of light with mechanical oscillators is the subject of the special field of optomechanics. The principle of interconnecting radiation fields with help of a mechanical mediator has been demonstrated in a number of experiments connecting optical and microwave fields [6–10]. Experiments have been reported connecting optical to optical [11–13] and microwave to microwave [14] fields. Theoretical proposals for building transducers connecting light and microwave radiation in the continuous-wave regime [15–21] have also been put forward.

To be fully compatible with modern hybrid quantum optics [22–25], pulsed versions of quantum optomechanics have been initiated in two regimes: exponentially modulated pulses with duration significantly exceeding the mechanical period [26] and high-intensity pulses which are very short compared to the mechanical period [27]. The former has been used to demonstrate Gaussian entanglement between microwave field and mechanical oscillator [28], quantum state transfer [29, 30], non-classical photon–phonon correlations [31, 32], entanglement between distant mechanical oscillators [33], and also motivated other theoretical ideas [34–36]. Likewise, the latter approach, also known as stroboscopic, has stimulated a number of experimental [37] and theoretical [38, 39] works. Recently, quantum transducers based on geometric phase effect have been proposed [40] and analysed in the regime of long pulses [41]. There it was shown that by proper optimization an entangling quantum non-demolition (QND) interaction [27, 42] can be established between two systems mediated by a mechanical oscillator, without the need to cool the latter close to the ground state. The idea has been applied to generate entanglement between optical and microwave field [28]. Such a scheme requires high-Q cavity systems, resolved-sideband regime, and intensive two-tone driving to eliminate the destructive free mechanical evolution and thereby reach nearly ideal performance. It, however, still remains unclear, whether the geometric phase effect will be sufficient to obtain a robust transducer in the stroboscopic regime with

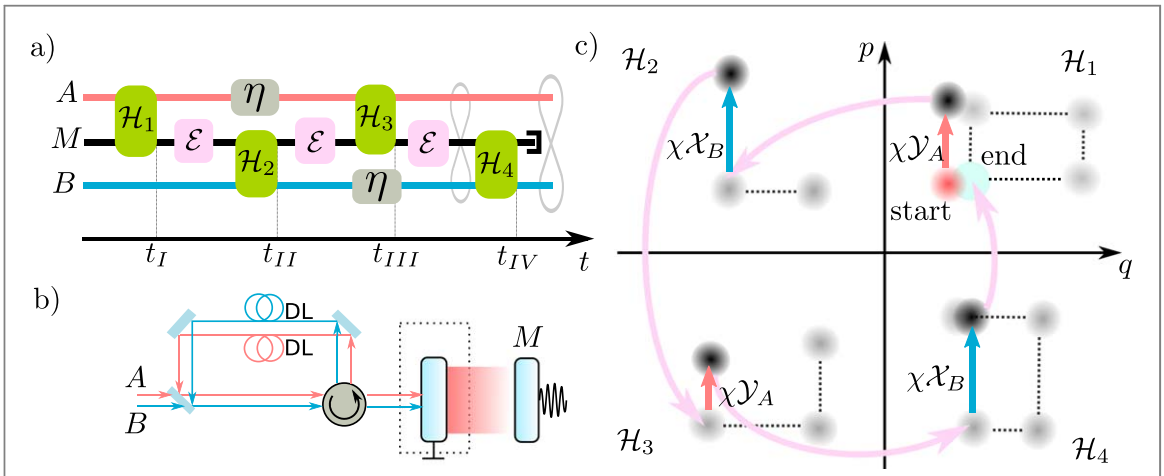

Figure 1. (a) The block-scheme of the transducer. Optical modes of possibly different wavelengths A and B interact sequentially with the mechanical system M by four QND interactions with Hamiltonians $\mathcal{H}_i$. Between these interactions the mechanical mode undergoes free evolution through one quarter of the mechanical period while interacting with the mechanical environment ($\mathcal{E}$) and the optical modes are subject to optical losses (η). t_i denote corresponding interaction end moments. (b) A possible experimental implementation of the protocol. The mirror (dashed) is optional. Optical modes A and B interact alternately with the mechanical system M. DL—delay lines. (c) Path of the mechanical mode of the transducer in phase-space. The mechanical system starts in the first quadrant. Then the momentum kick by the mode A occurs (red vertical arrow). After that the mechanical system evolves freely per one quarter of the mechanical period, ending up in the second quadrant (purple arrow). Subsequently the interaction with the mode B occurs. The procedure is repeated until the system reaches the 'end' point. In the ideal case the trajectory of the mechanical mode in the phase space is closed and this mode appears to be effectively decoupled from the optical ones. $\mathcal{X}_A$ and $\mathcal{Y}_B$ stand for amplitude and phase quadratures of systems A and B, respectively, and χ is the interaction strength.

ultrashort pulses without entering the sideband resolved regime, and potentially without cavity. Such a proposal will stimulate a much broader class of feasible quantum transducers mediated by mechanical systems.

In this paper we propose a pulsed stroboscopic quantum transducer based on the geometric phase effect, which generates a QND coupling between optical fields of possibly different frequencies. We show that for state-of-the-art optomechanical systems the proposed scheme performs very well under the influence of different decoherence processes and for an almost arbitrarily noisy mechanical mediator. We also analyse the gradual build-up of non-classical correlations, entangling power and quantum steering after different numbers of sequential pulses, demonstrating that even simplified versions of the protocol produce quantum correlations. It allows for a verification of its performance in the middle of the transducer protocol. In addition we prove that this protocol is also efficient in a system which does not contain an optical cavity.

2. Protocol

We propose a setup allowing to entangle two optical modes (possibly of different wavelengths), A and B, applying sequential interactions with a mechanical oscillator. We start by considering a mechanical mode of the optomechanical cavity (as in figure 1), although the protocol can be extended to a system without the cavity (see section 8). The optomechanical cavity is typically a system consisting of two modes, an optical and a mechanical one. In the presence of a strong classical optical pump at the cavity resonance, the inherently nonlinear optomechanical interaction [43] can be linearized. In the frame rotating with the pump frequency the Hamiltonian of the system including this linearized interaction, reads [44]

$$\mathcal{H}(t) = \frac{1}{2}\hbar\omega_m(q^2 + p^2) + \hbar g\alpha(t)(X\cos\theta + Y\sin\theta)q, \tag{1}$$

where the first summand describes the free evolution of the mechanical mode and the second one describes the optomechanical coupling of the optical mode with quadratures (X,Y) and the mechanical mode with dimensionless displacement q and momentum p, such that $[X, Y] = [q, p] = i$. Here g is the single-photon optomechanical coupling rate, ω_m is the mechanical frequency and θ is the optical quadrature phase. The mean intracavity amplitude $\alpha(t)$ induced by the pump is assumed to have constant value $\alpha = 4\sqrt{N/\kappa\tau}$ over the pulse duration τ, where κ is the energy decay rate of the cavity. This amplitude is normalized in such a way that the average number of photons in the corresponding pulse is $N = \alpha^2\tau\kappa/16$. If the interaction time is short compared to the mechanical period, as, for instance, in the experiment [37], the free evolution of the mechanical mode can approximately be ignored, so that only the second (coupling) term in the Hamiltonian (1) remains. Numerical estimations prove that the free mechanical evolution during the pulsed interaction does indeed not influence the entanglement of the modes significantly. This step significantly simplifies the resonant

optomechanical interaction, because we can reach two different QND interactions associated with $\theta = 0, \pi/2$ in (1), without any change in the non-demolition variables X, q and Y, q.

Our proposed protocol consists of four sequential pulsed QND interactions (two for each of the optical modes) separated by a quarter of the period of the free mechanical evolution during which there is no interaction with any of the optical modes (see figure 1(c)). Between the optomechanical interactions with the mechanical oscillator, each of the optical modes is directed to the delay line. The Hamiltonians of the individual pulsed interactions read (the quadratures of modes A and B are labelled with corresponding subscript)

$$\mathcal{H}_{1,3} = -4\hbar g\sqrt{N_{1,3}/\kappa\tau}\, Y_A q, \quad \mathcal{H}_{2,4} = 4\hbar g\sqrt{N_{2,4}/\kappa\tau}\, X_B q. \tag{2}$$

Each of the QND interactions shift the momentum of the mechanical mode and also one of the quadratures of the corresponding optical mode. Combined with the precisely timed free evolutions of the mechanical mode that effectively swap the mechanical quadratures $q \leftrightarrow p$ this ideally allows the mechanical mode to follow a closed path in phase space (figure 1 (c)). The geometric phase induced by this closed path enables coupling of the optical modes while keeping the mechanical mode decoupled from those.

For the QND interaction with Hamiltonian $\mathcal{H}_1 = -4\hbar g\sqrt{N_1/\kappa\tau}\, Y_A q$ (for the phase $\theta = 0$) the quantum Langevin equations take the following form [3, 45]:

$$\begin{aligned} \dot{X}_A &= -\frac{\kappa}{2}X_A + \sqrt{\kappa}X_A^{\mathrm{in}} - 4g\sqrt{N_1/\kappa\tau}\, q, \quad \dot{q} = 0, \\ \dot{Y}_A &= -\frac{\kappa}{2}Y_A + \sqrt{\kappa}Y_A^{\mathrm{in}}, \quad \dot{p} = 4g\sqrt{N_1/\kappa\tau}\, Y_A. \end{aligned} \tag{3}$$

Here X_A^{in}, Y_A^{in} are the quadratures of the input optical fluctuations with commutator $[X^{\mathrm{in}}(t),\, Y^{\mathrm{in}}(t')] = \mathrm{i}\delta(t - t')$.

We assume the optical decay rate κ to be much larger than other characteristic rates of the system—inverse pulse duration τ^{-1}, mechanical frequency ω_m and the enhanced optomechanical coupling strength $4g\sqrt{N/\kappa\tau}$ which is well justified in certain experiments [46, 47]. This corresponds to the adiabatic regime where the optical mode reacts instantaneously to influences. This allows us to set $\dot{X}_A = \dot{Y}_A = 0$ in (3). Thus with the help of the input–output relations [48] in the form

$$X_A^{\mathrm{out}}(t) = \sqrt{\kappa}X_A(t) - X_A^{\mathrm{in}}(t), \quad Y_A^{\mathrm{out}}(t) = \sqrt{\kappa}Y_A(t) - Y_A^{\mathrm{in}}(t) \tag{4}$$

we can write down the solution of (3):

$$\begin{aligned} X_A^{\mathrm{out}}(t) &= X_A^{\mathrm{in}}(t) - \frac{8g\sqrt{N_1}}{\kappa\sqrt{\tau}}q(0), \quad q(t) = q(0), \\ Y_A^{\mathrm{out}}(t) &= Y_A^{\mathrm{in}}(t), \quad p(t) = p(0) + \frac{8g\sqrt{N_1}}{\kappa\sqrt{\tau}}\int_0^\tau Y_A^{\mathrm{in}}(t)\mathrm{d}t. \end{aligned}$$

Now we introduce new optical modes with quadratures $\mathcal{Q} = \frac{1}{\sqrt{\tau}}\int_0^\tau Q(t)\mathrm{d}t$ and QND interaction strength $\chi_1 = \frac{8g\sqrt{N_1}}{\kappa}$, and integrate the equations for X^{out} and Y^{out} over the duration of the first pulsed interaction. We then obtain the standard QND form [49] of interaction:

$$\begin{aligned} \mathcal{X}_A^{\mathrm{out}} &= \mathcal{X}_A^{\mathrm{in}} - \chi_1 q(0), \quad q(\tau) = q(0), \\ \mathcal{Y}_A^{\mathrm{out}} &= \mathcal{Y}_A^{\mathrm{in}}, \quad p(\tau) = p(0) + \chi_1\mathcal{Y}_A^{\mathrm{in}}, \end{aligned} \tag{5}$$

valid when $\kappa \gg \tau^{-1} \gg \omega_m$. Equations (5) describe the ideal unitary coupling between the new temporal modes which are not affected by decoherence during the short period of the pulse. We apply the same approach for the remaining interactions.

3. Decoherence processes

In this section we describe the model of the decoherence processes in the system. The most fundamental decoherence processes are that of mechanical decoherence due to the coupling to the thermal environment and optical losses.

3.1. Mechanical thermal noise

Since the pulsed optomechanical interactions in our scheme are very short compared to the mechanical period ($\tau^{-1} \gg \omega_m$) and the thermal decoherence time ($\tau^{-1} \gg \Gamma n_{\mathrm{th}}$), it is safe to neglect the free evolution of the mechanical mode for the time of the interaction. Between the interactions, however, the mechanical mediator is subject to damped harmonic oscillations that last for a quarter of mechanical period ($\tau_* = \pi/(2\omega_m)$). This evolution is described by the following equations of motion

$$\dot{q} = \omega_m p, \quad \dot{p} = -\omega_m q + \sqrt{2\Gamma}\,\xi(t) - \Gamma p, \tag{6}$$

where Γ is the mechanical damping coefficient, $\xi(t)$ is the thermal noise operator that obeys the autocorrelation $\langle \xi(t)\xi(t')\rangle = (n_{\rm th} + \frac{1}{2})\delta(t - t')$ with $n_{\rm th}$ being the mean occupation number of the mechanical bath.

We can formally solve the equations (6) and find the transformation of the mechanical mode for a high-Q mechanical oscillator that satisfies $\Gamma \ll \omega_m$:

$$q(\tau_*) = \mathrm{e}^{-\Gamma\tau_*/2}[p(t) + \Delta q(\tau_*)], \quad p(\tau_*) = \mathrm{e}^{-\Gamma\tau_*/2}[-q(t) + \Delta p(\tau_*)], \tag{7}$$

with Δq, Δp being mechanical noise operators defined as:

$$\Delta q(t) = \sqrt{2\Gamma}\int_0^t \mathrm{d}t' \mathrm{e}^{\Gamma t'/2}\sin(\omega_m(t - t'))\xi(t'),$$
$$\Delta p(t) = \sqrt{2\Gamma}\int_0^t \mathrm{d}t' \mathrm{e}^{\Gamma t'/2}\cos(\omega_m(t - t'))\xi(t').$$

These operators have the following properties:

$$\langle \Delta q^2(\tau_*)\rangle = \langle \Delta p^2(\tau_*)\rangle = \left(n_{\rm th} + \frac{1}{2}\right)\frac{\pi\Gamma}{2\omega_m},$$
$$\langle \Delta q(\tau_*)\Delta p(\tau_*)\rangle = \left(n_{\rm th} + \frac{1}{2}\right)\frac{\Gamma}{\omega_m},$$

which resembles standard Markovian noise [50].

3.2. Optical losses

The optical losses in the system stem from imperfect coupling to the optomechanical cavity, mismatch of modes, propagating photon losses etc. Importantly, all these processes are linear and this leads to admixture of vacuum. Therefore the effect of losses on an optical mode with quadratures Q can be modelled as a beamsplitter with vacuum in the unused port. The corresponding phase-insensitive transformations of quadratures Q read

$$Q \to \sqrt{\eta}\,Q + \sqrt{1 - \eta}\,Q_N, \tag{8}$$

with Q_N being the quadrature of the optical vacuum noise ($\langle Q_N^2\rangle = \frac{1}{2}$) and η, the transmittance of the beamsplitter. For example, when $\eta = 1$ there are no optical losses in the system.

We introduce the optical loss after the first QND interaction for the optical mode A and after the second QND interaction for the optical mode B (see figure 1(a) for reference). The optical losses before the first and after the last interactions are not taken into account since they may be considered as not being inherent in the protocol itself and may be easily added to the final results if needed.

We have now described each of the evolution blocks constituting figure 1 in terms of input–output relations for the quadratures of the modes affected. Sequentially applying this formalism, we can obtain expressions for the quadratures at a certain instant of time, from which we can evaluate the required parameters, in particular, the covariance matrices.

4. Generalized squeezing, conditional squeezing, Gaussian entanglement and Gaussian quantum steering

A zero-mean Gaussian state $\hat{\rho}$ of a bipartite system $A + B$ with the quadratures forming a vector $f = (X_A, Y_A, X_B, Y_B)$ can be completely described by the covariance matrix [51, 52] with elements $V_{ij} = \frac{1}{2}\,\mathrm{Tr}\,[\hat{\rho}(f_i f_j + f_j f_i)]$. This matrix has the block structure

$$V = \begin{bmatrix} V_A & C \\ C^T & V_B \end{bmatrix},$$

where V_A, V_B and C are the 2×2 matrices describing individual variances and co-variances correspondingly. Superscript ^{T} means transposition.

The mathematical formalism for Gaussian states allows us to investigate different signatures of quantum mechanical correlations between two modes [53]. We will use four suitable Gaussian quantifiers: generalized squeezing, conditional squeezing, entanglement and steering. They have gradually higher demand on quantity of quantum correlations between A and B.

Generalized squeezing [54] specifies squeezing available in the system by global passive transformations. It is also the signature that the covariance matrix corresponds to a non-classical state. This quantity is defined as the minimal eigenvalue of the covariance matrix.

Conditional squeezing procedure may be described in the following way [55]. Let us perform homodyne detection of the amplitude quadrature of mode B. After this procedure the covariance matrix of system A is transformed in the following way:

$$V_A' = V_A - \frac{1}{V_{B,11}} C\Pi C^{\mathrm{T}}, \tag{9}$$

with $\Pi = \mathrm{diag}(1,\ 0)$. The conditional squeezing is possible when the smallest eigenvalue of V_A' (which we will later refer to as *conditional variance* and which in the simple case of diagonal V_A' corresponds to the variance of amplitude or phase quadrature of system A) is smaller than the shot-noise variance, established by the Heisenberg's uncertainty principle. An analogous procedure can be applied to check for the possibility of obtaining conditional squeezing of system B. Conditional squeezing justifies that generalized squeezing can be, at least partially, induced in one mode by a measurement of the other one.

The state ρ_{AB} of a bipartite system is called an entangled state if it cannot be presented in the form $\rho_{AB} = \sum_i c_i \rho_i^A \otimes \rho_i^B$ with $\rho_i^{A,B}$ being the states of the first and second systems correspondingly and c_i being the probabilities. A measure of entanglement is the logarithmic negativity defined for Gaussian states as follows [53]:

$$E_{\mathrm{N}} = \max\left[0,\ -\ln 2\nu_-\right], \tag{10}$$

where ν_- is the smallest symplectic eigenvalue of the covariance matrix of the partially transposed state. This eigenvalue can be calculated in the following way:

$$\nu_- = \frac{1}{\sqrt{2}}\sqrt{\Sigma_V - \sqrt{\Sigma_V^2 - 4\det V}}, \quad \Sigma_V = \det V_A + \det V_B - 2\det C.$$

The modes A and B are entangled when $E_{\mathrm{N}} > 0$.

The logarithmic negativity constitutes an upper bound to the distillable entanglement, and is a proper entanglement monotone that can be easily evaluated provided a covariance matrix and does not require complicated optimization. Therefore we prefer it to other entanglement measures, including Duan's criterion [51]. The latter could be used as well, but it requires a proper optimization of the combination of the quadratures of the subsystems A and B.

The state ρ_{AB} is $A\rightarrow B$ steerable if after performing measurements on subsystem A, it is possible to predict the measurement results of system B with an accuracy better than for a pure separable minimum uncertainty state. To quantify the steering of bipartite Gaussian systems we use the steerability [56]:

$$G_{A\rightarrow B} = \max\left\{0,\ -\sum_{j:0<\nu_j<1} \ln \nu_j^B\right\}, \tag{11}$$

where $\{\nu_j^B\}$ are the orthogonal eigenvalues of the matrix $|\mathrm{i}\Omega M^B|$ with $\Omega = \mathrm{antidiag}(1,\ -1)$ and $M^B = V_B - C^T V_A^{-1} C$. The steerability in opposite direction from party B to party A may be calculated by replacing matrices V_A and V_B.

5. Basic quantum transducer

To understand the process of building quantum correlations and entanglement, we will analyse the correlations after output of each step of the protocol. After only two QND interactions the transducer is capable of building correlations sufficient for conditional squeezing of at least one optical mode. The presence of this non-classical aspects of correlations would be a demonstration of the feasibility of the basic protocol.

We consider a sequence of interactions, where mode A first interacts with the mediator M with Hamiltonian $\mathcal{H}_1$, then the mechanical system evolves quarter of a mechanical period and after that mode B interacts with the mediator with Hamiltonian $\mathcal{H}_2$ (see figure 1(a)). We start with the simplest case when there is no decoherence in the system and all individual QND interaction strengths are equal to χ. The optical modes are initially in vacuum, and the mechanical mode in a thermal state with occupation n_0. When each of the two optical modes have interacted with the mediator, the transformations of quadratures are as follows:

$$\begin{aligned} &\mathcal{X}_A^{\mathrm{out}} = \mathcal{X}_A^{\mathrm{in}} - \chi q(0), \quad q^{\mathrm{II}} = -q(0) - \chi\mathcal{X}_B^{\mathrm{in}}, \quad \mathcal{X}_B^{\mathrm{out}} = \mathcal{X}_B^{\mathrm{in}}, \\ &\mathcal{Y}_A^{\mathrm{out}} = \mathcal{Y}_A^{\mathrm{in}}, \quad p^{\mathrm{II}} = -p(0) - \chi\mathcal{Y}_A^{\mathrm{in}}, \quad \mathcal{Y}_B^{\mathrm{out}} = \mathcal{Y}_B^{\mathrm{in}} - \chi p(0) - \chi^2\mathcal{Y}_A^{\mathrm{in}}, \end{aligned} \tag{12}$$

where $q(0)$ and $p(0)$ are the mechanical quadratures before the first optomechanical interaction.

After homodyning an arbitrary quadrature $X_B\cos\Theta + Y_B\sin\Theta$ of system B, the covariance matrix of system A takes the form: $V_A^{\mathrm{out}'} = \mathrm{diag}(\frac{1}{2} + \chi^2\langle q(0)^2\rangle,\ \sigma_A^{\mathrm{II}})$, where

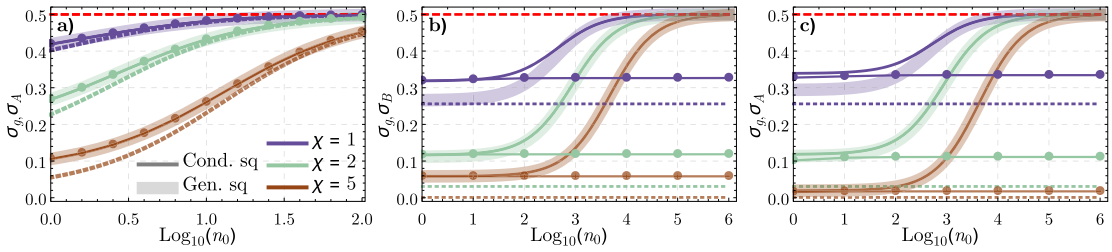

Figure 2. Generalized and conditional squeezing after two (a), three (b) and four (c) QND interactions as a function of the initial mechanical occupation (note different axis range in (a) and (b), (c)). Corresponding generalized (σ_g) and conditional variances ($\sigma_{A,B}$) after the phase quadrature of the system B (A) was homodyned as the function of initial occupation of the mechanical mode M for different values of the QND coupling strength. Darker colours denote conditional squeezing and lighter colours denote generalized one. Solid lines stand for the case including all the decoherence processes, dotted ones stand for ideal cases without any decoherence and lines with markers are responsible for the optimized values. Conditional squeezing coincides with generalized one for every case except the case of $\chi = 1$ in (b) and (c). Parameters used are the following: $\omega_m = 4 \times 10^{-3}\kappa$, $\Gamma = 6 \times 10^{-10}\kappa$, $g = 4 \times 10^{-7}\kappa$, $\tau = 16/\kappa$ what corresponds to the recent experiment [57]. We also assume $n_{\mathrm{th}} = 10^6$ and $\eta = 0.9$.

$$\sigma_A^{\mathrm{II}} = \frac{1}{2}\left[\frac{1 + 2\chi^2\langle p(0)^2\rangle \sin^2\Theta}{1 + \chi^2\sin^2\Theta(2\langle p(0)^2\rangle + 1)}\right] \leqslant \frac{1}{2}\left[1 - \frac{1}{1 + 2\chi^{-2}\langle p(0)^2\rangle + \chi^{-4}}\right]. \tag{13}$$

The diagonal elements of the covariance matrix of a Gaussian system (in the diagonal form) show uncertainties in its quadratures. When one of the elements is below the shot noise level, the system is squeezed. Therefore, homodyne detection on system B is capable of squeezing the mode of system A. This is already a nontrivial aspect of Gaussian quantum correlations build-up achieved using the mechanical mediator. The possibility of squeezing can be understood from the equations (12). Homodyne measurement of $\mathcal{Y}_B^{\mathrm{out}}$ effectively reduces its variance to zero. Since the quadrature $\mathcal{Y}_A^{\mathrm{in}}$ constitutes a part of this quadrature, its variance could as well be reduced as a result of this measurement, that is it will become squeezed. To achieve significant squeezing, however, one needs the coupling to be strong enough to secure $\chi^2 \gg \langle p(0)^2\rangle = n_0 + \frac{1}{2}$, so that the dominant term in the expression for $\mathcal{Y}_B^{\mathrm{out}}$ is provided by fluctuations in $\mathcal{Y}_A^{\mathrm{in}}$ and not by the initial mechanical fluctuations in $p(0)$. Formally this amounts to the need to decrease the denominator of the fraction in (13). This means that for realistic values of the coupling $\chi \leqslant 10$, squeezing can be observed for a mechanical occupancy of $n_0 \approx 100$. Cooling the phonon number to this level is achievable within the sideband unresolved regime using different techniques such as active feedback cooling [58], hybrid systems [59], optomechanically induced transparency [46] or dissipative optomechanics [60]. Experimentally, feedback cooling has allowed for an occupancy of $n_0 = 5$ of a mechanical oscillator [61, 62] which can be improved to yield ground state cooling using a higher detection efficiency or using squeezed state probing [63]. These experiments on near ground state cooling have been performed in a 4 K cryostat, but with the development of new high-Q mechanical oscillators [64–66], ground state cooling in a room temperature environment is within reach.

To determine the full dynamics, including mechanical decoherence and optical losses, we resort to numerical estimations. The results are presented in figure 2(a). The good correspondence between the lossless solution and the one with losses should be noted. This indicates that the approximate model captures the system really well and that the initial occupation is the main source of decoherence.

Our estimations show that in the case of two QND interactions conditional squeezing σ_A is identical to the generalized one σ_g meaning that the former reaches the maximal possible value of squeezing in this system (darker and lighter lines coincide in figure 2(a)).

Conditional squeezing of mode B is, however, not possible as no information about B is written into A after only two QND interactions.

Our analytical and numerical estimates of the logarithmic negativity and the steerability show that there is no entanglement between modes A and B and that steering is not possible in either direction.

6. Advanced quantum transducer

We now proceed to consider 3 interactions and investigate different measures of quantum correlations between the optical modes. In the ideal case without decoherence when the interaction strengths are equal, the transformations of quadratures take the following form:

$$\mathcal{X}_A^{\rm out} = \mathcal{X}_A^{\rm in} + \chi^2\mathcal{X}_B^{\rm in}, \quad q^{\rm III} = q(0) + \chi\mathcal{X}_B^{\rm in}, \quad \mathcal{X}_B^{\rm out} = \mathcal{X}_B^{\rm in},$$
$$\mathcal{Y}_A^{\rm out} = \mathcal{Y}_A^{\rm in}, \quad p^{\rm III} = -p(0), \quad \mathcal{Y}_B^{\rm out} = \mathcal{Y}_B^{\rm in} - \chi p(0) - \chi^2\mathcal{Y}_A^{\rm in}. \tag{14}$$

System B is not affected by the third interaction, thereby the measurement performed on it will provide the same squeezing of mode A as after only the two interactions. As we see from these equations the initial state of the mechanical oscillator is completely traced out from system A, and now quadrature $\mathcal{X}_A^{\rm out}$ contains information about $\mathcal{X}_B^{\rm in}$. From this we conclude that by homodyning system A in this ideal case one can perform squeezing of system B and the amount of squeezing does not depend on the initial occupation of the mechanical oscillator. The conditional variance in this case is expressed as $\sigma_B^{\rm III} = \frac{1}{2(1+\chi^4)}$ and is defined only by the value of the QND coupling strength.

When there are optical losses in the system, the conditional variance becomes dependent on the initial occupation of the mechanical system and may be approximated for small losses by:

$$\sigma_B^{\rm III} \simeq \frac{1}{2}\left[\frac{1}{1+\chi^4} + (1-\eta)\frac{\chi^4}{1+\chi^4} + n_0\frac{\chi^5(1-\eta)^2}{8(1+\chi^4)^2}\right]. \tag{15}$$

The optimization of σ_B with respect to unequal individual QND interaction strengths $\chi_{1,2,3}$ allows us to partially compensate for the influence of optical losses and to make σ_B independent of n_0 and equal to $\sigma_B|_{n_0=0}$. The presence of the mechanical bath defines the maximal achievable amount of squeezing and cannot be compensated by the optimization. In the case of a high mechanical quality factor $Q = \omega_m/\Gamma$ the conditional variance takes the following form:

$$\sigma_B^{\rm III} \simeq \frac{1}{2}\left[\frac{1}{1+\chi^4} + \frac{\pi\Gamma}{\omega_m}\frac{\chi^6}{(1+\chi^4)^2}n_{\rm th}\right]. \tag{16}$$

The reasoning above proves that the major impediment to successful performance is the initial thermal occupation n_0. In the lossless case it is automatically balanced out by the equal QND gains, and when the losses break the balance, the proper combination of unequal gains can help to alleviate the influence of n_0. Numerical estimations for the full dynamics including mechanical bath and optical losses are presented in the figure 2(b). The upper bound of the range of initial occupation, $n_0 = 10^6$, corresponds to the equilibrium occupation of a mechanical oscillator with frequency $\omega_m = 2\pi \times 100$ kHz at temperature of 5 K.

Comparison of the conditional squeezing with the generalized one shows that for the case of low QND coupling strengths ($\chi \lesssim 1$) the amount of squeezing produced by conditional measurement does not reach the maximal possible one (in both cases of the idealized dynamics without any decoherence and in the case of full model). To attain the maximally available squeezing the value χ should be increased. See figure 2(b) for details.

We now investigate the entanglement generated in this system. From (14) we conclude that logarithmic negativity should be sensitive to the initial occupation of the mechanical mode as the term $-\chi p(0)$ enters the expression for $\mathcal{Y}_B^{\rm out}$. In the ideal case, the logarithmic negativity is a monotonically increasing function of χ. Optical losses break this monotonicity. This is related to the fact that losses modify the trajectory of the mechanical system in phase space, displacing it away from the optimal final point, most pronounced for higher QND gains. Optimization with respect to QND couplings of individual interactions $\chi_{1,2,3}$ partially compensates the optical losses and makes the logarithmic negativity a monotonic function again. The presence of the mechanical bath imposes a limit on the maximal achievable amount of entanglement. The optimization with respect to unequal QND strengths partially compensates the influence of the mechanical bath and allows higher values of entanglement to be reached, compared to the non-optimized case. This is represented in the figure 3(a) together with estimates for non-optimized values.

The steerability properties are very similar to the ones of logarithmic negativity—optical losses break the monotonicity whereas the mechanical bath is responsible for limiting the maximal value of steerability. The optimization of this quantity with respect to $\chi_{1,2,3}$ partially compensates these two decoherence effects (see figure 3(b)). There is, however, a threshold value of optomechanical coupling necessary to achieve steering. For $G_{A\to B}$, in absence of the decoherence processes, it is defined by the value of n_0. The joint impact of optical losses and mechanical bath makes this threshold higher. In contrast, $G_{B\to A}$ does not demonstrate such a threshold in the ideal case, and only the presence of decoherence processes causes this limitation.

7. Full quantum transducer

In this section we finally consider the complete scheme of four sequential QND interactions (figure 1(a)). As above, we study different signatures of quantum correlations. In the idealized symmetric adiabatic case without decoherence the transformation of quadratures takes the following form:

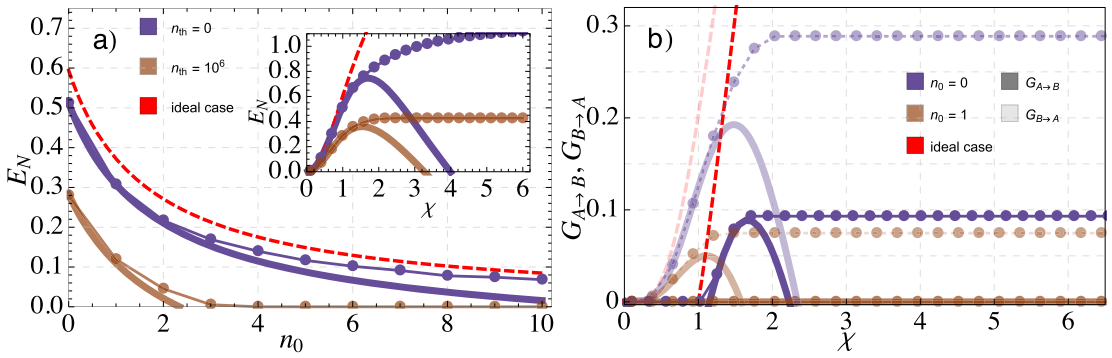

Figure 3. Entanglement and steerability after three interactions. (a) Logarithmic negativity as a function of the initial occupation of the mechanical mode n_0 for different values of the mechanical bath occupation number n_{th} and for $\chi = 1$. Inset: logarithmic negativity as a function of the QND coupling strength χ for different values of the mechanical bath occupation number n_{th}, $n_0 = 0$ and pulse photon numbers $0 \leqslant N \leqslant 10^{13}$. (b) Steering $G_{A\to B}$ and $G_{B\to A}$ as a function of the QND coupling χ for different values of the mechanical initial occupation n_0 and $\Gamma/\kappa = 3 \times 10^{-10}$. Dashed red lines represent the ideal case without any decoherence, whereas the solid lines represent the case with all decoherence processes included. Lines with markers indicate optimized parameter values. Parameters which are not mentioned separately are the same as in figure 2.

$$\begin{aligned} \mathcal{X}_A^{\mathrm{out}} &= \mathcal{X}_A^{\mathrm{in}} + \chi^2 \mathcal{X}_B^{\mathrm{in}}, \quad q' = q(0), \quad \mathcal{X}_B^{\mathrm{out}} = \mathcal{X}_B^{\mathrm{in}}, \\ \mathcal{Y}_A^{\mathrm{out}} &= \mathcal{Y}_A^{\mathrm{in}}, \quad p' = p(0), \quad \mathcal{Y}_B^{\mathrm{out}} = \mathcal{Y}_B^{\mathrm{in}} - \chi^2 \mathcal{Y}_A^{\mathrm{in}}, \end{aligned} \tag{17}$$

describing the QND interaction between the modes A and B with the Hamiltonian:

$$\mathcal{H} = \hbar \tau_{\mathrm{int}}^{-1} \chi^2 \mathcal{X}_B^{\mathrm{in}} \mathcal{Y}_A^{\mathrm{in}}.$$

As can be seen from (17) the mechanical mediator is finally traced out from the optical modes. This is a manifestation of the geometric phase effect.

We start by estimating the amount of conditional squeezing. System A is not involved in the fourth interaction, therefore measuring A yields the same conditional variance σ_B^{III} as after only three interactions, as analysed in section 6. System B does not contain any influence of the mechanical momentum and in the ideal case, the conditional variance $\sigma_A^{\mathrm{IV}} = \frac{1}{2(1+\chi^4)}$ is a function of only the QND coupling strength. The optical losses modify the trajectory of the mechanical system in phase-space and make it non-closed. As a consequence, σ_A^{IV} becomes dependent on n_0 and for small losses, it takes the following form:

$$\sigma_A^{\mathrm{IV}} \approx \frac{1}{2}\left[1 + \chi^4 \frac{\frac{1}{2}(1+\eta^2)}{1 + \frac{1}{2}\chi^2 n_0 (1-\eta)^2}\right]^{-1}. \tag{18}$$

Optimization with respect to individual QND couplings χ_i allows to bring this phase-space trajectory as close to the ideal one (figure 1(c)) as possible. The optimized value of σ_A becomes equal to $\sigma_A(n_0 = 0)$. The mechanical bath defines the maximal achievable value of conditional squeezing and its influence cannot be compensated in this case. The corresponding conditional variance for high mechanical quality factor Q approximately reads:

$$\sigma_A^{\mathrm{IV}} \simeq \frac{1}{2}\left[\frac{1}{1+\chi^4} + \frac{\pi\Gamma}{\omega_m}\frac{\chi^4}{(1+\chi^4)^2} n_{\mathrm{th}}\right]. \tag{19}$$

It is clear that the influence of n_0 is the major encumbrance for good protocol performance. In the absence of optical losses in the system, n_0 is automatically traced out from the equations by proper combination of QND gains. Once losses are introduced, they break this balance. This can be compensated by the optimization of unequal QND gains, which is presented in the figure 2(c).

Analogous to the case of three QND interactions, conditional squeezing coincide with the generalized one for large enough values of χ. For experimentally attainable values $\chi < 1$ the amount of conditional squeezing is lower than maximally possible one (see figure 2(c)).

We now study the entanglement and steerability. In the ideal case the logarithmic negativity and steerability are defined only by the value of the QND coupling χ. Optical losses modify them in a way that they become dependent on n_0. In the region of weak QND couplings and for small optical losses the eigenvalues defining the quantities (10), (11) can be approximately expressed by:

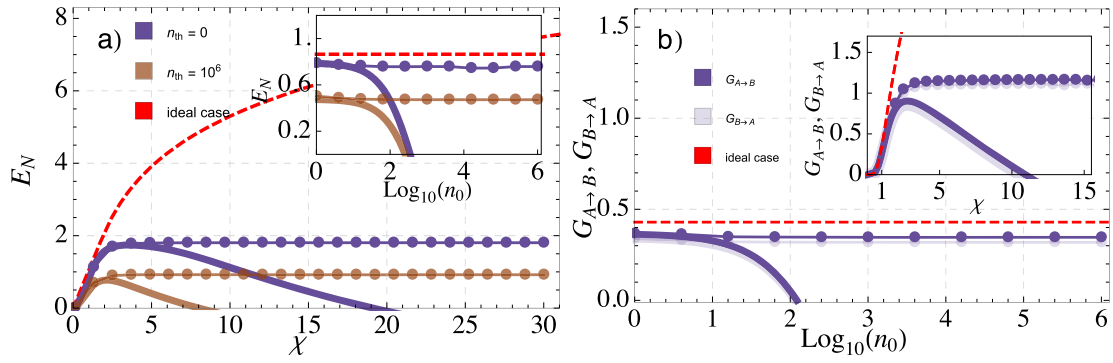

Figure 4. Entanglement and steerability after four interactions. (a): Logarithmic negativity as a function of QND coupling χ for different values of the mechanical bath occupation number n_{th}. Inset: logarithmic negativity as a function of the initial occupation of the mechanical mode for different values of mechanical bath occupation number n_{th} and $\chi = 1$. (b) Steerability $G_{A\to B}$ and $G_{B\to A}$ as a function of the initial occupation for $\chi = 1$. Inset: steerability as a function of QND interaction strength for $n_0 = 10$. Red dashed line shows the ideal case without any decoherence included, while the solid lines show the full dynamics. Lines with markers represent the case of optimized parameters. Mean photon number is varied in the region $0 \leqslant N \leqslant 10^{15}$. Other parameters are the same as in the figure 2.

$$\nu_{-}^{\mathrm{IV}} \approx \frac{1}{2}\left[1 - \chi^2 + \frac{1}{2}\chi^4 + \frac{1}{8}(1-\eta)^2\chi^2 n_0\right],$$
$$\nu_{\mathrm{A,B}}^{\mathrm{IV}} \approx 1 - \frac{\chi^4}{2} + \frac{1}{4}(1-\eta)^2\chi^2 n_0, \tag{20}$$

demonstrating that the optical losses are responsible for the appearance of the summand proportional to n_0. The influence of the mechanical bath is expressed by the additional term independent from n_0 and defining the maximal achievable entanglement and steerability. In the region of weak QND couplings and for high mechanical quality factor the eigenvalues are expressed as:

$$\nu_{-}^{\mathrm{IV}} \approx \frac{1}{2}\left[1 - \chi^2 + \frac{1}{2}\chi^4 + \frac{\Gamma}{2\omega_m}\pi\chi^2 n_{\mathrm{th}}\right],$$
$$\nu_{\mathrm{A,B}}^{\mathrm{IV}} \approx 1 - \frac{\chi^4}{2} + \frac{\Gamma}{2\omega_m}\pi\chi^2 n_{\mathrm{th}}. \tag{21}$$

It follows from the analysis above that n_0 is the main obstacle for the entanglement and steerability generation. The influence of optical losses and mechanical bath may be partially compensated by the optimization of individual unequal QND gains $\chi_{1,2,3,4}$. For the case of a cold mechanical bath and weak QND gains, the optimized values of logarithmic negativity and steerability tend to $E_{\mathrm{N}}(n_0 = 0)$ and $G_{A\to B,B\to A}(n_0 = 0)$ correspondingly. It is worthwhile to note that decoherence effects are responsible for the appearance of a threshold value of the QND coupling χ required to reach non-zero steerability. The numerical estimations for the full dynamics are presented in the figure 4.

8. Transducer without a cavity

The so-called bad cavity regime ($\kappa \gg \omega_m$) is advantageous for our transducer, because a cavity with higher decay rate does not distort the shape of pulses significantly, which allows us to consider the system in the adiabatic regime. Therefore a natural next step is to consider the transducer without the optical cavity, where the mechanical mode is coupled directly to the propagating light fields. The transducer without the cavity does not face the problem of mode matching between the propagating light and cavity so it does not need delicate cavity operation which is beneficial for the experiment. In this section we estimate the achievable amounts of entanglement and quantum steering for such a transducer.

The optomechanical system without a cavity may be presented by figure 1(b) without the mirror in a dashed box. We still consider four sequential QND interactions with the mechanical mediator as depicted in the figure 1(a). The transformations of the quadratures in the ideal case without any decoherence effects included take the same form as (17) with replacement $\chi \to \chi_i' = 4\pi x_0\sqrt{N_i}/\lambda$ [37] where $x_0 = \sqrt{\hbar/2m\omega_m}$ is the amplitude of zero-point fluctuations with m being the mass of the mechanical oscillator and λ—the optical wavelength.

The dynamics of the system without the cavity is completely equivalent to the one with the cavity, and the numerical estimation results replicate of figure 4 after the replacement $\chi \to \chi'$. Parameters used are the same with addition $\lambda = 1064$ nm, $m = 10^{-12}$ kg and $0 \leqslant N \leqslant 10^{16}$. The system without the cavity does not have the

advantage of resonant enhancement of the circulating power. Therefore, to achieve the same performance as in the system with the cavity, one has to supply the input power approximately $\mathcal{F}$ times higher, where $\mathcal{F}$ is the finesse of the cavity.

9. Conclusion

In this paper we explored the pulsed optomechanical transducer operating beyond the sideband resolved regime. This transducer allows to interconnect two optical modes A and B via a sequence of interactions with the same noisy mechanical mediator, which can be an element of an optomechanical cavity or just be coupled to freely propagating pulses. An advantage of the proposed scheme is that it is suitable for, in principle, arbitrary wavelengths of radiation, therefore it is capable of creating quantum correlations of pulses at different frequencies that would not interact otherwise.

We studied non-classical correlations after any number of sequential QND interactions in the adiabatic regime. We have shown that two QND interactions are enough to create conditional squeezing at least in one direction. Three sequential interactions allow conditional squeezing in both directions, entanglement between optical modes and quantum steering in both directions, provided that the mechanical mode is cooled close to its ground state. Finally, the full transducer with four sequential QND interactions is capable of producing sufficient values of conditional squeezing of both optical modes, entanglement and steerability in both directions at almost an arbitrary initial occupation of the mechanical mode.

The three negative effects that can degrade the performance of the transducer are the initial thermal occupation of the mechanical mode, its thermal environment and the losses in the modes of radiation. We have shown that the initial occupation is the most significant impediment to quantum correlations, until it is traced out from the optical modes by a proper combination of QND gains. The presence of optical losses breaks this balance and makes quantum correlations sensitive to the initial occupation again, whereas the interaction with the mechanical bath defines the maximally achievable amount of quantum correlations. Remarkably, the optimization of unequal gains of individual QND interactions allows to substantially compensate these two unwanted effects.

Thus, we have shown that the geometric phase effect allows for realizing an optomechanical transducer in the stroboscopic regime outside the sideband resolved limit for the systems with low-Q cavity, potentially without cavity. We have also demonstrated that it is feasible in the context of state-of-the-art optomechanical experiments. This investigation may stimulate further researches in the area of quantum transducers based on mechanical mediators.

Acknowledgments

NV, AAR and RF acknowledge the support of the project GB14-36681G of the Czech Science Foundation. AAR and RF have received national funding from the MEYS under grant agreement No. 731473 and from the QUANTERA ERA-NET cofund in quantum technologies implemented within the European Union's Horizon 2020 Programme (project TheBlinQC). AAR acknowledges support by the Development Project of Faculty of Science, Palacky University and COST Action CA15220 'QTSpace'. UBH and ULA acknowledge support from the Danish National Research Foundation (bigQ DNRF142) and the Villum foundation (grant no. 13300).

ORCID iDs

Andrey A Rakhubovsky https://orcid.org/0000-0001-8643-670X

References

[1] Kimble H J 2008 *Nature* **453** 1023
[2] Genes C, Mari A, Vitali D and Tombesi P 2009 *Adv. At., Mol. Opt. Phys.* **57** 33–86
[3] Aspelmeyer M, Kippenberg T J and Marquardt F 2014 *Rev. Mod. Phys.* **86** 1391
[4] Metcalfe M 2014 *Appl. Phys. Rev.* **1** 031105
[5] Zeuthen E, Schliesser A, Taylor J M and Sørensen A S 2017 arXiv:1710.10136
[6] Winger M, Blasius T D, Alegre T P M, Safavi-Naeini A H, Meenehan S, Cohen J, Stobbe S and Painter O 2011 *Opt. Express* **19** 24905–21
[7] Bochmann J, Vainsencher A, Awschalom D D and Cleland A N 2013 *Nat. Phys.* **9** 712
[8] Andrews R, Peterson R, Purdy T P, Cicak K, Simmonds R, Regal C A and Lehnert K 2014 *Nat. Phys.* **10** 321
[9] Bagci T *et al* 2014 *Nature* **507** 81–5
[10] Menke T, Burns P S, Higginbotham A P, Kampel N S, Peterson R W, Cicak K, Simmonds R W, Regal C A and Lehnert K W 2017 *Rev. Sci. Instrum.* **88** 094701
[11] Hill J T, Safavi-Naeini A H, Chan J and Painter O 2012 *Nat. Commun.* **3** 1196

[12] Liu Y, Davanco M, Aksyuk V and Srinivasan K 2013 *Phys. Rev. Lett.* **110** 223603
[13] Dong C, Fiore V, Kuzyk M C, Tian L and Wang H 2015 *Ann. Phys.* **527** 100
[14] Lecocq F Q, Clark J B, Simmonds R W, Aumentado J A and Teufel J D 2016 *Phys. Rev. Lett.* **116** 043601
[15] Regal C A and Lehnert W 2011 *J. Phys.: Conf. Ser.* **264** 012025
[16] Barzanjeh S, Vitali D, Tombesi P and Milburn G J 2011 *Phys. Rev.* A **84** 042342
[17] Barzanjeh S, Abdi M, Milburn G J, Tombesi P and Vitali D 2012 *Phys. Rev. Lett.* **109** 130503
[18] Wang Y D and Clerk A A 2012 *Phys. Rev. Lett.* **108** 153604
[19] Tian L 2012 *Phys. Rev. Lett.* **108** 153604
[20] Wang Y D and Clerk A A 2012 *New J. Phys.* **14** 105010
[21] McGee S A, Meiser D, Regal C A, Lehnert K W and Holland M J 2013 *Phys. Rev.* A **87** 053818
[22] Furusawa A and van Loock P 2011 *Quantum Teleportation and Entanglement: A Hybrid Approach to Optical Quantum Information Processing* (New York: Wiley)
[23] Morin O, Huang K, Liu J, Jeannic H L, Fabre C and Laurat J 2014 *Nat. Photon.* **8** 570–4
[24] Jeong H, Zavatta A, Kang M, Lee S W, Costanzo L S, Grandi S, Ralph T C and Bellini M 2014 *Nat. Photon.* **8** 564–9
[25] Makino K, Hashimoto Y, Yoshikawa J, Ohdan H, Toyama T, van Loock P and Furusawa A 2016 *Sci. Adv.* **2** e1501772
[26] Hofer S G, Wieczorek W, Aspelmeyer M and Hammerer K 2011 *Phys. Rev.* A **84** 052327
[27] Vanner M R, Pikovski I, Cole G D, Kim M S, Brukner Č, Hammerer K, Milburn G J and Aspelmeyer M 2011 *Proc. Natl Acad. Sci.* **108** 16182–7
[28] Palomaki T A, Teufel J D, Simmonds R W and Lehnert K W 2013 *Science* **342** 710–3
[29] Palomaki T A, Harlow J W, Teufel J D, Simmonds R W and Lehnert K W 2013 *Nature* **495** 210–4
[30] Reed A P *et al* 2017 *Nat. Phys.* **13** 1163
[31] Riedinger R, Hong S, Norte R A, Slater J A, Shang J, Krause A G, Anant V, Aspelmeyer M and Gröblacher S 2016 *Nature* **530** 313–6
[32] Hong S, Riedinger R, Marinković I, Wallucks A, Hofer S G, Norte R A, Aspelmeyer M and Gröblacher S 2017 *Science* **358** 203–6
[33] Riedinger R, Wallucks A, Marinković I, Löschnauer C, Aspelmeyer M, Hong S and Gröblacher S 2018 *Nature* **556** 473–7
[34] Rakhubovsky A A, Vostrosablin N and Filip R 2016 *Phys. Rev.* A **93** 033813
[35] Vostrosablin N, Rakhubovsky A A and Filip R 2016 *Phys. Rev.* A **94** 063801
[36] Kiesewetter S, Teh R Y, Drummond P D and Reid M D 2017 *Phys. Rev. Lett.* **119** 023601
[37] Vanner M R, Hofer J, Cole G D and Aspelmeyer M 2013 *Nat. Commun.* **4** 2295
[38] Hoff U B, Kollath-Bönig J, Neergaard-Nielsen J S and Andersen U L 2016 *Phys. Rev. Lett.* **117** 143601
[39] Bennett J S, Khosla K, Madsen L S, Vanner M R, Rubinsztein-Dunlop H and Bowen W P 2016 *New J. Phys.* **18** 053030
[40] Kupčík V and Filip R 2015 *Phys. Rev.* A **92** 022346
[41] Vostrosablin N, Rakhubovsky A A and Filip R 2017 *Opt. Express* **25** 18974
[42] Braginsky V B, Vorontsov Y I and Khalili F Y 1978 *JETP Lett.* **27** 276
[43] Law C K 1995 *Phys. Rev.* A **51** 2537–41
[44] Bowen W P and Milburn G J 2015 *Quantum Optomechanics* (Boca Raton, FL: CRC Press)
[45] Walls D F and Milburn G J 2007 *Quantum Optics* (Berlin: Springer)
[46] Ojanen T and Børkje K 2014 *Phys. Rev.* A **90** 013824
[47] Zhang Y X, Wu S, Chen Z B and Shikano Y 2016 *Phys. Rev.* A **94** 023823
[48] Gardiner C W and Collett M J 1985 *Phys. Rev.* A **31** 3761–74
[49] Grangier P, Levensen J and Poizat J P 1998 *Nature* **396** 537
[50] Gardiner C and Zoller P 2004 Quantum noise *A Handbook of Markovian and Non-Markovian Quantum Stochastic Methods with Applications to Quantum Optics* (Berlin: Springer)
[51] Duan L M, Giedke G, Cirac J I and Zoller P 2000 *Phys. Rev. Lett.* **84** 2722
[52] Simon R 2000 *Phys. Rev. Lett.* **84** 2726
[53] Laurat J, Keller G, Oliveira-Huguenin J A, Fabre C, Coudreau T, Serafini A, Adesso G and Illuminati F 2005 *J. Opt. B: Quantum Semiclass. Opt.* **7** S577
[54] Simon R, Mukunda N and Dutta B 1994 *Phys. Rev.* A **49** 1567
[55] Weedbrook C, Pirandola S, García-Patrón R, Cerf N J, Ralph T C, Shapiro J H and Lloyd S 2012 *Rev. Mod. Phys.* **84** 621–69
[56] Kogias I, Lee A R, Ragy S and Adesso G 2015 *Phys. Rev. Lett.* **114** 060403
[57] Brawley G A, Vanner M R, Larsen P E, Schmid S, Boisen A and Bowen W P 2016 *Nat. Commun.* **7** 10988
[58] Mancini S, Vitali D and Tombesi P 1998 *Phys. Rev. Lett.* **80** 688
[59] Jockel A, Faber A, Kampschulte T, Korppi M, Rakher M T and Treutlein P 2015 *Nat. Nanotechnol.* **10** 55–9
[60] Elste F, Girvin S M and Clerk A A 2009 *Phys. Rev. Lett.* **102** 207209
[61] Wilson D J, Sudhir V, Piro N, Schilling R, Ghadimi A and Kippenberg T J 2015 *Nature* **524** 325–9
[62] Poggio M, Degen C L, Mamin H J and Rugar D 2007 *Phys. Rev. Lett.* **99** 017201
[63] Schäfermeier C, Kerdoncuff H, Hoff U B, Fu H, Huck A, Bilek J, Harris G I, Bowen W P, Gehring T and Andersen U L 2016 *Nat. Commun.* **7** 13628
[64] Norte R A, Moura J P and Gröblacher S 2016 *Phys. Rev. Lett.* **116** 147202
[65] Reinhardt C, Muller T, Bourassa A and Sankey J C 2016 *Phys. Rev.* X **6** 021001
[66] Tsaturyan Y, Barg A, Polzik E S and Schliesser A 2017 *Nat. Nanotechnol.* **12** 776–83

Conclusion

The research conducted in this dissertation is very timely. We are on the verge of a second quantum revolution and quantum optomechanics is an important part of this process. By itself, this branch of quantum physics is very rapidly developing and promises many breakthroughs, both in terms of technology and in terms of a better understanding of the fundamental questions of quantum mechanics. We believe that this thesis advanced the field making important theoretical explorations that open the way for future experimental implementations and studies of other setups based on similar principles. In order not to be unsubstantiated, this section will present the main achievements of our research with reflections on their contribution to the field and the outlook of future exploration.

We proposed a new way to surpass the limit imposed on the transfer of highly nonclassical quantum states of light to the mechanical oscillator. The proposed setup can deterministically transfer an arbitrary state of light without any prior knowledge about this state. It was shown that with the help of only local Gaussian operation on the light it is possible to enhance the coupling of light to matter. This approach is proved to help to transfer negativity of Wigner function for the setups unable to do so previously. The impact of this work is the new possibility to merge developing pulsed quantum optomechanics with state-of-the-art quantum optics to produce a united physical platform for new experiments.

Next, we introduced and explored in detail a scheme allowing entanglement of two distant mechanical oscillators mediated by optical or microwave field. This work was very relevant as two similar mechanical oscillators coupled at the quantum level have not been demonstrated at that time. More importantly, the proposed scheme assumes a certain type of coupling between the mechanical oscillators - the quantum nondemolition one. This makes it useful for future quantum computing applications as this type of interaction is required for basic continuous-variable quantum gates, which are used to flexibly operate information in continuous-variable quantum processing. This work also might be of use in future studies of quantum synchronization of mechanical oscillators [136, 233, 225]. Additionally, such studies of quantum interaction of mechanical systems are important for potential connection with quantum thermodynamics [55, 237, 60, 32].

We then moved to the study of quantum transducers which are very important for

the development of unified quantum technology. We proposed to use a sequence of long-pulsed interactions between the systems of interest and the mediating system. The systems themselves do not interact directly with each other. We showed that by exploiting the power of the geometric phase effect it is possible to eliminate the noisy influence of the mediator. This approach is quite universal and opens the way for various experimental realizations. We explored and proved the feasibility for opto- and electromechanical experiments, however, this work might serve as an inspiration for combining other physical platforms, like atoms or NV centers (Chapter 14 in [12]).

To be fully compatible with modern hybrid quantum optics [72, 3], we explored a very similar transducer, but in the regime of high-intensive ultra-short pulses known as a stroboscopic regime. Before this exploration was done, it was unclear whether the geometric phase effect will be sufficient to obtain a robust transducer in this regime without entering the sideband resolved one. Our proposal is suitable for arbitrary wavelengths of radiation which might stimulate a much broader class of feasible quantum transducers mediated by mechanical systems. The work was performed in close collaboration with the experimental group of Prof. Ulrik Andersen from Denmark Technical University and there is big anticipation that the experimental realization will come in the near future. Moreover, further proposals from our team [176] and team of Prof. Michael Vanner at Imperial College London [102, 42, 144] show that stroboscopic optomechanics is an interesting future platform compatible with ultra-short quantum optics [87, 88].

Shrnutí v českém jazyce

Tato dizertační práce se zabývá aktuálními tématy vědeckého výzkumu. V současnosti se nacházíme na počátku druhé kvantové revoluce a kvantová optomechanika je důležitou součástí tohoto procesu. Kvantová optomechanika sama o sobě je velmi rychle se vyvíjející disciplína, která má potenciál pro mnoho průlomových objevů jak v technologiích, tak v hlubšímu porozumění kvantové fyziky. Věříme, že tato dizertační práce posouvá vpřed tento vědní obor tím, že činí důležitý teoretický výzkum, který otevírá cestu pro uskutečnění budoucích experimentů a studia dalších schémat založených na podobných principech. Tato sekce prezentuje hlavní výsledky našeho výzkumu s analýzou jejich příspěvků do kvantové opto-mechaniky a výhledu pro budoucí výzkum.

Navrhli jsme nový způsob jak překonat limity, které omezují přenos vysoce neklasických kvantových stavů světla do mechanického oscilátoru. Navrhované schéma může deterministicky přenést libovolný stav světla bez apriorní znalosti o tomto stavu. Ukázali jsme, že pouze pomocí lokálních Gaussovských operací na světle je možné zesílit interakci světla a látky. Tento nový postup prokazatelně pomáhá přenosu negativity Wignerovy funkce u schémat, která to dříve neumožňovala. Přínos této práce je nová možnost spojit vyvíjející se kvantovou optomechaniku s nejmodernější kvantovou optikou, aby bylo dosaženo jednotné fyzikální platformy pro nové experimenty.

Dále jsme zavedli a detailně zkoumali schéma dovolující vznik entanglementu mezi dvěma vzdálenými mechanickými oscilátory a to prostřednictvím optického nebo mikrovlnného pole. Tento výzkum byl je aktuální, protože dva podobné mechanické oscilátory spojené na kvantové úrovni nebyly předtím nikdy demonstrovány. Navíc toto navržené schéma předpokládá jistý typ interakce mezi mechanickými oscilátory – kvantově nedemoliční interakci. To je užitečné pro aplikace budoucího kvantového počítání, neboť tento typ interakce je potřebný pro základní kvantová hradla ve spojitých proměnných, která se využívají pro flexibilní zpracování informace ve spojitých proměnných. Tato práce by také mohla být využita pro budoucí studium kvantové synchronizace mechanických oscilátorů [136, 233, 225]. Navíc tento výzkum kvantové interakce mechanických systémů je důležitý pro potenciální spojení s kvantovou termodynamikou [55, 237, 60, 32].

Následně jsme zkoumali kvantové převodníky, které jsou velmi důležité pro vývoj univerzální kvantové technologie. Navrhli jsme aplikovat sekvenci pulzních interakcí mezi cílovými systémy a zprostředkujícími systémy. Samotné cílové systémy neinter-

agují přímo mezi sebou. Ukázali jsme, že pomocí efektu geometrické fáze je možné eliminovat vliv šumu mediátoru. Tento způsob je poměrně univerzální a otevírá cestu pro různé experimentální realizace. Zkoumali jsme a prokázali proveditelnost tohoto postupu v optických a elektrooptických experimentech. Tato práce však může sloužit jako inspirace pro kombinování jiných fyzikálních platforem jako jsou atomy nebo NV centra (kapitola 14 v [12]).

Abychom byli plně kompatibilní s moderní hybridní kvantovou optikou [72, 3], zkoumali jsme velmi podobný převodník v režimu ultra krátkých pulzů s vysokou intenzitou, což je známo jako stroboskopický režim. Předtím než byl proveden tento výzkum nebylo jasné, zda efekt geometrické fáze bude postačující pro získání robustního převodníku v tomto režimu. Náš návrh je přijatelný pro libovolnou vlnovou délku záření, což by mohlo stimulovat mnohem širší třídu proveditelných převodníků, které jsou zprostředkovány mechanickými systémy. Tato práce byla provedena v blízké spolupráci s experimentální skupinou prof. Ulrika Andersena z Technické Univerzity v Dánsku, kde očekáváme, že by se v budoucnu mohl uskutečnit experimentální realizace. Navíc, další návrhy našeho týmu [176] a týmu Prof. Michaela Vannera na Imperial College v Londýně [102, 42, 144] ukazují, že stroboskopická optomechanika je zajímavá budoucí platforma kompatibilní s kvantovou optikou se velmi krátkými pulsy [87, 88].

REFERENCES

[1] J. Aasi et al. Advanced LIGO. *Classical and Quantum Gravity*, 074001(32), 2015.

[2] B. P. Abbott et al. Observation of Gravitational Waves from a Binary Black Hole Merger. *Physical Review Letters*, 116(061102), 2016.

[3] U. L. Andersen, J. S. Neergaard-Nielsen, P. van Loock, and A. Furusawa. Hybrid discrete- and continuous-variable quantum information. *Nature Physics*, 11(9):713–719, 2015.

[4] M. H. Anderson, J. R. Ensher, M. R. Matthews, C. E. Wieman, and E. A. Cornell. Observation of Bose-Einstein Condensation in a Dilute Atomic Vapor. *Science*, (269):198–201, 1995.

[5] R. W. Andrews, R. W. Peterson, T. P. Purdy, K. Cicak, R. W. Simmonds, C. A. Regal, and K. W. Lehnert. Bidirectional and efficient conversion between microwave and optical light. *Nature Physics*, 10(4):321–326, 2014.

[6] R. W. Andrews, A. P. Reed, K. Cicak, J. D. Teufel, and K. W. Lehnert. Quantum-enabled temporal and spectral mode conversion of microwave signals. *Nature Communications*, 6(1):10021, 2015.

[7] O. Arcizet, P.-F. Cohadon, T. Briant, M. Pinard, and A. Heidmann. Radiation-pressure cooling and optomechanical instability of a micromirror. *Nature*, 444(7115):71–74, nov 2006.

[8] O. Arcizet, V. Jacques, A. Siria, P. S., P. Vincent, and S. Siedelin. A single nitrogen-vacancy defect coupled to a nanomechanical oscillator. *Nat. Phys.*, 879(7), 2011.

[9] G. Arnold, M. Wulf, S. Barzanjeh, E. S. Redchenko, A. Rueda, W. J. Hease, F. Hassani, and J. M. Fink. Converting Microwave and Telecom Photons with a Silicon Photonic Nanomechanical Interface. *arXiv:2002.11628 [cond-mat, physics:quant-ph]*, feb 2020.

[10] A. Ashkin. Acceleration and Trapping of Particles by Radiation Pressure. *Physical Review Letters*, 24:156–159, 1970.

[11] M. Aspelmeyer, T. J. Kippenberg, and F. Marquardt. Cavity optomechanics. *Rev. Mod. Phys.*, 86(4):1391–1452, dec 2014.

[12] M. Aspelmeyer, T. J. Kippenberg, and F. Marquardt. *Cavity Optomechanics Nano- and Micromechanical Resonators Interacting with Light*. Springer, 2014.

[13] H.-A. Bachor and T. C. Ralph. *A Guide to Experiments in Quantum Optics*. Wiley, 3rd editio edition, 2019.

[14] A. Barchielli and B. Vacchini. Quantum Langevin equations for optomechanical systems. *New Journal of Physics*, 17(8):083004, aug 2015.

[15] S. Barzanjeh, E. S. Redchenko, M. Peruzzo, M. Wulf, D. P. Lewis, G. Arnold, and J. M. Fink. Stationary Entangled Radiation from Micromechanical Motion. *Nature*, 570(7762):480, jun 2019.

[16] C. H. Bennett, G. Brassard, C. Crépeau, R. Jozsa, A. Peres, and W. K. Wootters. Teleporting an unknown quantum state via dual classical and Einstein-Podolsky-Rosen channels. *Phys. Rev. Lett.*, 70(13):1895–1899, mar 1993.

[17] J. S. Bennett and W. P. Bowen. Rapid Mechanical Squeezing with Pulsed Optomechanics. *New Journal of Physics*, 20(11):113016, 2018.

[18] J. S. Bennett, K. Khosla, L. S. Madsen, M. R. Vanner, H. Rubinsztein-Dunlop, and W. P. Bowen. A quantum optomechanical interface beyond the resolved sideband limit. *New Journal of Physics*, 18(5):053030, may 2016.

[19] J. S. Bennett, L. S. Madsen, M. Baker, H. Rubinsztein-Dunlop, and W. P. Bowen. Coherent control and feedback cooling in a remotely coupled hybrid atom–optomechanical system. *New J. Phys.*, 16(083036), 2014.

[20] M. V. Berry. J. Mod. Opt. *The adiabatic phase and Pancharatnam's phase for polarized light*, 34:1401–1407, 1987.

[21] D. G. Blair, E. N. Ivanov, M. E. Tobar, P. J. Turner, F. van Kann, and I. S. Heng. High Sensitivity Gravitational Wave Antenna with Parametric Transducer Readout. *Phys. Rev. Lett.*, 74(11):1908–1911, mar 1995.

[22] K. Børkje. Scheme for steady-state preparation of a harmonic oscillator in the first excited state. *Phys. Rev. A*, 90(2):23806, aug 2014.

[23] S. Bose, K. Jacobs, and P. L. Knight. Preparation of nonclassical states in cavities with a moving mirror. *Phys. Rev. A*, 56(5):4175–4186, nov 1997.

[24] D. Bothner, S. Yanai, A. Iniguez-Rabago, M. Yuan, Y. M. Blanter, and G. A. Steele. Cavity Electromechanics with Parametric Mechanical Driving. *arXiv:1908.08496 [cond-mat, physics:quant-ph]*, aug 2019.

[25] V. B. Braginski and Y. I. Vorontsov. Quantum-mechanical limitations in macroscopic experiments and modern experimental technique. *Soviet Physics Uspekhi*, 17:644–650, 1975.

[26] V. Braginskii and A. Manukin. Ponderomotive Effects of Electromagnetic Radiation. *Soviet Physics JETP*, 1967.

[27] V. Braginsky, A. Manukin, and M. Tikhonov. Investigation of dissipative ponderomotive effects of electromagnetic radiation. *Soviet Physics JETP*, 31(5), 1970.

[28] V. Braginsky and I. Minakova. Influence of the small displacements on the dynamical properties of mechanical oscillating systems. *Moscow Univ. Phys. Bull*, 1964.

[29] V. B. Braginsky, Y. I. Vorontsov, and K. S. Thorne. Quantum Non- demolition Measurements. *Science*, 209(4456):547–557, 1980.

[30] K. R. Brown, C. Ospelkaus, Y. Colombe, A. C. Wilson, D. Leibfried, and D. J. Wineland. Coupled quantized mechanical oscillators. *Nature (London)*, 196(471), 2011.

[31] M. Brunelli, D. Malz, A. Schliesser, and A. Nunnenkamp. Stroboscopic Quantum Optomechanics. *Physical Review Research*, 2(2):23241, may 2020.

[32] M. Brunelli, A. Xuereb, A. Ferraro, G. D. Chiara, N. Kiesel, and M. Paternostro. Out-of-equilibrium thermodynamics of quantum optomechanical systems. *New J. Phys.*, 035016(17), 2015.

[33] V. Buzek and P. L. Knight. *Quantum Interference, Superposition States of Light and Nonclassical Effects*. Elsevier, Amsterdam, 1995.

[34] A. O. Caldeira and A. J. Leggett. Influence of damping on quantum interference: An exactly soluble model. *Phys. Rev. A*, 1059(31), 1985.

[35] S. Camerer, M. Korppi, A. Jockel, D. Hunger, T. W. Hansch, and P. Treutlein. Realization of an Optomechanical Interface between Ultracold Atoms and a Membrane. *Phys. Rev. Lett.*, 223001(107), 2011.

[36] C. M. Caves. Quantum-mechanical noise in an interferometer. *Phys. Rev. D*, 23(8):1693–1708, apr 1981.

[37] C. M. Caves, K. S. Thorne, R. W. Drever, V. D. Sandberg, and M. Zimmermann. On the measurement of a weak classical force coupled to a quantum-mechanical oscillator. I. Issues of principle. *Rev. Mod. Phys.*, 52:341–392, 1980.

[38] J. Chen, M. Rossi, D. Mason, and A. Schliesser. Entanglement of Propagating Optical Modes via a Mechanical Interface. *Nature Communications*, 11(1):1–6, feb 2020.

[39] X. Chen, Y.-C. Liu, P. Peng, Y. Zhi, and Y.-F. Xiao. Cooling of macroscopic mechanical resonators in hybrid atom-optomechanical systems. *Phys. Rev. A*, 92(033841), 2015.

[40] Y. Chen. Macroscopic quantum mechanics: Theory and experimental concepts of optomechanics. *J. Phys. B*, 104001(46), 2013.

[41] J. B. Clark, F. Lecocq, R. W. Simmonds, J. Aumentado, and J. D. Teufel. Sideband cooling beyond the quantum backaction limit with squeezed light. *Nature*, (541):191–195, 2017.

[42] J. Clarke, P. Sahium, K. E. Khosla, I. Pikovski, I. Pikovski, M. S. Kim, and M. R. Vanner. Generating mechanical and optomechanical entanglement via pulsed interaction and measurement. *New Journal of Physics*, 22(6):063001, jun 2020.

[43] A. A. Clerk, K. W. Lehnert, P. Bertet, J. R. Petta, and Y. Nakamura. Hybrid Quantum Systems with Circuit Quantum Electrodynamics. *Nature Physics*, pages 1–11, mar 2020.

[44] P. F. Cohadon, A. Heidmann, and M. Pinard. Cooling of a Mirror by Radiation Pressure. *Phys. Rev. Lett.*, 83(16):3174–3177, oct 1999.

[45] G. P. Conangla, F. Ricci, M. T. Cuairan, A. W. Schell, N. Meyer, and R. Quidant. Optimal Feedback Cooling of a Charged Levitated Nanoparticle with Adaptive Control. *Physical Review Letters*, 122(22):223602, jun 2019.

[46] B. D. Cuthbertson, M. E. Tobar, E. N. Ivanov, and D. G. Blair. Parametric backaction effects in a high- Q cyrogenic sapphire transducer. *Review of Scientific Instruments*, 67(7):2435–2442, jul 1996.

[47] K. B. Davis, M. O. Mewes, M. R. Andrews, N. J. V. Druten, D. S. Durfee, D. M. Kurn, and W. Ketterle. Bose-Einstein condensation in a gas of sodium atoms. *Phys. Rev. Lett.*, (75):3969–3973, 1995.

[48] M. de Touzalin, C. Heijman, and C. Murray. Quantum Manifesto (qurope.eu/manifesto), feb 2016.

[49] R. D. Delaney, A. P. Reed, R. W. Andrews, and K. W. Lehnert. Measurement of Motion beyond the Quantum Limit by Transient Amplification. *Physical Review Letters*, 123(18):183603, oct 2019.

[50] S. Deleglise, I. Dotsenko, C. Sayrin, J. Bernu, M. Brune, J.-M. Raimond, and S. Haroche. Reconstruction of non-classical cavity field states with snapshots of their decoherence. *Nature (London)*, 510(455), 2008.

[51] U. Delic, D. Grass, M. Reisenbauer, T. Damm, M. Weitz, N. Kiesel, and M. Aspelmeyer. Levitated Cavity Optomechanics in High Vacuum. *Quantum Science and Technology*, 2020.

[52] U. Delić, M. Reisenbauer, K. Dare, D. Grass, V. Vuletić, N. Kiesel, and M. Aspelmeyer. Cooling of a Levitated Nanoparticle to the Motional Quantum Ground State. *Science*, 367(6480):892–895, feb 2020.

[53] U. Delić, M. Reisenbauer, D. Grass, N. Kiesel, V. Vuletić, and M. Aspelmeyer. Cavity Cooling of a Levitated Nanosphere by Coherent Scattering. *Physical Review Letters*, 122(12):123602, mar 2019.

[54] P. Dirac and F. Howard. The fundamental equations of quantum mechanics. *Proc. R. Soc. Lond. A*, 109:642–653, 1925.

[55] Y. Dong, K. Zhang, F. Bariani, and P. Meystre. Work measurement in an optomechanical quantum heat engine. *Phys. Rev. A*, 92(3):33854, sep 2015.

[56] L.-M. Duan, G. Giedke, J. I. Cirac, and P. Zoller. Inseparability Criterion for Continuous Variable Systems. *Phys. Rev. Lett.*, 84(12):2722–2725, mar 2000.

[57] L.-M. Duan, M. D. Lukin, J. I. Cirac, and P. Zoller. Long-distance quantum communication with atomic ensembles and linear optics. *Nature*, 414(6862):413–418, 2001.

[58] M. Eichenfield, J. Chan, R. Camacho, K. Vahala, and O. Painter. Optomechanical crystals. *Nature*, 462:78–82, 2009.

[59] A. Einstein. On a heuristic point of view concerning production and transformationof light. *Ann. Phys.*, 17:132–148, 1905.

[60] C. Elouard, M. Richard, and A. Auffèves. Reversible work extraction in a hybrid opto-mechanical system. *New Journal of Physics*, 17(5):055018, may 2015.

[61] F. Elste, S. M. Girvin, and A. A. Clerk. Quantum Noise Interference and Back-action Cooling in Cavity Nanomechanics. *Phys. Rev. Lett.*, 102(207209), 2009.

[62] G. Enzian, M. Szczykulska, J. Silver, L. D. Bino, S. Zhang, I. A. Walmsley, P. Del'Haye, and M. R. Vanner. Observation of Brillouin Optomechanical Strong Coupling with an 11 GHz Mechanical Mode. *Optica*, 6(1):7–14, jan 2019.

[63] A. Farace and V. Giovannetti. Enhancing quantum effects via periodic modulations in optome- chanical systems. *Phys. Rev. A*, 86(013820), 2012.

[64] S. A. Fedorov, N. J. Engelsen, A. H. Ghadimi, M. J. Bereyhi, R. Schilling, D. J. Wilson, and T. J. Kippenberg. Generalized Dissipation Dilution in Strained Mechanical Resonators. *Physical Review B*, 99(5), feb 2019.

[65] S. Felicetti, S. Fedortchenko, R. Rossi, S. Ducci, I. Favero, T. Coudreau, and P. Milman. Quantum communication between remote mechanical resonators. *Phys. Rev. A*, 95(2):22322, feb 2017.

[66] R. Filip. Excess-noise-free recording and uploading of nonclassical states to continuous-variable quantum memory. *Phys. Rev. A*, 78(012329), 2008.

[67] R. Filip. Quantum interface to a noisy system through a single kind of arbitrary Gaussian coupling with limited interaction strength. *Phys. Rev. A*, 80(022304), 2009.

[68] R. Filip. Squeezing restoration by a noisy probe from a classically correlated environment. *Phys. Rev. A*, 81(3):32330, mar 2010.

[69] R. Filip and V. Kupcik. Continous-variable entanglement mediated by a thermal oscillator. *Phys. Rev. A.*, 92(022346), 2015.

[70] R. Filip, P. Marek, and U. L. Andersen. Measurement-induced continuous-variable quantum interactions. *Phys. Rev. A*, 042308(71), 2005.

[71] M. Forsch, R. Stockill, A. Wallucks, I. Marinkovic, C. Gärtner, R. A. Norte, F. van Otten, A. Fiore, K. Srinivasan, and S. Gröblacher. Microwave-to-Optics Conversion Using a Mechanical Oscillator in Its Quantum Groundstate. *Nature Physics*, 16(1):69–74, jan 2020.

[72] A. Furusawa and P. van Loock. *Quantum Teleportation and Entanglement*. John Wiley Sons, New York, 2011.

[73] B. T. Gard, K. Jacobs, R. McDermott, and M. Saffman. Microwave-to-optical frequency conversion using a cesium atom coupled to a superconducting resonator. *Phys. Rev. A*, 96(013833), 2017.

[74] C. Gärtner, J. P. Moura, W. Haaxman, R. A. Norte, and S. Gröblacher. Integrated Optomechanical Arrays of Two High Reflectivity SiN Membranes. *Nano Letters*, 18(11):7171–7175, nov 2018.

[75] A. A. Geraci, S. J. Smullin, D. M. Weld, J. Chiaverini, and A. Kapitulnik. Improved constraints on non-Newtonian forces at 10 microns. *Phys Rev D*, 78:22002, 2008.

[76] R. P. Giffard. Ultimate sensitivity limit of a resonant gravitational wave antenna using a linear motion detector. *Phys. Rev. D*, 14:2478–2486, 1976.

[77] S. Gigan, H. R. Böhm, M. Paternostro, F. Blaser, G. Langer, J. B. Hertzberg, K. C. Schwab, D. Bäuerle, M. Aspelmeyer, and A. Zeilinger. Self-cooling of a micromirror by radiation pressure. *Nature*, 444(7115):67–70, nov 2006.

[78] R. J. Glauber. Coherent and Incoherent States of the Radiation Field. *Phys. Rev.*, 131(6):2766–2788, sep 1963.

[79] D. Goldwater, B. Stickler, L. Martinetz, T. E. Northup, K. Hornberger, and J. Millen. Levitated Electromechanics: All-Electrical Cooling of Charged Nano- and Micro-Particles. *Quantum Science and Technology*, 2018.

[80] C. Gonzalez-Ballestero, P. Maurer, D. Windey, L. Novotny, R. Reimann, and O. Romero-Isart. Theory for Cavity Cooling of Levitated Nanoparticles via Coherent Scattering: Master Equation Approach. *Physical Review A*, 100(1):13805, jul 2019.

[81] S. Gröblacher, K. Hammerer, M. R. Vanner, and M. Aspelmeyer. Observation of strong coupling between a micromechanical resonator and an optical cavity field. *Nature*, 460(7256):724–727, 2009.

[82] S. Gröblacher, J. B. Hertzberg, M. R. Vanner, G. D. Cole, S. Gigan, K. C. Schwab, and M. Aspelmeyer. Demonstration of an ultracold micro-optomechanical oscillator in a cryogenic cavity. *Nature Physics*, 5(7):485–488, 2009.

[83] B. Groisman, S. Popescu, and A. Wint. Quantum, classical, and total amount of correlations in a quantum state. *Phys. Rev. A*, 72(032317), 2005.

[84] J. Guo, R. A. Norte, and S. Gröblacher. Feedback Cooling of a Room Temperature Mechanical Oscillator Close to Its Motional Groundstate. *Physical Review Letters*, 123(22):223602, nov 2019.

[85] C. Gut, K. Winkler, J. Hoelscher-Obermaier, S. G. Hofer, R. M. Nia, N. Walk, A. Steffens, J. Eisert, W. Wieczorek, J. A. Slater, M. Aspelmeyer, and K. Hammerer. Stationary Optomechanical Entanglement between a Mechanical Oscillator and Its Measurement Apparatus. *arXiv:1912.01635 [cond-mat, physics:quant-ph]*, dec 2019.

[86] K. Hammerer, M. Aspelmeyer, E. S. Polzik, and P. Zoller. Estab- lishing Einstein-Poldosky-Rosen Channels between Nanome- chanics and Atomic Ensembles. *Phys. Rev. Lett.*, 020501(102), 2009.

[87] G. Harder, T. J. Bartley, A. E. Lita, S. W. Nam, T. Gerrits, and C. Silberhorn. Single-Mode Parametric-Down-Conversion States with 50 Photons as a Source for Mesoscopic Quantum Optics. *Phys. Rev. Lett.*, 116(14):143601, apr 2016.

[88] G. Harder, C. Silberhorn, J. Rehacek, Z. Hradil, L. Motka, B. Stoklasa, and L. L. Sánchez-Soto. Local Sampling of the Wigner Function at Telecom Wavelength with Loss-Tolerant Detection of Photon Statistics. *Phys. Rev. Lett.*, 116(13):133601, mar 2016.

[89] W. Heisenberg. Über den anschaulichen Inhalt der quantentheoretischen Kinematik und Mechanik. *Zeitschrift für Physik*, 43:172–198, 1927.

[90] L. Henderson and V. Vedral. Entanglement and Quantum Discord of Two Moving Atoms. *J. Phys. A*, 34(6899), 2001.

[91] H. Hertz. Über einen Einfluß des ultravioletten Lichtes auf die elektrische Entladung. *Ann. Phys.*, 31:983–1000, 1887.

[92] A. P. Higginbotham, P. S. Burns, M. D. Urmey, R. W. Peterson, N. S. Kampel, B. M. Brubaker, G. Smith, K. W. Lehnert, and C. A. Regal. Harnessing electro-optic correlations in an efficient mechanical converter. *Nature Physics*, 14(10):1038–1042, 2018.

[93] J. T. Hill, A. H. Safavi-Naeini, J. Chan, and O. Painter. Coherent optical wavelength conversion via cavity optomechanics. *Nature Communications*, 3, 2012.

[94] S. G. Hofer, W. Wieczorek, M. Aspelmeyer, and K. Hammerer. Quantum entanglement and teleportation in pulsed cavity optomechanics. *Phys. Rev. A*, 84(5):52327, nov 2011.

[95] U. B. Hoff, J. Kollath-Bönig, J. S. Neergaard-Nielsen, and U. L. Andersen. Measurement-Induced Macroscopic Superposition States in Cavity Optomechanics. *Phys. Rev. Lett.*, 117(14):143601, sep 2016.

[96] R. Horodecki, P. Horodecki, M. Horodecki, and K. Horodecki. Quantum entanglement. *Reviews of Modern Physics*, 81:865, 2009.

[97] K. Husimi. Some Formal Properties of the Density Matrix. *Proc. Phys. Math. Soc. Jpn.*, 22(264-314), 1940.

[98] J. D. Jackson. *Classical electrodynamics*. Wiley, 3rd edition, 1999.

[99] A. Jockel, A. Faber, T. Kampschulte, M. Korppi, M. T. Rakher, and P. Treutlein. Sympathetic cooling of a membrane oscillator in a hybrid mechanical-atomic system. *Nat. Nanotechnol.*, 55(10), 2015.

[100] M. Kavan, T. Paterek, S. Wonmin, V. Vlatko, and W. Mark. Unified View of Quantum and Classical Correlations. *Phys. Rev. Lett.*, 104(080501), 2010.

[101] F. Khalili, S. Danilishin, H. Miao, H. Müller-Ebhardt, H. Yang, and Y. Chen. Preparing a Mechanical Oscillator in Non-Gaussian Quantum States. *Phys. Rev. Lett.*, 105(7):70403, aug 2010.

[102] K. E. Khosla, G. A. Brawley, M. R. Vanner, and W. P. Bowen. Quantum optomechanics beyond the quantum coherent oscillation regime. *Optica*, 4(11):1382–1387, nov 2017.

[103] S. Kiesewetter, R. Y. Teh, P. D. Drummond, and M. D. Reid. Pulsed Entanglement of Two Optomechanical Oscillators and Furry's Hypothesis. *Physical Review Letters*, 119(2):23601, jul 2017.

[104] H. J. Kimble. The quantum internet. *Nature*, (453):1023–1030, 2008.

[105] I. Kogias, A. R. Lee, S. Ragy, and G. Adesso. Quantification of Gaussian Quantum Steering. *Phys. Rev. Lett.*, 114(6):60403, feb 2015.

[106] S. Kolkowitz, A. C. B. Jayich, Q. P. Unterreithmeier, S. D. Bennett, P. Rabl, J. G. E. Harris, and M. D. Lukin. Coherent sensing of a mechanical resonator with a single-spin qubit. *Science*, 1603(335), 2012.

[107] M. Kounalakis, Y. M. Blanter, and G. A. Steele. Flux-Mediated Optomechanics with a Transmon Qubit in the Single-Photon Ultrastrong-Coupling Regime. *arXiv:1911.05550 [cond-mat, physics:quant-ph]*, nov 2019.

[108] M. Kounalakis, Y. M. Blanter, and G. A. Steele. Synthesizing Arbitrary Mechanical Quantum States Using Flux-Mediated Three-Body Interactions with Superconducting Qubits. *arXiv:1905.10225 [quant-ph]*, may 2019.

[109] A. G. Krause, M. Winger, T. D. Blasius, Q. Lin, and O. Painter. A high-resolution microchip optomechanical accelerometer. *Nature Photonics*, 6(11):768–772, 2012.

[110] A. Kronwald, F. Marquardt, and A. A. Clerk. Arbitrarily large steady-state bosonic squeezing via dissipation. *Phys. Rev. A*, 88(6):63833, dec 2013.

[111] L. Lachman, S. Ivo, J. Hloušek, M. Ježek, and R. Filip. Faithful Hierarchy of Genuine n-Photon Quantum Non-Gaussian Light. *Phys. Rev. Lett.*, 123(4):43601, jul 2019.

[112] L. Landau and E. Lifshitz. *Mechanics and Electrodynamics*. Pergamon, 1972.

[113] H.-K. Lau and A. A. Clerk. High-fidelity bosonic quantum state transfer using imperfect transducers and interference. *npj Quantum Information*, 5(1):31, 2019.

[114] C. K. Law. Interaction between a moving mirror and radiation pressure: A Hamiltonian formulation. *Phys. Rev. A*, 2537(51), 1995.

[115] P. Lebedew. Untersuchungen über die Druckkräfte des Lichte. *Annalen der Physik*, 4(6):433–458, 1901.

[116] F. Lecocq, J. B. Clark, R. W. Simmonds, J. Aumentado, and J. D. Teufel. Mechanically Mediated Microwave Frequency Conversion in the Quantum Regime. *Phys. Rev. Lett.*, 116(4):43601, jan 2016.

[117] B.-B. Li, J. Bílek, U. B. Hoff, L. S. Madsen, S. Forstner, V. Prakash, C. Schäfermeier, T. Gehring, W. P. Bowen, and U. L. Andersen. Quantum enhanced optomechanical magnetometry. *Optica*, 5(7):850–856, jul 2018.

[118] J. Li, S. Gröblacher, S.-Y. Zhu, and G. S. Agarwal. Generation and Detection of Non-Gaussian Phonon-Added Coherent States in Optomechanical Systems. *Physical Review A*, 98(1):11801, jul 2018.

[119] J. Li, A. Wallucks, R. Benevides, N. Fiaschi, B. Hensen, T. P. M. Alegre, and S. Gröblacher. Proposal for Optomechanical Teleportation. *arXiv:2005.08860 [physics, physics:quant-ph]*, may 2020.

[120] Y. Li, L.-A. Wu, and Z. D. Wang. Fast ground-state cooling of mechanical resonators with time-dependent optical cavities. *Phys. Rev. A*, 043804(83), 2011.

[121] J.-Q. Liao and C. K. Law. Cooling of a mirror in cavity optomechanics with a chirped pulse. *Phys. Rev. A*, 84(053838), 2011.

[122] Q. Lin, B. He, and M. Xiao. Entangling Two Macroscopic Mechanical Resonators at High Temperature. *Physical Review Applied*, 13(3):34030, mar 2020.

[123] Q. Lin, J. Rosenberg, X. Jiang, K. J. Vahala, and O. Painter. Mechanical Oscillation and Cooling Actuated by the Optical Gradient Force. *Phys. Rev. Lett.*, 103(10):103601, aug 2009.

[124] F. Liu, S. Alaie, Z. C. Leseman, and M. Hossein-Zadeh. Sub-pg mass sensing and measurement with an optomechanical oscillator. *Opt. Express*, 21:19555–19567, 2013.

[125] R. Loudon. *The Quantum Theory of Light*. Oxford Science Publications, 3rd editio edition, 2000.

[126] Q. Lu, J. Bai, K. Wang, P. Chen, W. Fang, and C. Wang. Single Chip-Based Nano-Optomechanical Accelerometer Based on Subwavelength Grating Pair and Rotated Serpentine Springs. *Sensors (Basel, Switzerland)*, 18(7), jun 2018.

[127] S. Luo. Using measurement-induced disturbance to characterize correlations as classical or quantum. *Phys. Rev. A*, 77(022301), 2008.

[128] A. I. Lvovsky, B. C. Sanders, and W. Tittel. Optical quantum memory. *Nature Photonics*, 12(3):706–714, 2009.

[129] X. Ma, J. J. Viennot, S. Kotler, J. D. Teufel, and K. W. Lehnert. Nonclassical Energy Squeezing of a Macroscopic Mechanical Oscillator. *arXiv:2005.04260 [cond-mat, physics:quant-ph]*, may 2020.

[130] S. Machnes, J. Cerrillo, M. Aspelmeyer, W. Wieczorek, M. B. Plenio, and A. Retzker. Pulsed Laser Cooling for Cavity Optomechanical Resonators. *Phys. Rev. Letters*, 108(153601), 2012.

[131] S. Machnes, M. B. Plenio, B. Reznik, A. M. Steane, and A. Retzker. Superfast Laser Cooling. *Phys. Rev. Letters*, 104(183001), 2010.

[132] L. Magrini, R. A. Norte, R. Riedinger, I. Marinković, D. Grass, U. Delić, S. Gröblacher, S. Hong, and M. Aspelmeyer. Near-Field Coupling of a Levitated Nanoparticle to a Photonic Crystal Cavity. *Optica*, 5(12):1597–1602, dec 2018.

[133] S. Mancini, D. Vitali, and P. Tombesi. Scheme for teleportation of quantum states onto a mechanical resonator. *Phys. Rev. Lett.*, 90(137901), 2003.

[134] L. Mandel and E. Wolf. *Optical Coherence and Quantum Optics*. Cambridge University Press, 1995.

[135] P. Marek and R. Filip. Noise-resilient quantum interface based on quantum non-demolition interactions. *Phys. Rev. A*, 81(042325), 2010.

[136] A. Mari, A. Farace, N. Didier, V. Giovannetti, and R. Fazio. Measures of Quantum Synchronization in Continuous Variable Systems. *Phys. Rev. Lett.*, 111(10):103605, sep 2013.

[137] I. Marinković, A. Wallucks, R. Riedinger, S. Hong, M. Aspelmeyer, and S. Gröblacher. Optomechanical Bell Test. *Physical Review Letters*, 121(22):220404, nov 2018.

[138] F. Marquardt, J. P. Chen, A. A. Clerk, and S. M. Girvin. Quantum Theory of Cavity-Assisted Sideband Cooling of Mechanical Motion. *Phys. Rev. Lett.*, 99(9):93902, aug 2007.

[139] L. Martinetz, K. Hornberger, J. Millen, M. S. Kim, and B. A. Stickler. Quantum Electromechanics with Levitated Nanoparticles. *arXiv:2005.14006 [quant-ph]*, may 2020.

[140] J. C. Maxwell. A dynamical theory of the electromagnetic field. *Philosophical Transactions of the Royal Society of London.*, pages 459–512, 1865.

[141] F. M. Mayor, W. Jiang, C. J. Sarabalis, T. P. McKenna, J. D. Witmer, and A. H. Safavi-Naeini. Gigahertz phononic integrated circuits on thin-film lithium niobate on sapphire. jul 2020.

[142] S. A. McGee, D. Meiser, C. A. Regal, K. W. Lehnert, and M. J. Holland. Mechanical resonators for storage and transfer of electrical and optical quantum states. *Phys. Rev. A*, 87(5):53818, may 2013.

[143] S. M. Meenehan, J. D. Cohen, G. S. MacCabe, F. Marsili, M. D. Shaw, and O. Painter. Pulsed Excitation Dynamics of an Optomechanical Crystal Resonator near Its Quantum Ground State of Motion. *Phys. Rev. X*, 5(4):41002, oct 2015.

[144] C. Meng, G. A. Brawley, J. S. Bennett, M. R. Vanner, and W. P. Bowen. Mechanical Squeezing via Fast Continuous Measurement. *Phys. Rev. Lett.*, 125(4):43604, jul 2020.

[145] C. H. Metzger and K. Karrai. Cavity cooling of a microlever. *Nature*, 432(7020):1002–1005, dec 2004.

[146] N. Meyer, A. d. l. R. Sommer, P. Mestres, J. Gieseler, V. Jain, L. Novotny, and R. Quidant. Resolved-Sideband Cooling of a Levitated Nanoparticle in the Presence of Laser Phase Noise. *Physical Review Letters*, 123(15):153601, oct 2019.

[147] P. Meystre. A short walk through quantum optomechanics. *Ann. Phys. (Leipzig)*, 215(525), 2013.

[148] G. J. Milburn and M. J. Woolley. An introduction to quantum optomechanics. *Acta Phys. Slovaca*, 61:483 – 601, 2011.

[149] J. Millen, T. S. Monteiro, R. Pettit, and A. N. Vamivakas. Optomechanics with Levitated Particles. *Reports on Progress in Physics*, 83(2):26401, jan 2020.

[150] Y. Miwa, J.-i. Yoshikawa, N. Iwata, M. Endo, P. Marek, R. Filip, P. van Loock, and A. Furusawa. Exploring a New Regime for Processing Optical Qubits: Squeezing and Unsqueezing Single Photons. *Phys. Rev. Lett.*, 013601(113), 2014.

[151] C. B. Møller, R. A. Thomas, G. Vasilakis, E. Zeuthen, Y. Tsaturyan, M. Balabas, K. Jensen, A. Schliesser, K. Hammerer, and E. S. Polzik. Quantum Back-Action-Evading Measurement of Motion in a Negative Mass Reference Frame. *Nature*, 547(7662):191–195, jul 2017.

[152] M. Montinaro, G. Wust, M. Munsch, Y. Fontana, E. Russo-Averchi, M. Heiss, A. F. i. Morral, R. J. Warburton, and M. Poggio. Quantum dot opto-mechanics in a fully self-assembled nanowire. *Nano Letters*, 4454(14), 2014.

[153] E. Nichols and G. Hull. The Pressure due to Radiation. *The Astrophysical Journal*, 17(5):315–351, 1903.

[154] C. F. Ockeloen-Korppi, E. Damskägg, J.-M. Pirkkalainen, M. Asjad, A. A. Clerk, F. Massel, M. J. Woolley, and M. A. Sillanpää. Stabilized Entanglement of Massive Mechanical Oscillators. *Nature*, 556(7702):478–482, apr 2018.

[155] C. F. Ockeloen-Korppi, M. F. Gely, E. Damskägg, M. Jenkins, G. A. Steele, and M. A. Sillanpää. Sideband Cooling of Nearly Degenerate Micromechanical Oscillators in a Multimode Optomechanical System. *Physical Review A*, 99(2):23826, feb 2019.

[156] A. D. O'Connell, M. Hofheinz, M. Ansmann, R. C. Bialczak, M. Lenander, E. Lucero, M. Neeley, D. Sank, H. Wang, M. Weides, J. Wenner, J. M. Martinis, and A. N. Cleland. Quantum ground state and single-phonon control of a mechanical resonator. *Nature (London)*, 697(464), 2010.

[157] T. Ojanen and K. Børkje. Ground-state cooling of mechanical motion in the unresolved sideband regime by use of optomechanically induced transparency. *Phys. Rev. A*, 90(013824), 2014.

[158] H. Ollivier and W. H. Zurek. Quantum Discord: A Measure of the Quantumness of Correlations. *Phys. Rev. Lett.*, 88(017901), 2001.

[159] J. Oppenheim, M. Horodecki, P. Horodecki, and R. Horodecki. Thermodynamical Approach to Quantifying Quantum Correlations. *Phys. Rev. Lett.*, 89(180402), 2002.

[160] P. Ovartchaiyapong, K. W. Lee, B. A. Myers, and A. C. Jayich Bleszynski. Dynamic strain-mediated coupling of a single diamond spin to a mechanical resonator. *Nat. Commun.*, 4429(5), 2014.

[161] T. A. Palomaki, J. D. Teufel, R. W. Simmonds, and K. W. Lehnert. Entangling mechanical motion with microwave fields. *Science*, 710(342), 2013.

[162] Y. S. Park and H. Wang. Resolved-sideband and cryogenic cooling of an optomechanical resonator. *Nature Physics*, 5(7):489–493, 2009.

[163] S. Pautrel, Z. Denis, J. Bon, A. Borne, and I. Favero. An Optomechanical Discrete Variable Quantum Teleportation Scheme. *arXiv:2005.04080 [quant-ph]*, may 2020.

[164] G. A. Peterson, S. Kotler, F. Lecocq, K. Cicak, X. Y. Jin, R. W. Simmonds, J. Aumentado, and J. D. Teufel. Ultrastrong Parametric Coupling between a Superconducting Cavity and a Mechanical Resonator. *Physical Review Letters*, 123(24):247701, dec 2019.

[165] W. D. Phillips. Nobel Lecture: Laser cooling and trapping of neutral atoms. *Reviews of Modern Physics*, 70:721–741, 1998.

[166] S. Pirandola, S. Mancini, D. Vitali, and P. Tombesi. Continuous-variable entanglement and quantum-state teleportation between optical and macroscopic vibrational modes through radiation pressure. *Phys. Rev. A*, 68(6):62317, dec 2003.

[167] J. M. Pirkkalainen, S. U. Cho, J. L. G. S. Paraoanu, P. J. Hakonen, and M. A. Sillanpaa. Hybrid circuit cavity quantum electrodynamics with a micromechanical resonator. *Nature (London)*, 211(494), 2013.

[168] J.-M. Pirkkalainen, E. Damskägg, M. Brandt, F. Massel, and M. A. Sillanpää. Squeezing of Quantum Noise of Motion in a Micromechanical Resonator. *Phys. Rev. Lett.*, 115(24):243601, dec 2015.

[169] M. B. Plenio. Logarithmic Negativity: A Full Entanglement Monotone That is not Convex. *Phys. Rev. Lett.*, 95(9):90503, aug 2005.

[170] M. Poggio, C. L. Degen, H. J. Mamin, and D. Rugar. Feedback Cooling of a Cantilever's Fundamental Mode below 5 mK. *Phys. Rev. Lett*, 99(017201), 2007.

[171] J. Qian, A. A. Clerk, K. Hammerer, and F. Marquardt. Quantum Signatures of the Optomechanical Instability. *Phys. Rev. Lett.*, 109(25):253601, dec 2012.

[172] L. Qiu, I. Shomroni, P. Seidler, and T. J. Kippenberg. Laser Cooling of a Nanomechanical Oscillator to Its Zero-Point Energy. *Physical Review Letters*, 124(17):173601, apr 2020.

[173] A. Rakhubovsky, N. Vostrosablin, and R. Filip. Squeezer-based pulsed optomechanical interface. *Physical Review A*, 93(3), 2016.

[174] A. A. Rakhubovsky and R. Filip. Photon-phonon-photon transfer in optomechanics. *Scientific Reports*, 7(March):1–7, 2017.

[175] A. A. Rakhubovsky and R. Filip. Nonlinear stroboscopic quantum optomechanics. In *Quantum Information and Measurement (QIM) V: Quantum Technologies*, page F5A.68. Optical Society of America, 2019.

[176] A. A. Rakhubovsky and R. Filip. Stroboscopic high-order nonlinearity in quantum optomechanics. apr 2019.

[177] R. Riedinger, A. Wallucks, I. Marinković, C. Löschnauer, M. Aspelmeyer, S. Hong, and S. Gröblacher. Remote Quantum Entanglement between Two Micromechanical Oscillators. *Nature*, 556(7702):473–477, apr 2018.

[178] S. Rips, M. Kiffner, I. Wilson-Rae, and M. J. Hartmann. Steady-state negative Wigner functions of nonlinear nanomechanical oscillators. *New Journal of Physics*, 14(2):023042, feb 2012.

[179] R. Rivière, S. Deléglise, S. Weis, E. Gavartin, O. Arcizet, A. Schliesser, and T. J. Kippenberg. Optomechanical sideband cooling of a micromechanical oscillator close to the quantum ground state. *Phys. Rev. A*, 83(6):63835, jun 2011.

[180] I. C. Rodrigues, D. Bothner, and G. A. Steele. Coupling Microwave Photons to a Mechanical Resonator Using Quantum Interference. *arXiv:1907.01418 [cond-mat, physics:quant-ph]*, jul 2019.

[181] B. Rogers, N. L. Gullo, G. D. Chiara, G. M. Palma, and M. Paternostro. Hybrid optomechanics for Quantum Technologies. *Quantum Meas. Quantum Metrol.*, (2):11–43, 2014.

[182] E. Romero-Sánchez, W. P. Bowen, M. R. Vanner, K. Xia, and J. Twamley. Quantum Magnetomechanics: Towards the Ultrastrong Coupling Regime. *Physical Review B*, 97(2):24109, jan 2018.

[183] H. Rudolph, K. Hornberger, and B. A. Stickler. Entangling Levitated Nanoparticles by Coherent Scattering. *Physical Review A*, 101(1):11804, jan 2020.

[184] A. Rueda, W. Hease, S. Barzanjeh, and J. M. Fink. Electro-Optic Entanglement Source for Microwave to Telecom Quantum State Transfer. *arXiv:1909.01470 [quant-ph]*, sep 2019.

[185] A. C. S. Chu, J. E. Bjorkholm, A. Ashkin. Experimental Observation of Optically Trapped Atoms. *Phys. Rev. Lett*, 57:314–317, 1986.

[186] A. H. Safavi-Naeini and O. Painter. Proposal for an optomechanical traveling wave phonon-photon translator. *New Journal of Physics*, 13(1):013017, jan 2011.

[187] A. Schliesser, G. Anetsberger, R. Riviere, O. Arcizet, and T. J. Kippenberg. High-sensitivity monitoring of micromechanical vibration using optical whispering gallery mode resonators. *New Journal of Physics*, 10(095015), 2008.

[188] A. Schliesser, O. Arcizet, R. Rivière, G. Anetsberger, and T. J. Kippenberg. Resolved-sideband cooling and position measurement of a micromechanical oscillator close to the Heisenberg uncertainty limit. *Nature Physics*, 5(7):509–514, 2009.

[189] A. Schliesser, P. Del'Haye, N. Nooshi, K. J. Vahala, and T. J. Kippenberg. Radiation Pressure Cooling of a Micromechanical Oscillator Using Dynamical Backaction. *Phys. Rev. Lett.*, 97(24):243905, dec 2006.

[190] A. Schliesser, R. Riviere, G. Anetsberger, O. Arcizet, and T. Kippenberg. Resolved-sideband cooling of a micromechanical oscillator. *Nat. Phys.*, 4:415–419, 2008.

[191] M. Schlosshauer. Decoherence, the measurement problem, and interpretations of quantum mechanics. *Rev. Mod. Phys.*, 76(4):1267–1305, feb 2005.

[192] M. Schlosshauer. Quantum decoherence. *Physics Reports*, 831:1–57, 2019.

[193] J. Schmöle, M. Dragosits, H. Hepach, and M. Aspelmeyer. A micromechanical proof-of-principle experiment for measuring the gravitational force of milligram masses. *Classical and Quantum Gravity*, 33:125031, 2016.

[194] I. Shomroni, L. Qiu, D. Malz, A. Nunnenkamp, and T. J. Kippenberg. Optical Backaction-Evading Measurement of a Mechanical Oscillator. *Nature Communications*, 10(1):2086, may 2019.

[195] I. Shomroni, A. Youssefi, N. Sauerwein, L. Qiu, P. Seidler, D. Malz, A. Nunnenkamp, and T. J. Kippenberg. Two-Tone Optomechanical Instability and Its Fundamental Implications for Backaction-Evading Measurements. *Physical Review X*, 9(4):41022, oct 2019.

[196] R. Simon. Peres-Horodecki Separability Criterion for Continuous Variable Systems. *Phys. Rev. Lett.*, 84(12):2726–2729, mar 2000.

[197] R. Simon, N. Mukunda, and B. Dutta. Quantum-noise matrix for multimode systems: U(n) invariance, squeezing, and normal forms. *Phys. Rev. A*, 49(3):1567–1583, mar 1994.

[198] A. d. l. R. Sommer, N. Meyer, and R. Quidant. Strong Optomechanical Coupling at Room Temperature by Coherent Scattering. *arXiv:2005.10201 [physics, physics:quant-ph]*, may 2020.

[199] R. Stockill, M. Forsch, G. Beaudoin, K. Pantzas, I. Sagnes, R. Braive, and S. Gröblacher. Gallium Phosphide as a Piezoelectric Platform for Quantum Optomechanics. *Physical Review Letters*, 123(16):163602, oct 2019.

[200] E. C. G. Sudarshan. Equivalence of Semiclassical and Quantum Mechanical Descriptions of Statistical Light Beams. *Phys. Rev. Lett.*, 10(7):277–279, apr 1963.

[201] F. Tebbenjohanns, M. Frimmer, V. Jain, D. Windey, and L. Novotny. Motional Sideband Asymmetry of a Nanoparticle Optically Levitated in Free Space. *Physical Review Letters*, 124(1):13603, jan 2020.

[202] R. Y. Teh, S. Kiesewetter, P. D. Drummond, and M. D. Reid. Creation, Storage, and Retrieval of an Optomechanical Cat State. *Physical Review A*, 98(6):63814, dec 2018.

[203] J. Teissier, A. Barfuss, P. Appel, E. Neu, and P. Maletinsky. Strain Coupling of a Nitrogen-Vacancy Center Spin to a Diamond Mechanical Oscillator. *Phys. Rev. Lett.*, 020503(113), 2014.

[204] J. D. Teufel, T. Donner, D. Li, J. W. Harlow, M. S. Allman, K. Cicak, A. J. Sirois, J. D. Whittaker, K. W. Lehnert, and R. W. Simmonds. Sideband cooling of micromechanical motion to the quantum ground state. *Nature*, 475(7356):359–363, jul 2011.

[205] J. D. Teufel, J. W. Harlow, C. A. Regal, and K. W. Lehnert. Dynamical Backaction of Microwave Fields on a Nanomechanical Oscillator. *Phys. Rev. Lett.*, 101(19):197203, nov 2008.

[206] J. D. Teufel, D. Li, M. S. Allman, K. Cicak, A. J. Sirois, J. D. Whittaker, and R. W. Simmonds. Circuit cavity electromechanics in the strong-coupling regime. *Nature*, 471(7337):204–208, 2011.

[207] J. D. Thompson, B. M. Zwickl, A. M. Jayich, F. Marquardt, S. M. Girvin, and J. G. E. Harris. Strong dispersive coupling of a high-finesse cavity to a micromechanical membrane. *Nature*, 452(7183):72–75, mar 2008.

[208] K. S. Thorne, R. W. P. Drever, C. M. Caves, M. Zimmermann, and V. D. Sandberg. Quantum Nondemolition Measurements of Harmonic Oscillators. *Phys. Rev. Letters*, 40:667–671, 1978.

[209] L. Tian. Adiabatic State Conversion and Pulse Transmission in Optomechanical Systems. *Phys. Rev. Lett.*, 108(15):153604, apr 2012.

[210] L. Tian. Optoelectromechanical transducer: Reversible conversion between microwave and optical photons. *Annalen der Physik*, 527(1-2):1–14, 2015.

[211] M. Toroš and T. S. Monteiro. Quantum Sensing and Cooling in Three-Dimensional Levitated Cavity Optomechanics. *Physical Review Research*, 2(2):23228, may 2020.

[212] W. G. Unruh. Quantum nondemolition and gravity-wave detection. *Phys. Rev. D*, 19(10):2888–2896, 1979.

[213] M. R. Vanner, J. Hofer, G. D. Cole, and M. Aspelmeyer. Cooling-by-measurement and mechanical state tomography via pulsed optomechanics. *Nature Communications*, 4(1):2295, 2013.

[214] M. R. Vanner, I. Pikovski, G. D. Cole, M. S. Kim, C. Brukner, K. Hammerer, G. J. Milburn, and M. Aspelmeyer. Pulsed Quantum Optomechanics. *Proc. Natl Acad. Sci. USA*, 108:16182–16187, 2011.

[215] E. Verhagen, S. Deléglise, S. Weis, A. Schliesser, and T. J. Kippenberg. Quantum-coherent coupling of a mechanical oscillator to an optical cavity mode. *Nature*, 482(7383):63–67, 2012.

[216] D. Vitali, S. Gigan, A. Ferreira, H. R. Böhm, P. Tombesi, A. Guerreiro, V. Vedral, A. Zeilinger, and M. Aspelmeyer. Optomechanical Entanglement between a Movable Mirror and a Cavity Field. *Phys. Rev. Lett.*, 98(3):30405, jan 2007.

[217] B. Vogell, T. Kampschulte, M. T. Rakher, A. Faber, P. Treutlein, K. Hammerer, and P. Zoller. Long distance coupling of a quantum mechanical oscillator to the internal states of an atomic ensemble. *New J. Phys.*, 043044(17), 2015.

[218] N. Vostrosablin, A. A. Rakhubovsky, and R. Filip. Pulsed quantum interaction between two distant mechanical oscillators. *Physical Review A*, 94(6), 2016.

[219] D. Walls and G. Milburn. *Quantum Optics*. Springer, 2nd edition, 2008.

[220] A. Wallucks, I. Marinković, B. Hensen, R. Stockill, and S. Gröblacher. A Quantum Memory at Telecom Wavelengths. *Nature Physics*, pages 1–6, may 2020.

[221] X. Wang, S. Vinjanampathy, F. W. Strauch, and K. Jacobs. Ultraefficient Cooling of Resonators: Beating Sideband Cooling with Quantum Control. *Phys. Rev. Letters*, 177204(107), 2011.

[222] Y.-D. Wang and A. A. Clerk. Using Interference for High Fidelity Quantum State Transfer in Optomechanics. *Phys. Rev. Lett.*, 108(15):153603, apr 2012.

[223] C. Weedbrook, S. Pirandola, R. García-Patrón, N. J. Cerf, T. C. Ralph, J. H. Shapiro, and S. Lloyd. Gaussian quantum information. *Rev. Mod. Phys.*, 84(2):621–669, may 2012.

[224] R. Weiss. Electromagetically Coupled Broadband Gravitational Antenna. *Quarterly Progress Report, Research Laboratory of Electronics, MIT*, 105:54, 1972.

[225] T. Weiss, A. Kronwald, and F. Marquardt. Noise-induced transitions in optomechanical synchronization. *New J. Phys*, 013043(18), 2016.

[226] E. Wigner. On the Quantum Correction For Thermodynamic Equilibrium. *Phys. Rev.*, 40(5):749–759, jun 1932.

[227] I. Wilson-Rae, N. Nooshi, W. Zwerger, and T. J. Kippenberg. Theory of Ground State Cooling of a Mechanical Oscillator Using Dynamical Backaction. *Phys. Rev. Lett.*, 99(9):93901, aug 2007.

[228] D. Windey, C. Gonzalez-Ballestero, P. Maurer, L. Novotny, O. Romero-Isart, and R. Reimann. Cavity-Based 3D Cooling of a Levitated Nanoparticle via Coherent Scattering. *Physical Review Letters*, 122(12):123601, mar 2019.

[229] E. E. Wollman, C. U. Lei, A. J. Weinstein, J. Suh, A. Kronwald, F. Marquardt, A. A. Clerk, and K. C. Schwab. Quantum squeezing of motion in a mechanical resonator. *Science*, 349(6251):952 LP – 955, aug 2015.

[230] L. Yan, J.-Q. Zhang, S. Zhang, and M. Feng. Fast optical cooling of a nanomechanical cantilever by a dynamical Stark-shift gate. *Scientific Reports*, 5(14977), 2015.

[231] C. Yang and Others. Squeezed cooling of mechanical motionbeyond the resolved-sideband limit. *EPL*, 122(14001), 2018.

[232] I. Yeo, P.-L. de Assis, A. Gloppe, E. Dupont-Ferrier, P. Verlot, N. S. Malik, E. Dupuy, J. Claudon, J.-M. Gerard, A. Auffeves, G. Nogues, S. Seidelin, J.-P. Poizat, O. Arcizet, and M. Richard. Strain-mediated coupling in a quantum dot–mechanical oscillator hybrid system. *Nat. Nanotechnol.*, 106(9), 2014.

[233] L. Ying, Y.-C. Lai, and C. Grebogi. Quantum manifestation of a synchronization transition in optomechanical systems. *Phys. Rev. A*, 90(5):53810, nov 2014.

[234] H. D. Zeh. On the interpretation of measurement in quantum theory. *Foundations of Physics*, 1(1):69–76, 1970.

[235] H. Zhan, G. Li, and H. Tan. Preparing Macroscopic Mechanical Quantum Superpositions via Photon Detection. *arXiv:1910.04608 [quant-ph]*, oct 2019.

[236] H. Zhang, X.-K. Song, Q. Ai, M. Zhang, and F.-G. Deng. Transitionless intracavity quantum state transfer in optomechanical systems. oct 2016.

[237] K. Zhang, F. Bariani, and P. Meystre. Theory of an optomechanical quantum heat engine. *Phys. Rev. A*, 90(2):23819, aug 2014.

[238] W. H. Zurek. Decoherence, einselection, and the quantum origins of the classical. *Rev. Mod. Phys.*, 715(75), 2003.

LIST OF PUBLICATIONS

1. **Squeezer-based pulsed optomechanical interface**
   Andrey A. Rakhubovsky, Nikita Vostrosablin, and Radim Filip
   PHYSICAL REVIEW A 93, 033813 (2016)

2. **Pulsed quantum interaction between two distant mechanical oscillators**
   Nikita Vostrosablin, Andrey A. Rakhubovsky, and Radim Filip
   PHYSICAL REVIEW A 94, 063801 (2016)

3. **Pulsed quantum continuous-variable optoelectromechanical transducer**
   Nikita Vostrosablin, Andrey A. Rakhubovsky, and Radim Filip
   OPTICS EXPRESS Vol. 25, No.16 (2017)

4. **Quantum optomechanical transducer with ultrashort pulses**
   Nikita Vostrosablin, Andrey A. Rakhubovsky, Ulrich B. Hoff, Ulrik L. Andersen, and Radim Filip
   NEW JOURNAL OF PHYSICS 20, 083042 (2018)